NAVAL POSTGRADUATE SCHOOL

MONTEREY, CALIFORNIA

THESIS

OPTIMIZATION OF LIGHTNING WARNING AREAS AT CAPE CANAVERAL/KENNEDY SPACE CENTER

by

Erin M. Ceschini

June 2013

Thesis Advisor:	Patrick A. Harr
Second Reader:	Eva Regnier

Approved for public release; distribution is unlimited

THIS PAGE INTENTIONALLY LEFT BLANK

REPORT DOCUMENTATION PAGE			Form Approved OMB No. 0704-0188
Public reporting burden for this collection of information is estimated to average 1 hour per response, including the time for reviewing instruction, searching existing data sources, gathering and maintaining the data needed, and completing and reviewing the collection of information. Send comments regarding this burden estimate or any other aspect of this collection of information, including suggestions for reducing this burden, to Washington headquarters Services, Directorate for Information Operations and Reports, 1215 Jefferson Davis Highway, Suite 1204, Arlington, VA 22202-4302, and to the Office of Management and Budget, Paperwork Reduction Project (0704-0188) Washington DC 20503.			
1. AGENCY USE ONLY *(Leave blank)*	**2. REPORT DATE** June 2013	**3. REPORT TYPE AND DATES COVERED** Master's Thesis	
4. TITLE AND SUBTITLE OPTIMIZATION OF LIGHTNING WARNING AREAS AT CAPE CANAVERAL/KENNEDY SPACE CENTER		**5. FUNDING NUMBERS**	
6. AUTHOR(S) Erin M. Ceschini			
7. PERFORMING ORGANIZATION NAME(S) AND ADDRESS(ES) Naval Postgraduate School Monterey, CA 93943-5000		**8. PERFORMING ORGANIZATION REPORT NUMBER**	
9. SPONSORING /MONITORING AGENCY NAME(S) AND ADDRESS(ES) N/A		**10. SPONSORING/MONITORING AGENCY REPORT NUMBER**	
11. SUPPLEMENTARY NOTES The views expressed in this thesis are those of the author and do not reflect the official policy or position of the Department of Defense or the U.S. Government. IRB Protocol number ____N/A____.			
12a. DISTRIBUTION / AVAILABILITY STATEMENT Approved for public release; distribution is unlimited		**12b. DISTRIBUTION CODE**	

13. ABSTRACT (maximum 200 words)

Lightning is the primary weather hazard to spaceflight operations. At CCAFS/KSC, there are 13 individual lightning warning circles centered on locations with considerable outdoor operational activity. Reducing the number of individual lightning warning circles by combining existing warning circles or creating new warning areas based on lightning patterns has the potential benefit of reducing the workload of the forecasters on duty. However, this must be balanced against the impact of over-warning to the customers. Principal component analysis was conducted on lightning warnings issued by the 45 WS and on 4DLSS data to evaluate co-variability of the current warning circles. Additionally, lightning warnings issued by 45 WS for CCAFS/KSC were evaluated to quantify the temporal overlap of the lightning warnings for adjacent circles. "Perfect warnings" were simulated using 4DLSS data to determine lightning warning overlap in a "perfect" scenario for comparison against actual operations. The results of the principal component analysis and temporal overlap calculations were used to identify possible alternative warning areas. Finally, multi-objective decision analysis was performed to make a recommendation for the consolidation of warning circles.

14. SUBJECT TERMS lightning, multi-objective decision analysis, Cape Canaveral, Kennedy Space Center, 45 WS, resource protection			**15. NUMBER OF PAGES** 137
			16. PRICE CODE
17. SECURITY CLASSIFICATION OF REPORT Unclassified	**18. SECURITY CLASSIFICATION OF THIS PAGE** Unclassified	**19. SECURITY CLASSIFICATION OF ABSTRACT** Unclassified	**20. LIMITATION OF ABSTRACT** UU

NSN 7540-01-280-5500 Standard Form 298 (Rev. 2-89)
Prescribed by ANSI Std. 239-18

THIS PAGE INTENTIONALLY LEFT BLANK

Approved for public release; distribution is unlimited

OPTIMIZATION OF LIGHTNING WARNING AREAS AT CAPE CANAVERAL/KENNEDY SPACE CENTER

Erin M. Ceschini
Lieutenant Commander, United States Navy
B.S., The Pennsylvania State University, 2003

Submitted in partial fulfillment of the
requirements for the degree of

MASTER OF SCIENCE IN METEOROLOGY AND PHYSICAL OCEANOGRAPHY

from the

NAVAL POSTGRADUATE SCHOOL
June 2013

Author: Erin M. Ceschini

Approved by: Patrick Harr
Thesis Advisor

Eva Regnier
Second Reader

Wendell Nuss
Chair, Department of Meteorology

THIS PAGE INTENTIONALLY LEFT BLANK

ABSTRACT

Lightning is the primary weather hazard to spaceflight operations. At CCAFS/KSC, there are 13 individual lightning warning circles centered on locations with considerable outdoor operational activity. Reducing the number of individual lightning warning circles by combining existing warning circles or creating new warning areas based on lightning patterns has the potential benefit of reducing the workload of the forecasters on duty. However, this must be balanced against the impact of over-warning to the customers. Principal Component Analysis was conducted on lightning warnings issued by the 45 WS and on 4DLSS data to evaluate co-variability of the current warning circles. Additionally, lightning warnings issued by 45 WS for CCAFS/KSC were evaluated to quantify the temporal overlap of the lightning warnings for adjacent circles. "Perfect warnings" were simulated using 4DLSS data to determine lightning warning overlap in a "perfect" scenario for comparison against actual operations. The results of the Principal Component Analysis and temporal overlap calculations were used to identify possible alternative warning areas. Finally, multi-objective decision analysis was performed to make a recommendation for the consolidation of warning circles.

THIS PAGE INTENTIONALLY LEFT BLANK

TABLE OF CONTENTS

LIST OF FIGURES

THIS PAGE INTENTIONALLY LEFT BLANK

LIST OF TABLES

THIS PAGE INTENTIONALLY LEFT BLANK

LIST OF ACRONYMS AND ABBREVIATIONS

3-D:	3-Dimensional
45 WS:	45th Weather Squadron
AC-67:	Atlas/Centaur-67
4DLSS:	4-Dimensional Lightning Surveillance System
AFWX:	Air Force Weather
ALDF:	Advanced Lightning Direction Finding
CaPE:	Convective and Precipitation/Electrification
CC:	Cloud-to-Cloud
CCAFS:	Cape Canaveral Air Force Station
CG:	Cloud-to-Ground
CGLSS:	Cloud-to-Ground Lightning Surveillance System
CX:	Complex
EOF:	Empirical Orthogonal Function
hPa:	Hectopascal
IA:	Industrial Area
ITL:	Integrate-Transfer-Launch
IMPACT-ESP:	Improved Accuracy from Combined Technology-Enhanced Sensitivity and Performance
JAX:	ICAO for Jacksonville, FL
kA:	Kiloampere
KABLE:	Kennedy Space Center Atmospheric Boundary Layer Experiment
km:	Kilometers
KSC:	Kennedy Space Center
LDAR:	Lightning Detection and Ranging
LDAR-II:	Lightning Detection and Ranging, Second Generation
LF:	Low Frequency
MDF:	Magnetic Direction Finder
MHz:	Megahertz
MIA:	ICAO for Miami, FL
NASA:	National Aeronautics and Space Administration

NGM:	Nested Grid Model
NLDN:	National Lightning Detection Network
PAFB:	Patrick Air Force Base
PCA:	Principal Component Analysis
PC:	Principal Component
RAOB:	Rawinsonde Observation
SLF:	Shuttle Landing Facility
SVD:	Singular Value Decomposition
TOA:	Time of Arrival
TBX:	ICAO for Tampa Bay, FL
TLS-200:	Total Lightning Sensor Model-200
VAB:	Vehicle Assembly Building
VHF:	Very High Frequency

ACKNOWLEDGMENTS

I would like to thank my advisor, Dr. Pat Harr, for his guidance and support during the writing of this thesis, especially in understanding the Principal Component Analysis. Additionally, I would like to thank Dr. Eva Regnier for her patience and guidance as I stepped outside my comfort zone and into the field of decision analysis. Her input as my second reader ensured that my thesis was written to a broader audience. I must also extend my appreciation to Ms. Mary Jordan of the Department of Meteorology, Naval Postgraduate School, who provided programming and data processing assistance, saving me hours of MATLAB coding and frustration.

This research was funded by the 45th Operations Group at Patrick Air Force Base, Fl. Additionally, I could not have completed this thesis without the data, support and expert local knowledge of Mr. William Roeder and Mr. Todd McNamara of the 45th Weather Squadron.

To my classmates Paul Kutia, Angela Lefler, Casey Gon, Steve McIntyre, and Kate Longley: You guys made this tour great, and I am lucky to have gotten to know you. I look forward to working with you all again in the future.

And last, but not least, to my husband, Joe, and our two daughters, Abby and Evelyn, thank you for your love and support in all I do.

THIS PAGE INTENTIONALLY LEFT BLANK

I. INTRODUCTION

A. CONSEQUENCES OF LIGHTNING STRIKES

In 2009, lightning in the United States killed 34 people, hurt 201 others, and caused more than $43 million dollars in property damage. Cloud-to-ground lightning is the single largest cause of transients, faults and outages in electrical power transmission and distribution systems in lightning prone areas. Additionally, it is a major cause of electromagnetic interference that affects all electronic systems (Cummins and Murphy 2009, Cummins et al. 1998).

Lightning is one of the primary weather hazards to spaceflight operations, affecting three primary aspects of operations: 1) space launch, 2) ground processing in preparation for space launch, and 3) personnel safety and resource protection. Located along the central eastern coast of Florida, an area with the highest lightning flash density in the United States (Figure 1), Cape Canaveral Air Force Station/Kennedy Space Center experiences significant lightning impacts on operations. As documented by Merceret et al. (2010), rocket-triggered lightning strikes to ascending launch vehicles can inject currents in excess of 100 kA into those launch vehicles. Even if the primary lightning current is conducted entirely by the vehicle's metal skin, the resulting electromagnetic fields can induce secondary currents to interior structures leading to destruction of the vehicle. These induced currents can reduce the lifetime of electronics in the payloads, induce faults in the control electronics of the space launch vehicle, and even destroy the space launch vehicles. Of particular concern is interference with the proper operation of the flight termination system, so that if the space launch vehicle were to go too far off course, Range Safety could not destroy the rocket before it became a threat to public safety (Merceret et al. 2010). Two incidents of triggered lightning highlight the danger of lightning strikes to equipment. In 1969, Apollo 12 suffered two triggered lightning strikes during its launch. This mission was completed successfully; however, in flight maintenance was required on some systems due to the strikes. In 1987, the launch of Atlas/Centaur-67 (AC-67) triggered a lightning strike, which disrupted the vehicle guidance electronics ultimately leading to break up and intentional destruction of the

rocket and payload for safety reasons (McNamara et al. 2010; Roeder and McNamara 2006).

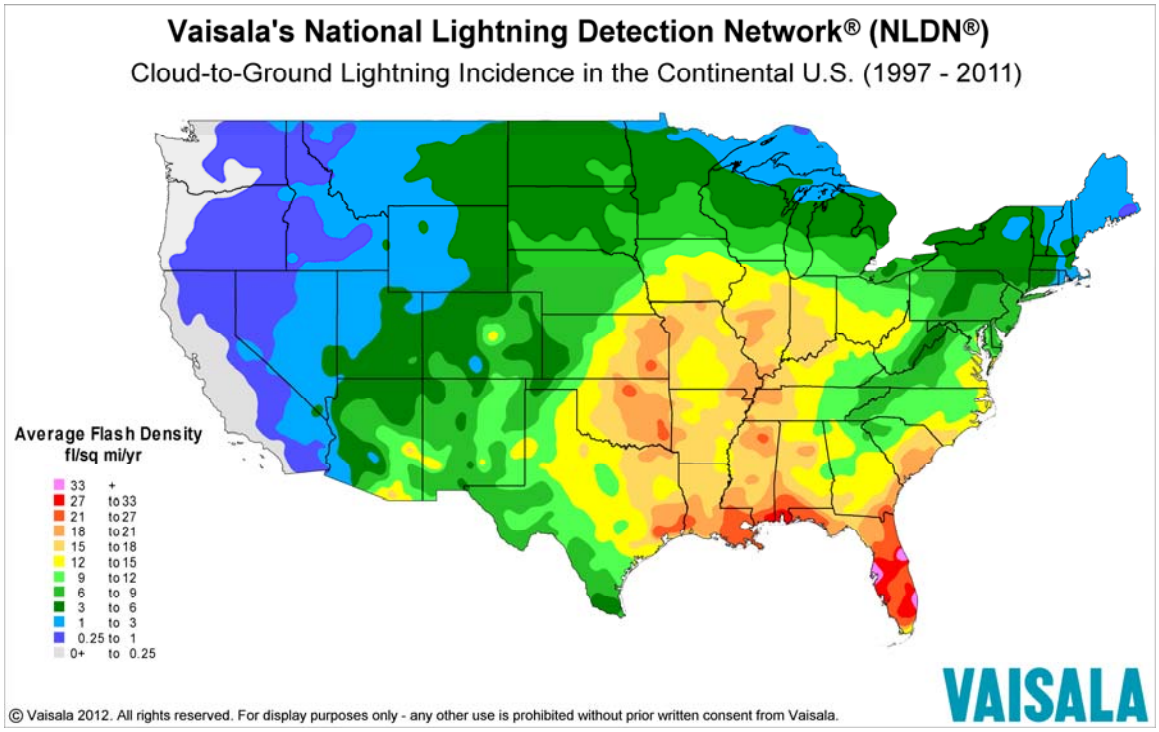

Figure 1. Average flash density (flash per square mile per year) in the United States as detected by the National Lightning Detection Network from 1997 to 2011. (From Vaisala 2012a)

Lightning can also impact ground processing operations in preparation for space launch. Nearby lightning strikes can induce potentially damaging electric currents in the electronics of satellite payloads, space launch vehicles, ground support equipment and key facilities (Flinn et al. 2010a, 2010b). Damage from lightning strikes to or near payloads, space launch vehicles, and ground equipment used in operations at Cape Canaveral Air Force Station/Kennedy Space Station (CCAFS/KSC) has significant impact on operations (Flinn et al. 2010a, 2010b).

In addition to the potential damage to or loss of equipment, injury to personnel is also a hazard of lightning. A prime example of this is an incident at Hurlburt Field, Florida, in 1996, when one person was killed and ten were injured in a lightning strike from a thunderstorm 5 to 7 nm away (McNamara 2002). Significant outdoor processing

required to prepare for space launch, occurs at CCAFS/KSC, including considerable work on launch pads, which are tall isolated structures in large open areas, creating a potentially large safety hazard during thunderstorms.

B. LIGHTNING ADVISORIES AT CAPE CANAVERAL AIR FORCE STATION/KENNEDY SPACE CENTER

The 45th Weather Squadron (45 WS) is responsible for providing comprehensive weather support to CCAFS/KSC, Patrick Air Force Base (PAFB) and other locations. This weather support includes providing for the safety of over 25,000 personnel and resource protection for over $20B of facilities as well as weather support to America's space program for pre-launch, launch and post-launch operations CCAFS/KSC (Flinn et al. 2010a, 2010b). Due to the location of CCAFS/KSC in central Florida and the potential for loss of life or severe damage, lightning is the primary hazard warned against, with approximately 1,500 lightning advisories issued each year on average by the 45 WS.

There are two types of lightning advisories issued by the 45 WS. A Phase I Lightning Watch is issued when lightning is expected to occur within 5 nm of the center of that lightning warning circle with a desired lead-time of 30 minutes. When a Phase I Lightning Watch is issued, agencies and personnel in the affected area are alerted to take preliminary actions to protect personnel and resources. Some work may continue under a Phase I Watch depending on proximity of lightning shelter and mission priority of the work. A Phase II Lightning Warning is issued when lightning is imminent or occurring within 5 nm of the center of the lightning warning circle. When a Phase II Lightning Warning is issued, agencies and personnel in the affected area are alerted to complete all actions to protect personnel and resources. All outdoor work stops in the lightning warning circle under a Phase II Lightning Warning (45th Space Wing 2007).

At CCAFS/KSC, there are currently 13 individual warning circles that cover 13 specific assets located at the center of each circle (Figure 2). The warning circles identify locations with considerable outside operational activity that require notification of lightning hazards. Each circle is 5 nm in radius based on the Air Force Occupational Safety and Health Standard 91-66 (Department of the Air Force 1997). The 5 nm radius

provides a safety buffer for the center point, since a watch or warning is issued when lightning is expected or imminent/occurring anywhere inside the circle, respectively.

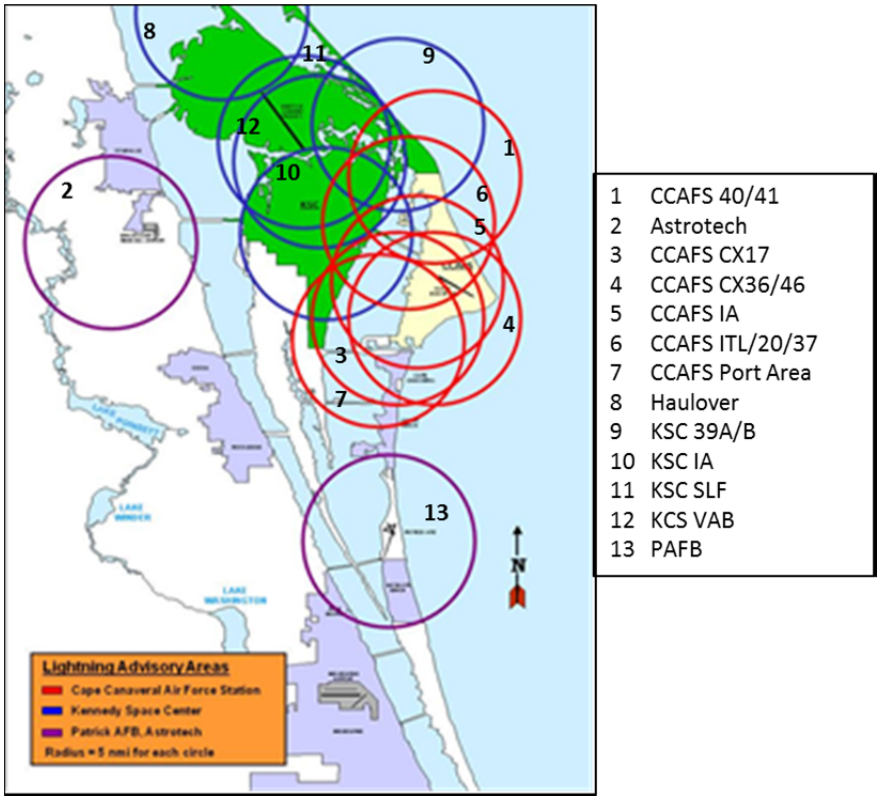

Figure 2. Lightning warning circles at Cape Canaveral Air Force Station/Kennedy Space Center and other locations.

C. RESEARCH MOTIVATION AND SCOPE

The 45 WS typically has two forecasters on duty 24/7 to provide all required weather support to CCAFS/KSC and other locations, which includes the Phase I and II Lightning Watches and Warnings. During the summer thunderstorm season, an additional forecaster serves as the thunderstorm coordinator and works a late day shift (1200-2000 L). The thunderstorm coordinator is a civil servant with years of local weather experience and a specialist in the radar and lightning detection systems. The main job of the thunderstorm coordinator during the busy summer lightning season is to issue and cancel the lightning watches and warnings and other weather advisories. On convectively active days, when multiple lightning warning areas are affected by

thunderstorm activity nearly simultaneously, the workload of these forecasters can increase dramatically, which is compounded by frequent inquiries from various customers as to when lightning advisories will end. Air Force weather policy and procedure requires the forecasters to maintain constant situational awareness of the current and expected conditions with stringent lead-time expectations for advisories and warnings. The desired lead times are in place to minimize the impact to operations due to longer than required warnings. Given the high number of individual lightning warning circles at CCAFS/KCS, their close proximity to each other, the lightning patterns and the state-of-the-art in precise lightning prediction, forecasters can quickly become overwhelmed by trying to meet lead-time requirements for each individual circle. This often leads to forecasters simultaneously issuing lightning warnings for multiple, adjacent circles which is often but not always meteorologically justified.

A preliminary study (Bowman 2009) into the feasibility of combining warning circles was conducted in the summer of 2009. Three years (2006-2008) of Phase II Lightning Warnings were compared to determine how often they overlapped in time across multiple circles. Results of this study showed that 85% of Phase II Lightning Warnings overlapped with at least one other circle. This study was only a preliminary examination of the amount of temporal overlap in the lightning advisories and excluded all Phase I Lightning Watches and did not verify lightning strike data with the issued warnings (Bowman 2009). This study also only examined the temporal overlap of pairs of lightning warning circles, not the amount of overlap of triplets or higher order combinations of lightning warning circles. This information is needed not only to identify which combinations of lightning circles would be most effective, but also to justify to the operators that the proposed combinations would not cause them to lose too much time for outdoor work. The work by Bowman was done under the Air Force Academy Cadet Summer Research Program.

Reducing the number of individual lightning warning circles by combining existing warning circles or creating new warning areas based on lightning patterns has the potential benefit of reducing the workload of the forecasters. For example, if the circles for KSC 39 A/B and KSC VAB were combined into one warning area, and lightning

occurred within any part of KSC 39 A/B or KSF VAB, a warning would be issued for the area encompassed by the previously defined KSC 39 A/B and KSC VAB circles and would end when lightning was no longer impacting either circle (Figure 3).

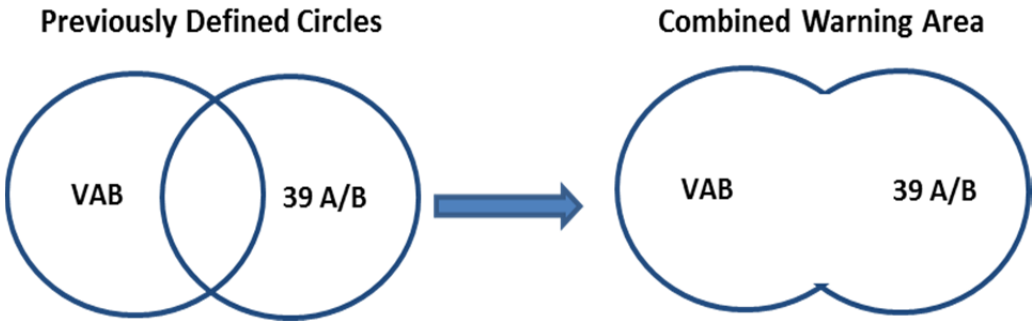

Figure 3. Example of combined warning circles KSC VAB and KSC 39A/B.

This workload reduction would allow forecasters increased time to focus on all watch responsibilities as well as increased focus on the lead-time requirements of the lightning warnings and especially canceling the lightning warnings. This would allow increased attention to the timing of active warnings, enabling the forecasters to more accurately and precisely start and stop warnings, ultimately reducing minutes (and cumulatively hours) of lost work by personnel on station. After-the-fact analysis of the 45 WS lightning warnings shows that the warnings remain active longer than required due to the lack of reliable objective high-performance guidance on lightning cessation. Lightning cessation is the top technical improvement requirement of the 45 WS and anything that can improve the prediction of the end of lightning, including more efficient lightning warning circles is desired. Operations at the 45 WS and the Bowman (2009) study led to the request by the 45 WS to examine frequency of temporal overlap of lightning watches and warnings at CCAFS/KCS for pairs, triplets and higher combinations of the current 45 WS lightning warning circles and recommend optimum lightning warning areas.

The primary hypothesis of this thesis is that the current warning circles (Figure 2) at Cape Canaveral Air Force Station/Kennedy Space Station overlap spatially and overlap temporally enough to allow consolidation of pairs, triplets or higher combinations of

warning circles due to warning criteria conditions. The secondary hypothesis of this thesis is that lightning warning circles are linked spatially and temporally by specific weather processes/regimes.

Principal component analysis was conducted on lightning warnings issued by the 45 WS and on 4-Dimension (4DLSS) data to evaluate co-variability of the current warning circles. Additionally, lightning warnings issued by 45 WS for CCAFS/KSC were evaluated to quantify the temporal overlap of the lightning watches and warnings for adjacent circles. "Perfect warnings" were simulated using 4DLSS data to determine lightning warning overlap in a "perfect" scenario for comparison against actual operations. The results of the Principal Component Analysis and temporal overlap calculations were used to identify possible alternative warning areas. Finally, multi-objective decision analysis was performed to make a recommendation for the consolidation of warning circles.

THIS PAGE INTENTIONALLY LEFT BLANK

II. BACKGROUND

A. LIGHTNING

Lightning is the essential, defining part of a thunderstorm. In the absence of lightning that generates the thunder, a thunderstorm fails to exist (MacGorman and Rust 1998). The classic thunderstorm develops in three stages: cumulus, mature and dissipating. During the cumulus stage, there are updrafts throughout the primary convective cell and no precipitation at the surface. Once precipitation reaches the ground, the thunderstorm has reached the mature stage of development and has both updrafts and downdrafts. During the mature stage, the thunderstorm begins generating lightning. Heavy rain, sometimes strong winds and occasionally hail occur at the surface. The final stage of development, the dissipating stage, is reached when only downdrafts exist in the cell. While new electrical charge is usually not being generated, lightning can continue to occur from previously generated electrical charge. Frontal thunderstorms are considered more electrically active than convective (air mass) thunderstorms (Malan 1963).

The classic model of the main charge within a thunderstorm as described by Walin (1986), MacGorman and Rust (1998), Uman (2001) and Rakov and Uman (2003) is a positive dipole where the lower portion of a thundercloud is predominantly negatively charged and the top portion is predominantly positively charged. Occasionally, a small pocket of positive charge will be found near the base of the cloud. When this occurs, it is commonly referred to as a tripole. The dipole/tripole conceptual model describes the basic charge distribution of a thunderstorm, but actual charge distributions are much more complex (Figure 4).

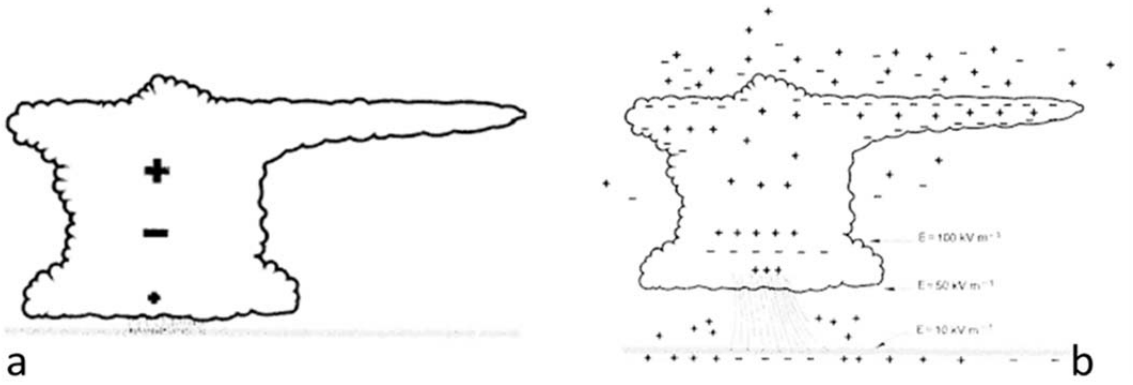

Figure 4. a. Thunderstorm described as a simple tripole model. The lower positive charge in this model may not always be present. In that case, there is a positive dipole charge structure. b. Example of the more realistic complex charge distribution of an actual thunderstorm. (After MacGorman and Rust 1998).

There are two types of theories for the generation of the main charge dipole/tripole in a thunderstorm. In the first theory, heavy, falling precipitation particles interact with lighter particles, which are carried upward in the updrafts. The interaction of these two particles serves to charge the heavy particles negatively and the lighter particles positively. This non-inductive collisional graupel-ice mechanism is a precipitation theory whereby in the presence of water droplets, falling graupel transfers negative charge to lower portions of the cloud while ice crystals transfer positive charge to upper portions of the cloud. The charging depends on temperature and liquid water content, size of ice crystals colliding with graupel, impact velocity and contamination in the water particles (MacGorman and Rust 1998, Rakov and Uman 2003). The small positively charged region near the cloud base might be caused by one or more processes. These processes include those that are similar to the main dipole charging method, such as the release of positive corona at the ground and subsequent upward motion to the cloud base and deposition by lightning (Uman 2001). The second type of theory is convective, where charge accumulated near the Earth's surface or across regions of varying air/cloud conductivity is moved in bulk to the observed locations by air flow associated with thunderstorms (Uman 2001). There is growing consensus that the

graupel-ice mechanism is the dominant electrification mechanism and explains the tripole cloud structure (Rakov and Uman 2003).

Once sufficient charge is generated in the thunderstorm, the first flash of lightning will occur. A typical thunderstorm takes approximately twenty minutes to generate the charge required for the first flash of lightning but only seconds are required for the ensuing flashes (Wahlin 1986). The flash rate may vary from one to ten or more per minute with a maximum flash rate of ten to twenty flashes per minute after the first flash. The mean flash rate is two to three flashes per minute per cell within a storm. An average thunderstorm consists of two cells per storm with three to four flashes per minute per storm (Golde 1977). All lightning can be grouped into two types: intra-cloud and cloud-to-ground (Bazelyan and Razier 2000).

1. Intra-Cloud Lightning

The majority of all flashes are wholly located within the cloud. Technically, the term "intra-cloud lightning" refers only to flashes within the thunderstorm cloud. While admittedly the majority of lightning aloft is intra-cloud, inter-cloud or cloud-to-cloud lightning and cloud-to-air lightning also occur. The term "lightning aloft" would be completely inclusive, but as the term "intra-cloud lightning" is well ingrained in the literature and common usage, it will be used for all types of lightning aloft throughout this thesis. Intra-cloud lightning serves to reduce the spatial differences in charge within or between clouds and typically precedes cloud-to-ground discharges by minutes to tens of minutes (Cummins and Murphy 2009). Intra-cloud flashes can be several to dozens of kilometers long (Bazelyan and Raizer 2000). Diffuse illumination by the flash can be seen, and occasionally the channel can also be seen (Malan 1963).

Intra-cloud flashes outnumber cloud-to-ground flashes by a factor of two to ten (Cummins and Murphy 2009). The average ratio of intra-cloud flashes to cloud-to-ground flashes varies by location, but Malan (1963), Wahlin (1986), Bazelyan and Raizer (2000) agree that the average ratio is around three times as many intra-cloud flashes as cloud-to-ground. An active thundercloud can produce hundreds of intra-cloud flashes without a single discharge to the ground (Malan 1963).

Intra-cloud lightning occurs between oppositely charged regions of the cloud with a typical duration of one second. The intra-cloud lightning process begins with a continuously propagating leader that generates a weak return stroke called a recoil streamer, when it comes into contact with pockets of space charge opposite to its own (Uman and Krider 1989, Uman 2001). A typical cloud flash begins in or near the main negatively charged region of the cloud (located at approximately four to eight kilometers above the surface) and propagates toward an upper positively charged region of the cloud (located at approximately eight to twelve kilometers above the surface) (Cummins and Murphy 2009). The return stroke is likely a concurrent leader coming into contact with the initial leader (Bazelyan and Raizer 2000). Most of, if not all, intra-cloud lightning discharges occur in the region of the cloud containing water in the form of frozen particles (Malan 1963).

2. Cloud-to-Ground Lightning

Cloud-to-ground lightning is defined by Malan (1963) as "an electrical discharge between the negatively charged region in the thundercloud and the ground. The net effect produced by the flash is the lowering and final dissipation of the negative charge from the cloud to earth." Flashes that transport the negative charge to the ground are called negative polarity lightning. A small minority of cloud-to-ground flashes transport positive charge to the ground (more accurately negative charge to the cloud), which are called positive polarity lightning (Uman and Krider 1989). An electric field is produced between the negatively charged cloud and positive charge induced on the ground by the negatively charged cloud. The positive charge at the surface is carried upward by the electrical field at approximately 1 cm s^{-1} and by the wind at approximately 10 m s^{-1}. The positive charge in the ground is not uniformly distributed due to varying conductivity, object height and gusty winds. The distribution of charge in the cloud, which induces the positive charge in the ground, also contributes to the lack of uniform distribution of charge in the ground (Malan 1963).

Cloud-to-ground lightning is sometimes also classified according to the source of the lightning: cellular thunderstorms, anvil cloud and debris cloud. The vast majority of

flashes come from cellular thunderstorms. Cloud-to-ground lightning from anvil clouds is much less frequent than from cellular thunderstorms. Anvil cloud-to-ground lightning can be produced a surprisingly long distance from the parent thunderstorms, easily many tens of miles to over 100 miles in extreme cases. Cloud-to-ground lightning from debris cloud is even less frequent than from anvil cloud. Debris cloud is the remnant cloud leftover after a thunderstorm decays. Debris cloud can carry remnant electrical charge that can produce a last set of cloud-to-ground lightning a surprisingly long time after the thunderstorm decayed, tens of minutes to over an hour in extreme cases (Roeder and McNamara 2011).

The basic negative CG leader and return stroke cloud-to-ground lightning process is described by Malan (1963), MacGorman and Rust (1998) Uman (2001) and Rakov and Uman (2003). The preliminary breakdown within the cloud begins the process though there is disagreement about the exact form and location. Following the preliminary breakdown, the discharge begins at the cloud and progresses toward the ground as a stepped-leader, branching in a downward direction. The leader leaves behind an ionized channel where the advancing conductor lowers negative charge toward the ground. As the leader comes close to the ground, it creates a strong electrical field. A streamer discharge moves upward from the ground to meet the leader. At this point, electrical continuity is established and the leader channel is neutralized which is manifested by the flash of lightning along the channel from ground to cloud. This neutralization is known as the return stroke. The rapid release of energy from the return stroke also heats the leader channel and generates a high-pressure channel that expands and creates shockwaves, which quickly lose intensity and changes from a shockwave into a normal acoustic wave known as thunder. In a single stroke flash, the process ends here. For multi-stroke flashes where additional charge is available at the top of the channel, following the initial stroke, a continuous dart leader replaces a stepped leader traveling to the ground and initiating a second and all subsequent return strokes. Dart leaders and return strokes are typically not branched, however dart leaders may deviate from the original channel leading to cloud-to-ground flashes with multiple contact points to the ground. Recent research has shown that about half of cloud-to-ground flashes have

multiple contact points with the ground and the typical distance between these multiple contact points is three kilometers and can be over ten kilometers (Valine and Krider, 2002). The leader for most cloud-to-ground strokes originates within the cloud (descending leader), but the process can also originate at the surface (ascending leader) sometimes called ground-to-cloud lightning (Uman and Krider 1989).

The main lightning channel is usually branched. Branches, most of which do not reach the ground, are less luminous and slope downwards away from the main channel. Branching occurs when the leader encounters multiple pockets of positive charge as it moves toward the ground. The leader splits into multiple channels and the first channel to meet the ground becomes the main channel (Malan 1963).

Flashes of lightning have multiple separate partial discharges known as component return strokes of the flash (Malan 1963). The number of strokes per flash is referred to as multiplicity (Cummins and Murphy 2009). A typical flash has three to four component return strokes, but as many as 42 strokes per flash have been reported (Wahlin 1986). Discharges do not progress in a "steady, orderly fashion" (Golde 1977). While subsequent component return strokes may follow the original main channel, 30-50% of all cloud-to-ground flashes have strokes that produce different ground strike points separated by up to several kilometers (Cummins and Murphy 2009). Cloud-to-ground strokes in a single flash tend to strike within ten kilometers in of the first stroke (Uman and Krider 1989). For this reason, some researchers define a cloud-to-ground flash as "the ensemble of all CG strokes that strike within ten kilometers of each other within a one second interval" (Cummins and Murphy 2009).

Flashes can be negatively or positively charged. This is referred to as the polarity of the flash. The classification of charge is based on the charge of the region from which they originate. Negative flashes originate from negatively charged regions (cloud or ground) and positive flashes originate from positively charged regions. Of all cloud-to-ground flashes worldwide, 90% are negatively charged and 10% are positively charged (Uman 2001). There are several notable differences between positive and negative flashes. Negative flashes usually have stepped leaders and multiple return strokes (Bazelyan and Raizer 2000). Positive discharges are continuous and only have one return

stroke (Uman and Krider 1989, Uman 2001). Positive strokes are ten times more powerful and have ten times more charge than negative strokes (Wahlin, 1986). As a result, strong positive cloud-to-ground lightning is especially damaging and more likely to cause fires. Additionally, positive flashes occur mostly in winter as most snowstorm flashes are positive (only 1-15% of summer flashes are positive), and increase in frequency with latitude and height of terrain (Uman and Krider 1989, Uman 2001). Anvil lightning also produces positive lightning (MacGorman and Rust 1998).

B. LIGHTNING ALONG OF THE CENTRAL FLORIDA COAST

Located along the central eastern coast of Florida, CCAFS/KSC averages 83 thunderstorm-days each year (14th Weather Squadron, 2009). Hodanish et al. (1997) found as part of a 10-year lightning climatology that an annual flash density maximum occurred near Cape Canaveral with flash densities exceeding 12 flashes km^{-2} yr^{-1}. The lightning frequency at CCAFS/KSC depends on the position of the subtropical ridge axis and the resultant low-level flow regimes over the peninsula (Lericos et al. 2002). A study of lightning ground flash density and thunderstorm duration by Huffines and Orville (1999) found that the maximum annual thunderstorm hours in the United States occurred over the Florida peninsula. This study also found a pronounced maximum of 45+ flashes per flash hour over the Florida coast, which they found to be highly indicative of sea breeze convection (Huffines and Orville 1999). The flash density climatology local to CCAFS/KSC from 1992-2004 is illustrated in Figure 5. This climatology shows that the flash density increases along an axis oriented south-southeast to north-northwest.

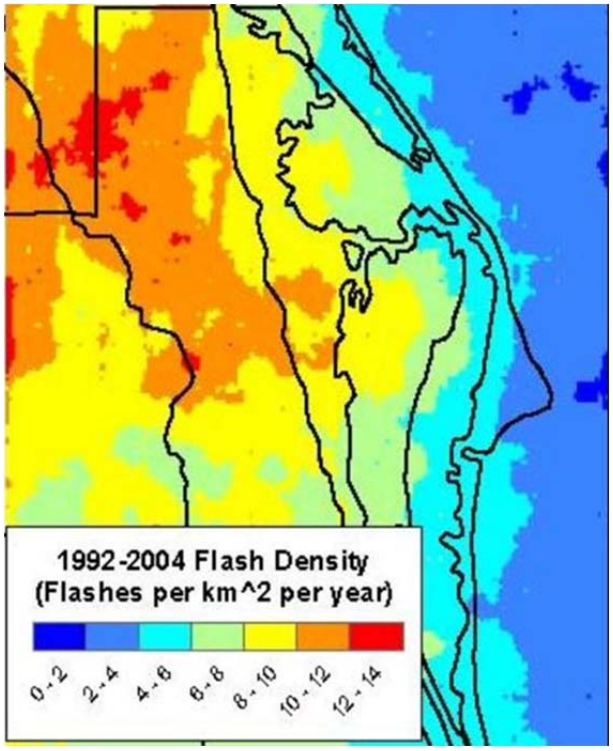

Figure 5. Lightning flash density climatology at CCAFS/KSC from 1992–2004. (From Stano 2007)

1. Sea Breeze Circulations Near Cape Canaveral

The geography of the Florida peninsula is unique and conducive to the formation of thunderstorms. Surrounded by water on three sides, there is significant opportunity for differential heating between the land and water surfaces, leading to mesoscale sea/land-breeze circulations across the Florida Peninsula (Hodanish et al. 1997). The sea breeze circulation sets up during the day, when the land heats up faster than the adjacent water so that the air over the land rises. Over the cooler sea, the air sinks and onshore flow of cooler air from over the nearby water replaces the rising air with a return flow aloft that completes the circulation. Often the sea breeze has an identifiable leading edge called the sea breeze front that interacts with synoptic scale flow and other low-level flows and can result in deep convection and thunderstorms. The Florida peninsula experiences two coastal sea breezes, one along the east coast off the Atlantic Ocean and one along the west coast off the Gulf of Mexico. Each of these sea breezes develops along the coast, but the exact location of these sea breezes throughout the day is highly dependent upon

the synoptic scale flow patterns (Lericos et al. 2002). Due to the narrowness of the Florida peninsula and depending on the flow pattern, one of the sea breeze fronts can move across the width of the peninsula over the course of the day and potentially interact with the sea breeze front from the other side of the peninsula.

The localized sea breeze tends to be perpendicular to the orientation of the nearest shore and the resulting sea breeze fronts parallel to the nearest shore. Coastline shape, such as the convex protrusion of Cape Canaveral, has been shown to change the shape of the sea breeze along irregular coastlines. The sea breeze front is then roughly the same shape as the coastline. At Cape Canaveral, there is a distinct bend in the coastline that under certain flow regimes can effectively create two sections of the local sea breeze front, one along the northern part of the Cape and one along the southern portion. These variations in the coastline can lead to persistent zones of convergence within the sea breeze air. Laird et al. (1995) using data collected as part of the Convective and Precipitation/Electrification (CaPE) Experiment, showed that a persistent convergence line developed as the two sections of the sea breeze front moved inland. The resultant "Trailing Convergence Line" extended from the intersection of the two sea breeze fronts toward the outer coast of Cape Canaveral. This convergence increased the depth of the sea breeze air and created circulations at the top of the sea breeze, which supported the development of convection (Laird et al. 1995).

In addition to being surrounded on three sides by water, Florida has numerous bodies of land-locked water totaling 11,500 km^2. Just as the sea is typically cooler than the land, these bodies of water are cooler than the surrounding land and can also generate areas of localized subsidence. As the air sinks and diverges over the water, convergence typically occurs along the shore, affecting convection and thunderstorm development (Hodanish et al. 1997). Three bodies of water near Cape Canaveral, which affect local thunderstorm development, are the Banana River, Indian River and Mosquito Lagoon (Figure 6). Two experiments conducted in the CCAFS/KSC area, the Kennedy Space Center Atmospheric Boundary Layer Experiment (KABLE) and the CaPE Experiment, found that the presence of the Banana and Indian Rivers and to a lesser degree Mosquito Lagoon significantly changed the expected sea breeze convergence pattern. Using data

collected as part of the CaPE Experiment, Laird et al. (1995) found that sufficient divergence over the relatively cooler waters of the Indian River was sufficient to create and maintain a quasi-stationary convergence zone that, when interacting with the sea breeze front, triggered thunderstorms.

A climatology of the sea breeze at Cape Canaveral (Cetola 1997) found that on 60% of sea breeze days, there are also Banana and/or Indian River breezes. He found that these river breezes are less prevalent and weaker than the sea breeze due to the weaker temperature gradient between the river and land. Additionally, the Indian River breeze was typically stronger and lasted longer than the Banana River breeze due to its increased distance from the coast, which delays interaction with the coastal sea breeze (Cetola 1997).

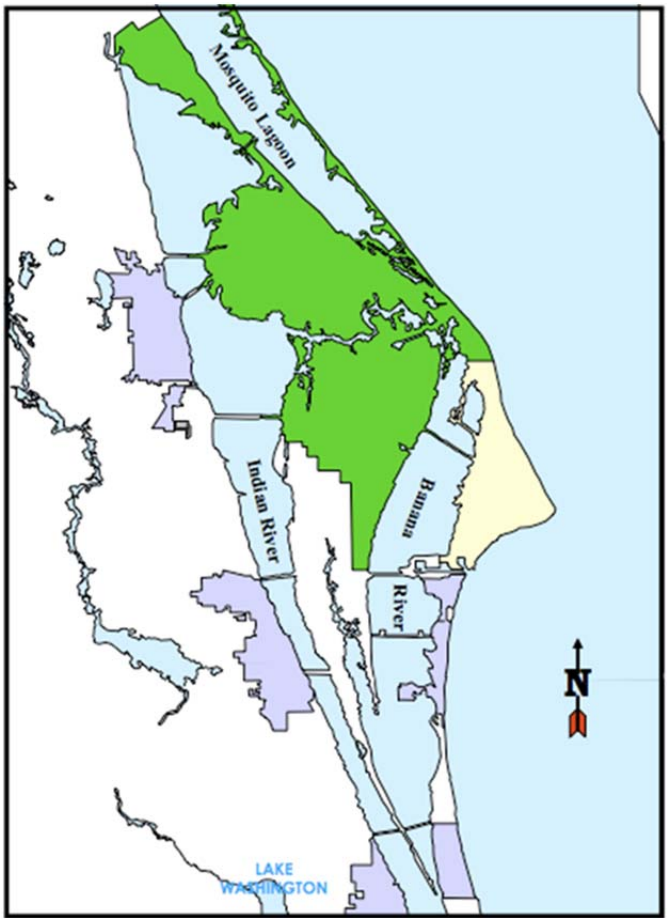

Figure 6. Bodies of water near Cape Canaveral, Florida.

2. Synoptic Patterns Associated with Lightning Distributions

There are numerous studies of the synoptic flow patterns and associated phenomena that lead to thunderstorms on the Florida Peninsula. Lericos et al. (2002) summarize several of these studies, which specifically focus on convective development over the Florida peninsula and the effects of sea breezes, prevailing flow, and frictional convergence and divergence. The two most relevant to this thesis are Reap (1994) and Lericos et al. (2002).

The study by Reap (1994) focused on the relationship between sea and lake breeze convergence zones and the prevailing synoptic low-level flow patterns. The objectives of that research included determining the effects of synoptic-scale forcing under a variety of flow patterns on lightning distributions and developing and analyzing the spatial and temporal characteristics of lightning in each flow. Reap evaluated warm season (1 March – 30 September) NGM (Nested Grid Model) 18-hour sea-level pressure and 950 hPa height data from 1987-1989 and used a linear correlation technique for synoptic pattern classification. He found seven patterns with a 0.8 R threshold. Of these seven, three accounted for 66% of the total lightning flashes and 66% of the total days studied, which he classified as map types A, B and C (Figure 7).

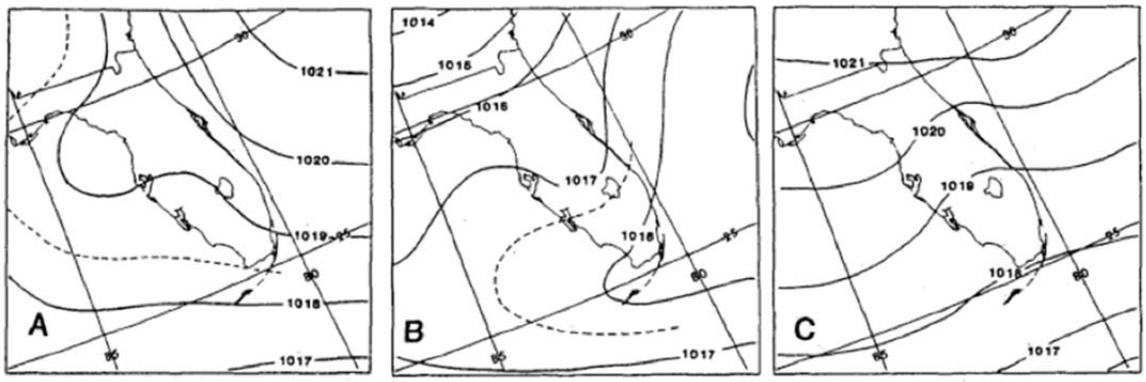

Figure 7. Mean NGM 18-h forecast sea level pressure patterns associated with map types A-C. (After Reap 1994)

Type A is an east-west ridge over Florida, producing generally southeasterly flow over central and southern Florida. Type B is southward movement of the east-west ridge

over Florida, producing southwesterly flow across the Florida Peninsula. Type C is predominantly easterly flow over the peninsula. Of these three, Type B, produced a relative maximum of lightning along the eastern Florida coast, with a maximum flash density just west of Cape Canaveral. Type B produced the most convectively active days, and is characterized by the early appearance of convection along both coasts and the interior near Lake Okeechobee. The southwesterly flow moves the west coast sea breeze front to the interior of the peninsula eventually merging with the east coast sea breeze. The east coast sea breeze front remains relatively stationary along the east coast due to relatively high mean synoptic scale wind speeds. Type B events are also characterized by an east-west band of thunderstorm activity stretching along an axis between Cape Canaveral and Tampa (Reap 1994).

Lericos et al. (2002) focus on the 1989-1998 warm seasons (May through September) and specifically relate the horizontal distribution and timing of lightning to the position of the sub-tropical ridge axis and its interaction with the mesoscale circulations that produce thunderstorms, especially the east coast and west coast sea breezes. Synoptic regimes were classified using the 1000-700 hPa mean vector wind at three radiosonde stations (TBX, JAX and MIA). The top six regimes are identified for comparison, four of which describe the position of the subtropical ridge axis, one describes a more mid-latitude flow pattern and the sixth represents calm flow. The eight regimes containing the fewest days were not considered due to insufficient sample size. From the six regimes considered, three produced a relative increase in lightning near CCAFS/KSC: 1. the sub-tropical ridge axis located south of the Florida peninsula, 2. the sub-tropical ridge axis located between Tampa Bay and Miami, and 3. northwesterly flow across the entire Florida peninsula (Figure 8) (Lericos et al. 2002).

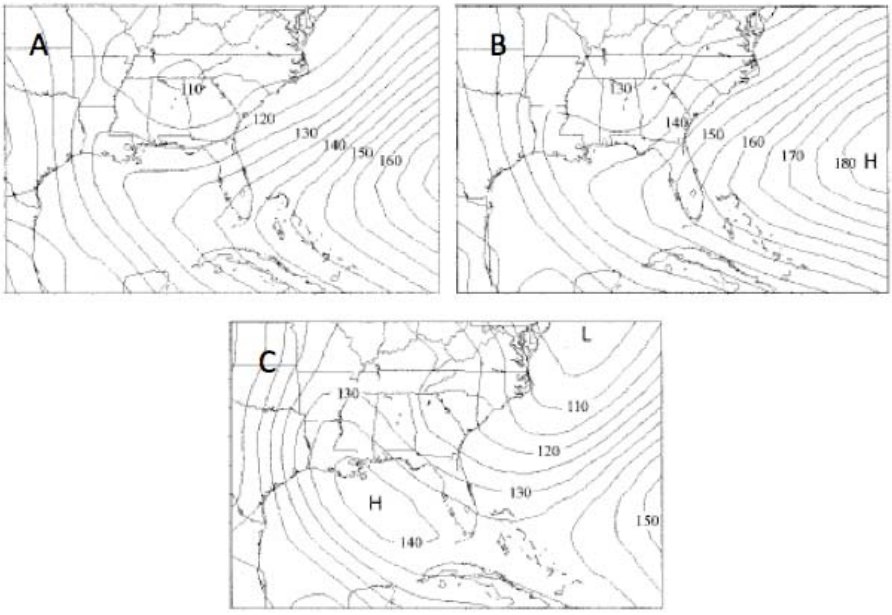

Figure 8. Averaged 1000-mb height contours for individual flow regimes: (A) sub-tropical ridge to the south, (B) sub-tropical ridge between Miami and Tampa, (C) northwest flow. (After Lericos et al. 2002)

In the first regime, the sub-tropical ridge axis is located south of the Florida peninsula. This is the most common flow regime identified by Lericos et al. (2002) with 24% of all study days and the regime that also produces the greatest number of flashes over the Florida peninsula. Under this regime, the peninsula experiences southwesterly flow. As also found in Reap's (1994) Type B, the southwesterly flow in this regime led to a better defined east coast sea breeze and greatest flash densities were confined along the east coast near Cape Canaveral and Palm Beach (Lericos et al. 2002).

In the next regime, the sub-tropical ridge axis is located between Tampa Bay and Miami. This regime has a similar influence on the lightning distribution areas with enhanced lightning activity near Tampa, Cape Canaveral, Miami and Fort Myers due to the convex shape of the coastline in those areas. The maximum near Cape Canaveral is the most pronounced of the four. In this regime, flash patterns along the east and west coasts are comparable (Lericos et al, 2002).

The final regime considered is northwesterly flow across the entire peninsula. There are two main causes of this regime, including frontal passage (especially in May and September) and a lobe of sub-tropical high pressure over the Gulf of Mexico. In either scenario, relatively dry air from the north covers the peninsula. In this regime, the greatest flash densities are again observed along the east coast, indicating influence from the east coast sea breeze. There is little evidence of a west coast sea breeze in this regime. There is also enhanced lightning between Tampa and Cape Canaveral as in the first regime; however, the orientation is more southeastward (Lericos et al. 2002).

The use of lightning flow regimes has proven very useful. The Applied Meteorology Unit has developed a lightning probability tool for the 45 WS. The flow regime was selected statistically as the second most important predictor variable, after one or two traditional RAOB (Rawinsonde Observation) thunderstorm indices. More information on this lightning probability tool is available in Lambert and Roeder (2008), Lambert et al. (2006) and Lambert et al. (2005). Other statistically significant variable for lightning probability at CCAFS/KSC in this tool were daily climatology, one-day persistence and mid-level humidity.

C. LIGHTNING DETECTION EQUIPMENT

1. National Lightning Detection Network

In the United States, a network of lightning sensors detects and locates cloud to ground strikes and intra-cloud lightning flashes. This network, known as the National Lightning Detection Network (NLDN) is owned and operated by the private company, Vaisala. The most recent system wide upgrade to the NLDN occurred in 2002-2003, when Vaisala replaced all its existing lightning sensors with the Improved Accuracy from Combined Technology-Enhanced Sensitivity and Performance (IMPACT-ESP) sensor and added a few additional sensors to improve network geometry. Following this upgrade, there are currently 113 lightning sensors in the network (Figure 9) (Grogan 2004).

Figure 9. NLDN lightning sensor locations in the Continental United States. (From Grogan 2004)

The IMPACT-ESP sensors use a combination of Magnetic Direction Finding (MDF) and Time of Arrival (TOA) technologies (Vaisala 2011). Both MDF and TOA methods take advantage of the magnetic and electric fields radiated by lightning processes to detect and locate cloud-to-ground lightning. The MDF technology detects magnetic waveforms that are characteristic of return strokes that propagate radially outward from the strike along the ground. The electric field is also measured to determine stroke polarity. By using a network of MDFs, the location of the stroke is determined by triangulation. The direction of the strike from each pair of sensors generates a candidate location for the strike. At least two sensors are required to generate a candidate location by MDF (Roeder 2010). The TOA sensors are based on measuring the time-of-arrival of a radio pulse emitted by the lightning flash at several stations that are precisely synchronized (Cummins et al. 1998). Each pair of sensors generates a hyperbola on which the strike must lie. The intersection of three or more hyperbola sensors determines the strike location. At least three sensors are required to generate a candidate location by TOA. By combining the MDF and TOA methods from many sensors, multiple candidate locations for the same strike are developed. The most likely location is then determined by Chi-squared minimization statistics that minimize the location error (Roeder 2010). Vaisala states a 80-85% detection efficiency of all cloud-

to-ground flashes and approximately a 30-50% detection efficiency of cloud flashes for the IMPACT-ESP sensor (Vaisala 2011). Detection efficiency is defined as the fraction of actual strokes or flashes that are detected and reported by the network (Cummins et al. 1998). The NLDN has a 90% or greater network detection efficiency for cloud-to-ground and 10-30% or greater network detection efficiency for cloud flashes (Vaisala 2011). Vaisala states a 60-80% stroke detection efficiency and a stroke location accuracy of 500 meter median error for the NLDN (Grogan, 2004).

The combined MDF/TOA technology used by the sensors requires only two sensors to accurately locate an event while still maintaining one excess degree of freedom. This allows the network to detect low amplitude cloud-to-ground flashes and as well as cloud flashes. The configurable waveform and noise-rejection criteria allow the sensor to accept or reject a waveform and categorize it based on a set of rules that can be changed by location or as scientific understanding of lightning waveforms changes and improves. While the IMPACT-ESP sensor has improved the ability to detect cloud flashes, only 10-30% are detected and the classification algorithms used still misclassify some cloud flashes as cloud-to-ground (Cummins et al. 2006).

2. 4-Dimension Lightning Surveillance System

The 4-Dimension Lightning Surveillance System (4DLSS) employed at CCAFS/KCS was implemented operationally in April 2008. This system is a major upgrade to the Lightning Detection and Ranging (LDAR) system as well as an upgrade to the Cloud-to-Ground Lightning Surveillance System (CGLSS) and integrated it into the 4DLSS (Roeder 2010). 4DLSS monitors lightning activity within a 100 kilometer area centered on CCAFS/KSC.

The cloud-to-cloud (CC) detection system uses Lightning Detection and Ranging, Second Generation (LDAR-II) sensors. They detect inter-cloud and intra-cloud lightning, and measure the relative signal strength with polarity. The CC sensors can detect cloud-to-ground lightning, in the form of step leaders, down to approximately one kilometer in altitude, but they cannot provide the final ground strike location. These sensors measure Very High Frequency (VHF) radiation emitted by lightning at frequencies of 60-70 MHz

and locate the lightning via triangulation from TOA measurements (45th Weather Squadron, 2011). Similar to cloud-to-ground lightning TOA detection, each pair of sensors generates a 3-dimensional (3-D) hyperbolic surface on which the step leader must lie. Since 3-D locating is being done, four pairs of sensors are required to generate a solution in 3-D space. Time is the fourth dimension of the 4DLSS solution (Roeder 2010). There are nine total CC sensors (Figure 10).

The cloud-to-ground (CG) sensors are the IMPACT Model 141-T Low-Frequency (LF) Advanced Lightning Direction Finding (ALDF) sensors. They detect cloud-to-ground lightning strike points and relative signal strength magnitudes with polarity using TOA and MDF technology. A minimum of two CG sensors is required to locate and display the lightning strike. Additional sensors increase the accuracy of the location and the detection rate. There are six CG sensors at CCAFS/KCS (Figure 10) (45th Weather Squadron 2011). A major upgrade of 4DLSS is in-progress as of January 2013 to change the six CG sensors and nine CC sensors to 11 CG/CC combined Total Lightning Sensor-200 (TLS-200) sensors. Total Lightning Sensor TLS-200 combines VHF interferometry with LF magnetic direction finding and time-of-arrival technologies for the highest level of total lightning mapping detection capabilities with calibrated lightning parameters (Vaisala 2012b). This will improve the CC detection capability and significantly improve the CG detection capability of 45 WS, however the height of CC lightning will no longer be provided. In addition, the Shilo site is being relocated slightly to reduce radio interference and a new site at Patrick AFB is being added to replace the Melbourne site which will not be usable for the sensors since it is too tall and will interfere with flight safety at the Melbourne airport. The nine in-range NLDN sensors will also have their data integrated into the new network to help reduce lost CG detections from strong local strokes (Ward et al. 2008), which causes 4.9% of all strokes to be missed (Sun 2012). Additional technical characteristics of the NLDN and 4DLSS are outlined in Table 1.

Figure 10. 4DLSS Remote Site Sensor Locations. (From 45th Weather Squadron 2011)

Table 1. Technical Characteristics of the NLDN and 4DLSS used at CCAFS/KCS. (After 45th Weather Squadron 2011)

	NLDN	4DLSS	
Sensor Type	Hybrid[1] (CG/CC)	Hybrid[1] (CG)	VHF/TOA (CC)
Number of Sensors	113	6	9
Sensor Spacing	200-400 km	20 km	6-10 km
Effective Range	National	100 km	111km
Lightning Detected	Cloud-to-Ground Cloud-to-Cloud	Cloud-to-Ground	Cloud-to-Cloud
Flash Detection Efficiency	90% [3] (CG) 10-30% (CC)	98% [2]	>99% (within 37 km)[5] 90% (within 111 km)[5]
Lightning Process Located	Return Stroke, Ground Stroke	Return Stroke, Ground Stroke	VHF Radiation
Locating Accuracy	~ 0.5 km[3]	0.3 km [2]	0.1-0.25 km (within 37 km)[5] <2 km (within 111 km)[5]
Locations per Flash	~ 1[3,4]	1-5	20-1000
Peak Location Rate	800 $mins^{-1}$	74 $mins^{-1}$	1100 s^{-1}
Display	Stand-alone	Stand-alone and MIDDS	Stand-alone
Source	Commercial Service	Commercial Product	Commercial Product

1. Integrated MDF/TOA technology.
2. With all six sites operational.
3. Based on most recent evaluation of system performance when using only MDF technology.
4. System typically resolves only one ground strike point per flash.
5. With all nine sites operational.

THIS PAGE INTENTIONALLY LEFT BLANK

III. DATA AND METHODOLOGY

A. DATA

1. Warning Data

The 45 WS provided data on the lightning warnings issued from January 2008 through November 2010. These data include the warning location, number, forecaster initials, Phase I issue and cancel times, Phase I begin time, Phase II issue and cancel times, lead time, timing error, Phase I total time and Phase II total time (Figure 11). Each lightning warning circle was assigned a number 1 through 13 for identification (Table 2). The decision was made to focus on the Phase II lightning warning data, as these are issued when lightning is actually occurring. There are numerous instances throughout the lightning warning logs when a Phase I lightning watch was issued, and no Phase II lightning warning followed. These Phase I watches may have been justified meteorologically. For example, a developing cumulus cell may have been expected to achieve a height such that lightning would occur, prompting the issuance of a Phase I lightning watch. Subsequently, the cell did not reach the expected height, no lightning occurred and a Phase II lightning warning was not issued. Since the lightning warning areas should be combined based on actual lightning occurrence, it was decided that the focus of this research would be on the Phase II lightning warnings. All further manipulations and calculations use only the Phase II data.

PHASE 1 & PHASE 2 LIGHTNING

FOR THE MONTH OF: **May** YEAR: **2008**

									Phase 2 # 2		Phase 2 # 3		Phase 2 # 4		Phase 2 # 5					
	LOCATION	#	FCSTR INITLS	Issue Time L (Phase 1) dd mmm yy hhmm	Begin Time L (Phase 1)	Cancel Time L (Phase 1) dd mmm yy hhmm	Time of Occurrence L (Phase 2) dd mmm yy hhmm	Cancel Time L (Phase 2) dd mmm yy hhmm	Time of Occurrence L (Phase 2) dd mmm yy hhmm	Cancel Time L (Phase 2) dd mmm yy hhmm	Time of Occurrence L (Phase 2) dd mmm yy hhmm	Cancel Time L (Phase 2) dd mmm yy hhmm	Time of Occurrence L (Phase 2) dd mmm yy hhmm	Cancel Time L (Phase 2) dd mmm yy hhmm	Time of Occurrence L (Phase 2) dd mmm yy hhmm	Cancel Time L (Phase 2) dd mmm yy hhmm	LEAD TIME	TIMING ERROR	Phase 1 Total Time	Phase 2 Total Time
8	CCAFS 40/41	05-505	MP	22-May-08 12:40		22-May-08 16:26	22-May-08 12:22	22-May-08 12:55	22-May-08 13:22	22-May-08 14:41							N/A	N/A	03:46	01:52
9	CCAFS 40/41	05-506	MP	23-May-08 14:20		23-May-08 20:00	23-May-08 17:09	23-May-08 18:25									2:43	02:19	05:40	01:16
10	CCAFS 40/41	05-507	JNF	23-May-08 22:12		24-May-08 1:15	23-May-08 22:55	23-May-08 23:30									0:43	00:13	03:03	00:35
11	CCAFS 40/41	05-508	CGW	24-May-08 13:05		24-May-08 21:00	24-May-08 17:11	24-May-08 17:51									4:06	03:36	07:55	00:40
12	CCAFS ASTROTECH	05-503	GS	19-May-08 11:52		19-May-08 16:35											N/A	N/A	04:43	00:00
13	CCAFS ASTROTECH	05-504	KJ	20-May-08 11:49		20-May-08 13:34	20-May-08 12:14	20-May-08 12:58									0:25	-0:05	01:45	00:44
14	CCAFS ASTROTECH	05-505	MP	22-May-08 12:40		22-May-08 16:28	22-May-08 13:50	22-May-08 14:41									1:10	00:40	03:48	00:51
15	CCAFS ASTROTECH	05-506	MP	23-May-08 14:20		23-May-08 20:00											N/A	N/A	05:40	00:00
16	CCAFS ASTROTECH	05-507	JNF	23-May-08 21:50		24-May-08 1:15	23-May-08 22:25	23-May-08 23:30									0:35	00:05	03:25	01:05
17	CCAFS CX 17	05-503	GS	19-May-08 11:52		19-May-08 16:35											N/A	N/A	04:43	00:00
18	CCAFS CX 17	05-505	MP	22-May-08 12:40		22-May-08 16:26	22-May-08 12:22	22-May-08 12:55	22-May-08 13:50	22-May-08 14:41							N/A	N/A	03:46	01:24
19	CCAFS CX 17	05-506	MP	23-May-08 14:20		23-May-08 20:00	23-May-08 17:09	23-May-08 18:25									2:43	02:19	05:40	01:16
20	CCAFS CX 17	05-507	JNF	23-May-08 22:35		24-May-08 1:15	23-May-08 23:00	23-May-08 23:30									0:25	-0:05	02:40	00:30
21	CCAFS CX 17	05-508	CGW	24-May-08 13:05		24-May-08 21:00	24-May-08 17:11	24-May-08 17:51									4:06	03:36	07:55	00:40
22	CCAFS CX 36/46	05-503	GS	19-May-08 11:52		19-May-08 16:35											N/A	N/A	04:43	00:00

Figure 11. Example 45 WS Phase I and Phase II lightning warning log.

Table 2. Lightning warning circle identification number and circle name.

Circle ID Number	Circle Name
1	CCAFS 40/41
2	ASTROTECH
3	CCAFS CX 17
4	CCAFS CX 36/46
5	CCAFS IA
6	CCASF ITL/20/37
7	CCAFS PORT AREA
8	HAULOVER
9	KSC 39A/B
10	KSC IA
11	KSC SLF
12	KSC VAB
13	PAFB

Further formatting of the Phase II lightning data was necessary for calculations. The data were sorted by start time and then grouped by warning circle into separate variables, creating 12 matrices containing the start and stop times of the warnings issued for each circle. After reviewing the data, four types of data entry errors were identified. Type 1 errors are duplicate warnings. Type 2 errors are warnings for a warning circle with the same start time and different end times. Type 3 errors are warnings for a warning circle with different start times and the same end time. Type 4 errors are warnings with start times that were after the end times. To correct these data entry errors, all Type 2, 3 and 4 errors were removed from the data set and one of the duplicate warnings was removed in the case of Type 1 errors.

After the data entry errors were removed, the Phase II data were converted from start and stop times for each location to a monthly matrix, W, of 12 rows (1 for each circle) by 44,640 columns (1 for each minute in a 31 day month) that contained 1s and 0s for each minute of the month such that:

$$W_{it} = \begin{Bmatrix} 1, \text{ if a Phase II lightning warning was in effect} \\ \quad \text{for circle, i, during minute, t} \\ 0, \text{ otherwise} \end{Bmatrix}$$

2. 4DLSS Data

The 4DLSS data containing LDAR-II and CGLSS lightning data (date, time and location for each strike) from May 2008 through September 2009, were used to create a matrix containing the distances from the center of each circle to each strike. For each month, a matrix, L, of 12 rows (1 for each circle) by 44640 columns (1 for each minute in a 31 day month) was created that contained 1's and 0's for each minute of the month such that:

$$L_{it} = \begin{Bmatrix} 1, \text{ if lightning occurred within 5 nm of the center of circle, i,} \\ \quad \text{in minute, t, or within the 15 minutes prior} \\ 0, \text{ otherwise} \end{Bmatrix}$$

The matrix, L, for 4DLSS data indicates a "perfect warning" scenario where there is no delay in the issuance or cancelation of the warnings and is in the same format as the Phase II warning data. The inclusion of the 15 minutes following the last lightning strike is based on the results from Stano et al. (2010) that suggested a 10 minute wait time following the last flash as a suitable end time for a Phase II lightning warning. To err on the side of safety the 45 WS implemented a minimum wait time since last flash of 15 minutes before canceling a lightning warning. Analysis of the actual warning lengths for January 2008 through November 2010 found no warnings were issued for less than 17 minutes confirming the use of a 15 minute wait time (Figure 12).

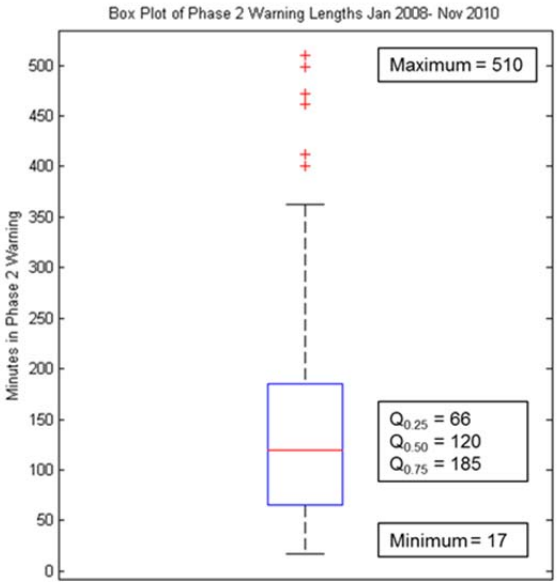

Figure 12. Boxplot of Phase 2 warning lengths for January 2008 to November 2010.

B. METHODOLOGY

1. Principal Component Analysis

From 2008 to 2010, the 45 WS issued 3,579 Phase II lightning warnings. Many of the warnings applied to individual circles overlapped temporally with one or more warnings applied to other circles during that period. The PAFB warning circle was excluded from this analysis due to its geographic separation from the CCAFS/KSC circles, different lightning pattern and different timing. This warning circle has no geographical overlap with any of the other warning circles and so it is not a prime candidate for consolidation. In addition, the barrier island at the southern tip of Merritt Island in and around PAFB is too narrow to initiate any river breeze fronts that could interact with the sea breeze front. As a result, the lightning patterns for the PAFB lightning warning area are much different than for the other lightning warning circles making it unlikely that the PAFB circle would be consolidated with any of the other areas. Even more important is that the timing of the PAFB flashes is often much different than for CCAFS/KSC, tending to occur under southwest synoptic flow (Reap (1994) Type B) and so occurs later in the day, while CCAFS/KSC gets lightning under both southwest and to a lesser degree southeast flow (Reap (1994) Type A) generating

lightning later in the day and earlier in the day, respectively. Based on this, the PAFB lightning warning circle was excluded from the analysis and so the number of warning circles in the analysis is 12, vice the total of 13 warning circles supported by 45 WS.

There are thousands of ways that 12 circles can be grouped together in combinations ranging from one to 12. Even when only evaluating pairs (two circles grouped together) or triples (three circles grouped together), the number is still high at 66 and 220 respectively for a total of 286 pair or triple combinations. From a practical standpoint, evaluating all possible combinations of circles for temporal and spatial overlap is unnecessary. Many of the possible combinations are not likely to provide significant benefit to the problem based on their location relative to each other and the nature of lightning within thunderstorms. Therefore, to reduce the number of possible combinations to be evaluated, a Principal Component Analysis (PCA) was performed to examine the co-variability of warnings among individual circles.

Principal component analysis, also commonly referred to as empirical orthogonal function (EOF) Analysis, is a useful tool when dealing with large, multivariate datasets and can potentially provide insight into the spatial and temporal variations exhibited by the field analyzed. PCA divides the data into modes that explain the most co-variability among variables, however, the modes that explain co-variability among variables are not necessarily indicative of physical variability. Subjective interpretation of the modes and data is necessary to determine if the modes are associated with physical characteristics (Bjornsson and Venegas 1997).

The first step in PCA is to organize the data as an m x n matrix, [X], where m is the number of variables and n is the number of observations in the sample. Next, the mean from each variable type is removed. The third step is to calculate the singular value decomposition (SVD) of the covariance matrix of the data. The covariance matrix is calculated as,

$$\left[\sigma^2\right]_{\mathrm{m\,x\,m}} = \left[X\right]_{\mathrm{m\,x\,n}} \left[X\right]^T_{\mathrm{n\,x\,m}}$$

where the superscript T indicates the matrix transpose. The SVD expresses the spectral decomposition of a matrix, which is analogous to Fourier decomposition. In SVD, the

eigenvalues are analogous to the Fourier amplitudes and the principal component matrix corresponds to the cosine function (Wilks 2006). The original data, x, can be reconstructed using the principal components, [PC] and EOFs, [E] such that

$$x(t) = \sum_{i=1}^{m} [PC_i][E_i]$$

The SVD is expressed as

$$[A]_{\text{m x m}} = [E]_{\text{m x m}} [\Omega]_{\text{m x m}} [E]^T_{\text{m x m}}$$

The matrix $[\Omega]_{\text{m x m}}$ is a diagonal matrix containing the variance of each column vector of [E]. The variances in $[\Omega]_{\text{m x m}}$ are ordered from largest to smallest on the diagonal and the sum of the diagonal elements is equal to the total variance of the dataset. The [E] matrix is an orthogonal matrix that contains the eigenvectors, $\mathbf{e}_k$, such that $[E] = [\boldsymbol{e_1}, \boldsymbol{e_2}, \boldsymbol{e_{e,}} \cdots \boldsymbol{e_k}]$. The number of eigenvectors is equal to the number of variables. The columns of [E] are the EOFs for the dataset. The first column is EOF 1 and contains the EOF values for each of the variables. The EOF values identify variables that vary together. As the signs of individual EOF values are arbitrary, variables with positive EOF values vary together while variables with negative values vary together, and in an opposite sense to the positive values. EOF 1 explains the greatest variance in the dataset and its associated variance is the first value listed in the $[\Omega]_{\text{m x m}}$ matrix. The percent of variance explained by each EOF is

$$\sigma_i^2 = \frac{e_i}{\sum_{i=1}^{k} e_i} \text{ x } 100\%$$

Subsequent EOFs (two and higher), identify which variables explain the most variability not already explained by previous EOFs. As PCA is a purely statistical technique, it therefore only explains how the variability is structured in the data and not why it is structured that way. This is why subjective interpretation of the modes and data is necessary to determine if the modes are associated with physical characteristics.

While each EOF mathematically explains a portion of the total variance, there is a number of EOFs beyond which the additional variance explained is no longer significant. This variance "floor" can be determined using the methods of North et al. (1982) where

EOFs with spacing of variance less than one standard deviation apart are not meaningful. The third matrix in the SVD is the transpose of [E] (Wilks 2006).

The principal components (PCs) define how each mode is represented in each sample and because the observations are ordered in time, the PCs therefore represent a time series of co-variability among the variables. The PCs are calculated by multiplying the transpose of the eigenvector matrix by the original data matrix, [X].

$$[PC]_{m \times n} = [E]^{T}_{m \times m} [X]_{m \times n}$$

The first PC is the linear combination of [X] that explains the largest variance. The second PC is a linear combination of [X] that explains the next largest variance and so on. The number of measurement types defines the number of PCs. All PCs are mutually uncorrelated in time (Wilks 2006, Bjornsson and Venegas 1997).

To gain a broad sense of the co-variability of Phase II warnings between circles, a 12 x 1098 matrix containing the number of minutes in Phase II Lightning warning per day for each circle for 2008-2010 was created using the warning data provided by the 45 WS. The mean number of minutes in warning for each day was removed, the SVD was conducted and the corresponding PCs were calculated. By examining only the daily co-variability of Phase II warnings between circles, any diurnal or shorter term co-variability was not captured.

2. Temporal Overlap Calculation

The percentage of temporal overlap gives a measure of how often warning circles were in warning together. The measurement of temporal overlap for a set of k warning circles is a ratio of the number of minutes of overlap to the number of minutes the consolidated area would be warned such that

$$\% \text{ Temporal Overlap} = \frac{O}{W}$$

where O is the number of minutes of overlap for any combination of k circles (indexed i=1,...,k) over all times, t=1,...,T:

$$O = \sum_{t=1}^{T} \prod_{i=1}^{k} L_{it}$$

and W is the length of warning for the combined area of k circles over all times, t:

$$W = \sum_{t=1}^{T} \underbrace{\left(1 - \underbrace{\prod_{i=1}^{k} (1 - L_{it})}_{\text{Indicator that combined area is not warned}} \right)}_{\text{(Equals 1 if any circle, i, is warned at time, t)}}$$

3. Alternative Warning Area Selection

To reduce the number of possible alternative warning areas, specific criteria were selected. Alternative warning area sets must:

(1) Partition all 12 circles represented (e.g., pair 1 and 5, triple 7, 8, 9 and singles 2, 3, 4, 6, 10, 11, 12),

(2) Contain only multi-circle combinations with a percent of temporal overlap greater than or equal to 66%,

(3) Be composed of combinations of singles, pairs, triples, quadruples and/or quintuples of circles, and

(4) Contain only multi-circle combinations whose component circles overlap spatially with at least one other circle in the combined area (i.e., circles 11 and 12 (SLF and VAB) could be considered, but not 7 and 8 (Port Area and Haulover)) (Figure 2).

Criterion one ensures that all areas currently supported by the 45 WS remain supported. The 66% of temporal overlap in criterion two was selected somewhat arbitrarily to limit the number of possible alternatives to a reasonable number for evaluation. In addition, 45 WS indicated that proposed combinations of lightning warning circles with a temporal overlap of about less than 90% would likely not be accepted by their customers. The much lower threshold of 66% provides a large margin of error for the uncertainty in the 45 WS estimate and allows flexibility if a somewhat lower threshold would provide significant consolidation/simplification of the lightning warning circles. Criterion three was limited to quintuples because there were no combinations of greater than five circles that also met criteria two. From an operational

standpoint, criterion four groups circles together spatially as well as temporally which provides operational simplification and ultimately the goal of this research.

4. Multi-objective Decision Analysis

Decision making in an operational setting is inherently challenging, especially when there are multiple stakeholders, time pressures and decision makers often find themselves relying on incomplete information, "gut-feelings" and/or anecdotal experience. There are many structured methods to gather and analyze stakeholder preferences that can improve decision making. Multi-objective decision analysis is one such method that allows a decision maker to consider the tradeoffs among multiple competing objectives. Kirkwood (1997) defines an essential trait of a decision as the existence of at least two alternatives from which one must be selected. The most significant decisions have alternatives with differing results. A five-step approach to decision making can provide the necessary structure to decision making (Kirkwood 1997):

> "(1) Specify objectives and scales for measuring achievement with respect to these objectives.
>
> (2) Develop alternatives that potentially might achieve the objectives.
>
> (3) Determine how well each alternative achieves each objective.
>
> (4) Consider tradeoffs among the objectives.
>
> (5) Select the alternative that, on balance, best achieves the objectives, taking into account uncertainties."

The first step in the decision making process is to determine what is important and how to measure how well alternatives perform with respect to what is important. Kirkwood (1997) sets forth a set of definitions for the various terms of multi-objective decision analysis. The "important things" in the decision process are evaluation considerations and are defined as any matters "significant enough to be taken into account while evaluating alternatives." A goal is a "threshold of achievement with respect to an evaluation consideration which is either attained or not by any alternative that is being evaluated." An objective is defined as an indication of the "preferred

direction of movement with respect to an evaluation consideration." Objectives typically use terms such as "minimize" or "maximize." Finally an attribute is defined as a "measure of performance in relation to an objective" (Kirkwood 1997).

A value hierarchy is a way to display and organize the entire set of evaluation considerations, goals, objectives and attributes for a particular decision analysis. These are often called value trees because they look like an upside-down tree. In a value hierarchy, evaluation considerations at the same distance from the top of the hierarchy create a layer or tier. Desirable properties of a value hierarchy include completeness, non-redundancy, independence, operability and small size (Kirkwood 1997).

Evaluation considerations and objectives are qualitative in nature, while attributes are quantitative and provide an unambiguous rating of how well an alternative does with respect to each objective. Attributes can be defined as natural or constructed as well as direct or proxy. Natural scales are those that are familiar to the general public with a common interpretation such as "number of fatalities." Constructed scales are developed for a particular decision problem to measure the degree of attainment of an objective. A direct scale directly measures the degree of attainment of an objective, such as profit, in dollars. A proxy scale reflects (approximates) the degree of attainment of its associated objective but does not directly measure it. Gross national product is an example of a proxy attribute for the economic well-being of a country (Kirkwood 1997).

In multi-objective decision analysis, alternatives with stronger performance with respect to one attribute will often have worse performance with respect to another attribute. In this case, trade-offs between attributes must be considered to determine which alternative is most preferred. To do this, the attributes must be combined into a single index of overall desirability of an alternative known as a multi-objective value function. This index incorporates weights and single-dimension value functions for each attribute. Assuming a linear or a directly proportional relationship between attribute values is often inaccurate. For example, an attribute value of 40 is often not twice as desirable as a value of 20. There may be a threshold above or below which any levels of the attribute are equally desirable. There may also be a threshold or region in which small changes in attribute values have large changes in desirability. To capture these

preferences, single-dimension value functions are used. One method to determine the single-dimension value functions is the Direct Rating Method. In this method, the alternatives are ranked in terms of a specific attribute from least preferred to most preferred. The least preferred alternative for this attribute is given a value of 0 while the most preferred alternative is given a value of 100. The decision maker or a subject matter expert is then asked to rate the other alternatives so that the space between the values given for each alternative represents the strength of preference for one alternative over another in terms of the attribute being evaluated. In this method, it is the interval between points on the scale that is compared. For example, an alternative, A, given a rating of 10 would indicate that an improvement from A to the attribute level of for the most preferred alternative is 9 times more important than an improvement in the attribute from the least preferred alternative to A's level (from 0 to 10). Once preference values are assigned to each alternative, they can be plotted against the actual attribute values to generate a piece-wise linear function that represents the single-dimension value function. This process is repeated for each attribute.

Weights are used to assign relative importance to attributes based on the preferences of the decision maker. Weights are conventionally determined such that they sum to 1. Many methods for determining weights are available depending on the number of attributes and level of stakeholder participation.

Using an additive model, the final multi-objective value function is:

$$v(X) = \sum_{i=1}^{n} w_i v_i(X_i)$$

where X is the entire set of attributes ($X = (X_1, X_2, \ldots X_n)$) for an alternative, w_i are the attribute weights and $v_i(X_i)$ are the single-dimension value functions.

Once the final multi-objective value function is calculated, sensitivity analysis can be conducted to examine how robust the choice of an alternative is to changes in the various model assumptions, such as the single-dimension value functions and their weights (Kirkwood 1997, Goodwin and Wright 2009). In a case where the decision maker is worried about the weight of one attribute versus another, a plot of the value of one alternative for weights ranging from 0 to 1 can quickly illustrate the alternative that

would be preferred for a given weight of one of the attributes. The sample in Figure 13 shows the value of seven alternatives in a two attribute model and their values for weights ranging from w_a=0 to w_a=1. The lines for each alternative show the value each alternative would have for each value of w_a on the x-axis. The alternative with the top-most line for any given w_a is the alternative that is best (most desirable) for that weight. In this example, A is best for weights w_a=0 to 0.272, B is best for weights w_a=0.272 to 0.667 and D is best for w_a=0.667 to 1. A similar method can be used to evaluate the sensitivity of the results to the single-dimension value functions.

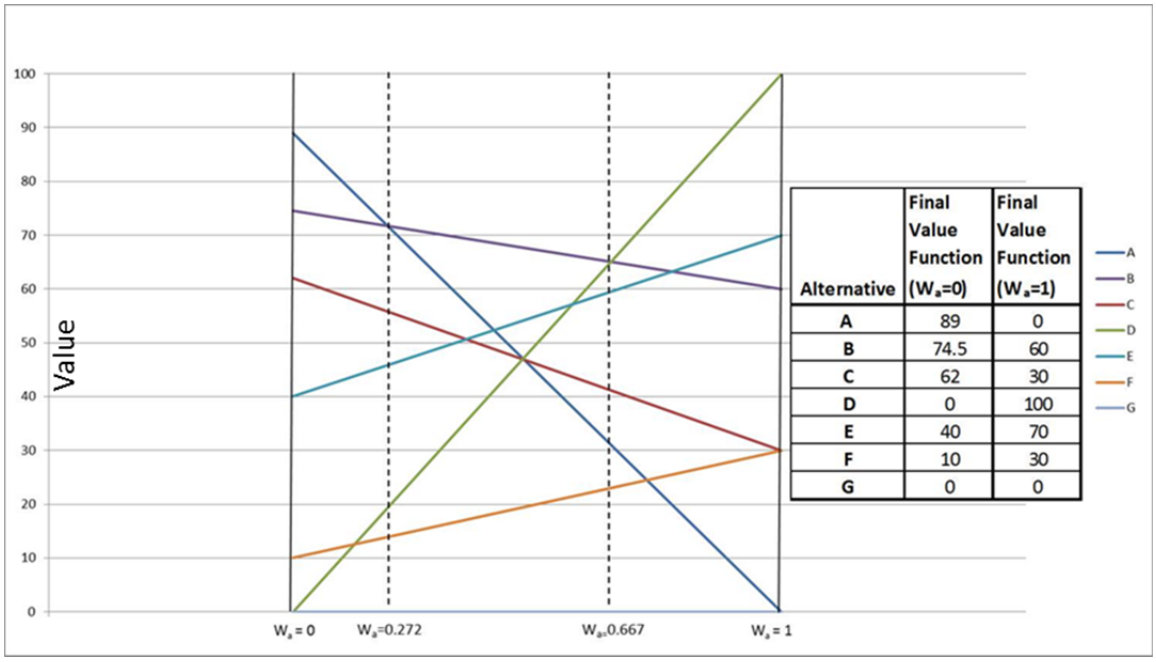

Alternative	Final Value Function (W_a=0)	Final Value Function (W_a=1)
A	89	0
B	74.5	60
C	62	30
D	0	100
E	40	70
F	10	30
G	0	0

Figure 13. Sample sensitivity analysis.

a. Attribute Selection and Calculation

The goal of this thesis is to optimize warning circles at CCAFS/KCS. The two primary groups of stakeholders in this decision and their concerns led to the selection of evaluation considerations, objectives and attributes. The first stakeholder is the 45 WS who desires an alternative that will reduce the workload while continuing to provide excellent operational support to their customers and to meet the policies and standards of Air Force Weather in issuing warnings. The second group of stakeholders is the

customers of the lightning watches and warning, who are concerned with keeping personnel and equipment safe with thunderstorms while minimizing the amount of work lost due to those watches and warnings. The two primary evaluation considerations are cost and workload. Cost is related to both man-hours to issue warnings, but primarily man-hours lost due to over-warning. Workload is primarily related to the forecasters issuing the lightning advisories. Another important factor is that the reduced workload could allow forecasters more time to analyze the changing weather and perhaps terminate lightning warnings sooner than done at present. This has the potential benefit of reducing lost work time by customers. This is important since it is known from after-the-fact analysis that the lightning warnings at CCAFS/KSC are not terminated at an optimal time due to the lack of high-skill easy-to-use guidance on forecasting lightning cessation. The improvement in terminating lightning warnings is not quantifiable and is not considered in this thesis.

A value tree was constructed based on the specific objectives to be evaluated (Kirkwood 1997) (Figure 14). The four objectives that represent the concerns of the stakeholders with respect to warning areas are shown in red. The objectives that capture the concerns of the 45 WS are the forecaster workload and meeting Air Force Weather (AFWX) standards. The objectives that capture the concerns of the customers are safe operations and the minimization of man-hours lost. The attribute for each objective is shown in green. Attribute 1 is the number of warnings issued. Attribute 2 is the amount of lead time error in the Phase I Lightning Watches. Attribute 3 is the number of minutes under-warned; personnel and/or equipment may be at risk if a warning is not issued in a timely manner. Attribute 4 is the number of minutes over-warned, because personnel are needlessly prevented from performing required tasks during over-warning.

After reviewing the attributes initially suggested by the concerns of the stakeholders and the alternative areas suggested, attribute 3 (Safe Operations) was found to not distinguish between the alternatives. Since the alternative areas suggested will maintain the 5 nm radius as required by on the Air Force Occupational Safety and Health Standard 91-66 (Department of the Air Force 1997), there is no increased risk of under-

warning for any area when compared to the current warning circles. For this reason, attribute 3 can be removed from the final value tree. While attribute 2 (Meet AFWX Standards) serves as a measure of how well the forecasters at the 45 WS meet Air Force weather standards, discussions with personnel at 45 WS indicate that workload and safety far out-weigh concerns associated with meeting the lead time standard, so lead time error can be excluded from the analysis (Roeder 2013, personal communication). Figure 15 defines the resulting final value tree.

The remaining attributes, 1 and 4, were calculated for each alternative using the LDAR data, as described in section III.A.2. For attribute 1, the number of warnings that would have been issued based on the new warnings areas in each alternative were counted. For attribute 4, the number of minutes over warned for each alternative consisting of m consolidated areas is equal to:

$$\text{Minutes Over-warned} = \sum_{n=1}^{m}\sum_{t=1}^{T}\sum_{i=1}^{k_n}\left(\underbrace{(1-L_{it})}_{=1 \text{ if, i, is not warned at time, t}} \quad S_{nt} \right)$$

where

$$S_{mt} = \begin{Bmatrix} 1, \text{ if the consolidated area, m,} \\ \quad \text{should be warned at time, t} \\ 0, \text{ otherwise} \end{Bmatrix}$$

and where m is the number of new warning areas and k_m is equal to the number of circles consolidated into warning area, m.

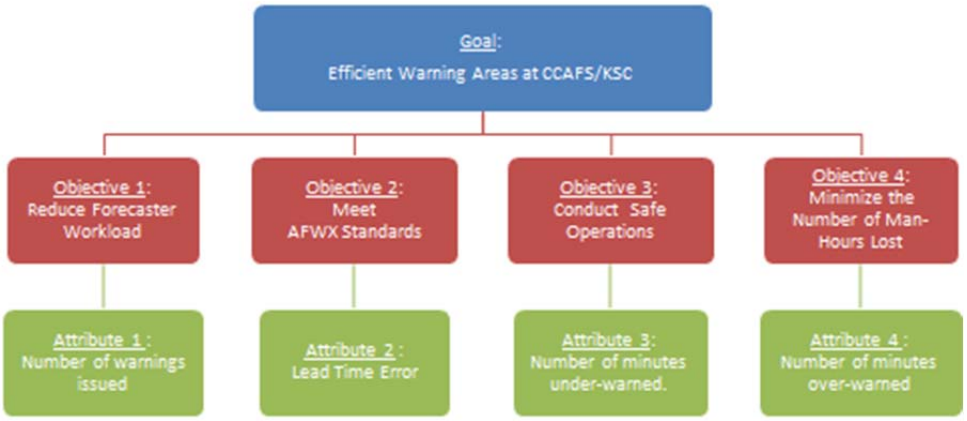

Figure 14. Initial value tree for the problem of optimizing the warning circles at CCAFS/KSC. The goal is listed in blue. Each objective is listed in the four red boxes. The attributes are listed in the green boxes.

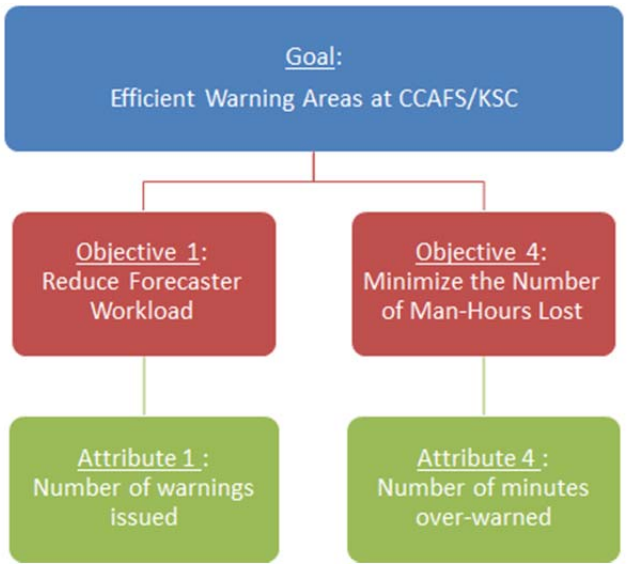

Figure 15. Initial value tree for the problem of optimizing the warning circles at CCAFS/KSC. The goal is listed in blue. Each objective is listed in the four red boxes. The attributes are listed in the green boxes.

IV. RESULTS

A. PRINCIPAL COMPONENT ANALYSIS

1. Empirical Orthogonal Functions

The Phase II lightning warnings and 4DLSS data used in this EOF analysis are minutes of warning per day for each warning circle.

a. Phase II Lightning Warnings

The amount of variance (in percentage) explained by the first six EOFs from the Principal Component Analysis of Phase II Lightning Warnings is listed in Table 3 and shown graphically in Figure 16. The resulting first six EOFs are displayed in Table 4. The lightning warning circles are ordered from north to south and color coded based on their location on either Kennedy Space Center (light blue) or Cape Canaveral Air Force Station (light green).

Table 3. Percent of variance explained by EOFs 1– 6 of Phase II Lightning Warnings for CCAFS/KSC warning circles.

EOF	Variance
1	45.2%
2	17.2%
3	14.1%
4	8.1%
5	3.8%
6	3.6%

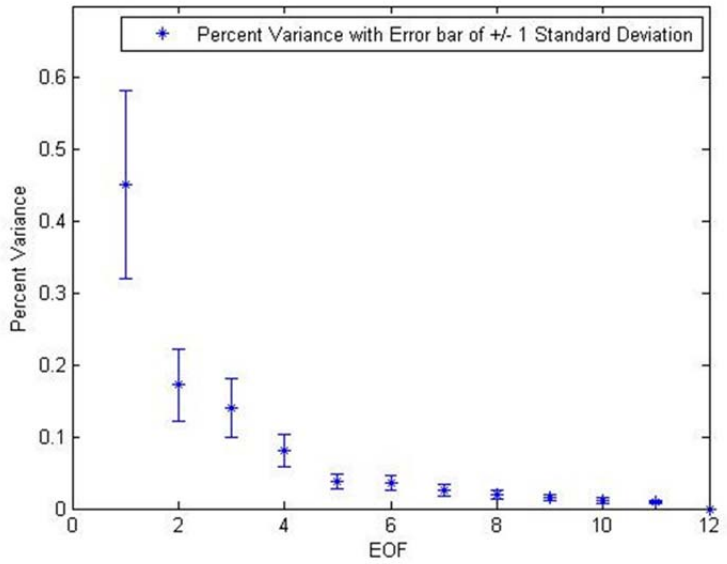

Figure 16. Percent variance explained by each EOF of the Phase II lightning warnings. Error bars are defined by +/- 1 standard deviation.

Table 4. Empirical Orthogonal Functions (EOFs) 1 – 6 of Phase II Lightning Warnings for CCAFS/KSC warning circles. Locations shaded in light blue are located on Kennedy Space Center. Locations shaded in light green are located on Cape Canaveral Air Force Station. Locations not shaded are not located on either CCAFS or KSC. EOF values with red fill and dark red text are positive values. EOF values with yellow fill and dark yellow text are negative values.

	EOF1	EOF2	EOF3	EOF4	EOF 5	EOF 6
Haulover	-0.3615	0.625493	-0.58112	-0.20108	-0.08366	0.010181
39 A/B	-0.20099	-0.33765	-0.21502	0.141958	0.604549	0.161166
SLF	-0.27838	-0.31738	-0.02964	-0.19604	-0.29191	0.185372
VAB	-0.21503	-0.39078	-0.0386	-0.14872	-0.00372	0.178663
40/41	0.126239	-0.03769	-0.21166	0.585452	0.175729	-0.20044
Astrotech	-0.47247	0.341814	0.711929	0.250554	0.068236	0.024855
KSC IA	-0.08315	-0.2784	0.098967	-0.26244	-0.31915	-0.52953
ITL/20/37	0.192039	0.013194	-0.09687	0.392644	-0.29006	-0.34937
CCAFS IA	0.2867	0.017222	0.013549	0.125023	-0.31371	0.309193
CX36/46	0.348746	0.097641	0.077799	-0.05032	-0.13289	0.373585
CX17	0.361027	0.129996	0.1358	-0.19765	0.165498	0.24666
Port Area	0.296765	0.136543	0.134879	-0.43939	0.421082	-0.41035

The first EOF, which accounts for 45.2% of the overall variability (Table 3), indicates that the KSC and Astrotech circles vary together in warning and the CCAFS circles vary together in warning. This is defined by the negative EOF values for the KSC and Astrotech circles and the positive EOF values for the CCAFS circles. In PCA, the sign of the variation is not physically meaningful, only the variables that are grouped by sign. Variables, in this case warning circles, that have the same sign will vary together and oppositely from those with the opposing sign. The EOF1 values indicate a facility-based co-variability in warning in that the northern circles (KSC/Astrotech) warn together and opposite from the southern circles (CCAFS). The amount of shading in Figure 17 indicates relative magnitude of the EOF value.

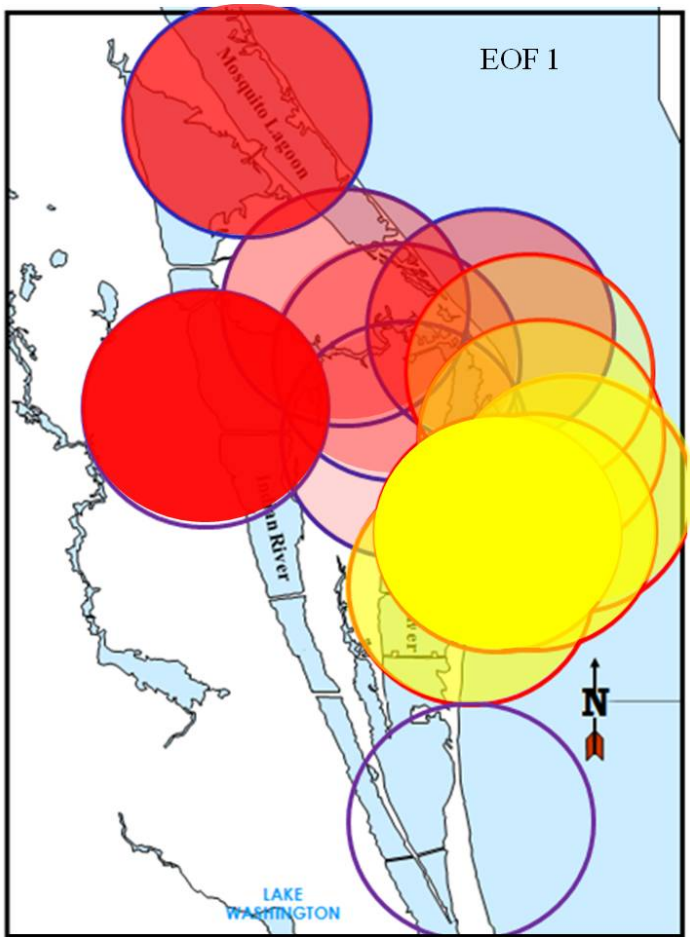

Figure 17. Values for EOF 1 of Phase II Lightning Warnings. Red shaded circles indicate negative values; yellow shaded circles indicate positive values. Level of shading indicates relative magnitude of the EOF value (more transparency indicates less magnitude).

The second EOF accounts for 17.2% of the overall variability (Table 3). Much like EOF1, there appears to be a north-south pattern of the circles in variability as four of the five KSC circles have negative values and 5 of the 6 CCAFS circles have positive values. In EOF2, the Haulover and Astrotech circles vary opposite of EOF1. These locations are relative geographical outliers from the other KSC circles, which are also centered farther to the west than the other circles. This likely accounts for the difference in variability in EOF2 as alternating EOFs must be orthogonal to each other. Complex 40/41 also varies from EOF1 in that it varies with the KSC circles. Complex 40/41 is the northern-most circle located on CCAFS and the most likely of the CCAFS circles to vary with KSC based on the apparent north-south split in variability. Additionally, in EOF2, Complex 40/41 has the smallest negative value, which indicates that it does not vary as strongly with the other negative circles. The shift from negative to positive values for the Haulover and Astrotech circles is clearly identified in Figure 18.

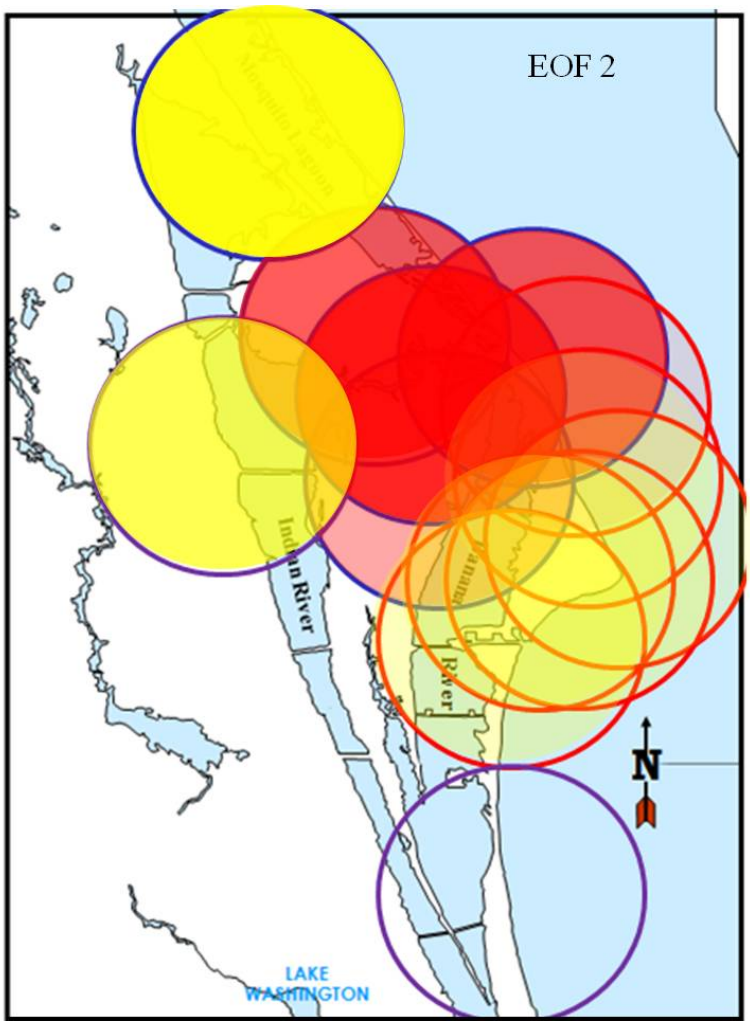

Figure 18. Values for EOF 2 of Phase II Lightning Warnings. Red shaded circles indicate negative values; yellow shaded circles indicate positive values. Level of shading indicates relative magnitude of the EOF value (more transparency indicates less magnitude).

The third EOF explains 14.1% of the overall variability (Table 3). There is again a north-south pattern in variability, however the five circles in the middle appear to vary the most from EOFs 1 and 2. The Vehicle Assembly Building (VAB) and Complex 40/41 circles are centered at the same latitude, however VAB is located inland of Complex 40/41. Astrotech, KSC Industrial Area and ITL Area/Complex 20/37 are centered at the same latitude. Astrotech is the most inland, KSC Industrial Area is located in the middle and ITL Area/Complex 20/37 is closest to the coast. Additionally, the EOF values are less than EOFs 1 and 2 as clearly seen in Figure 19.

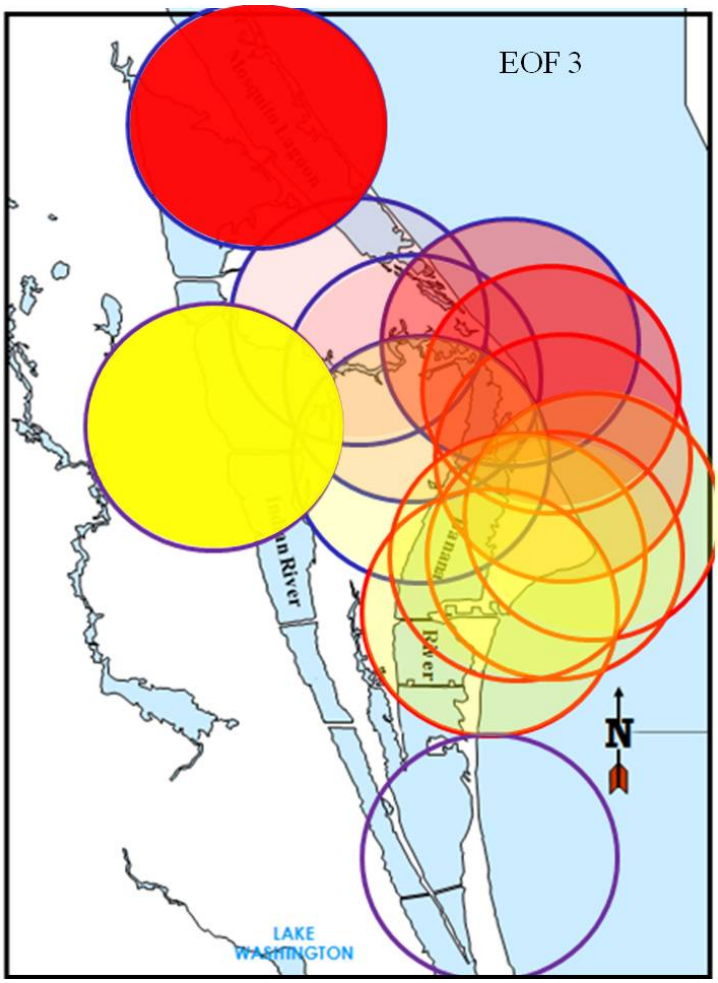

Figure 19. Values for EOF 3 of Phase II Lightning Warnings. Red shaded circles indicate negative values; yellow shaded circles indicate positive values. Level of shading indicates relative magnitude of the EOF value (more transparency indicates less magnitude).

The fourth EOF explains 8.1% of the overall variability (Table 3). There is a clear east-west pattern to the co-variability in this EOF (Figure 20).

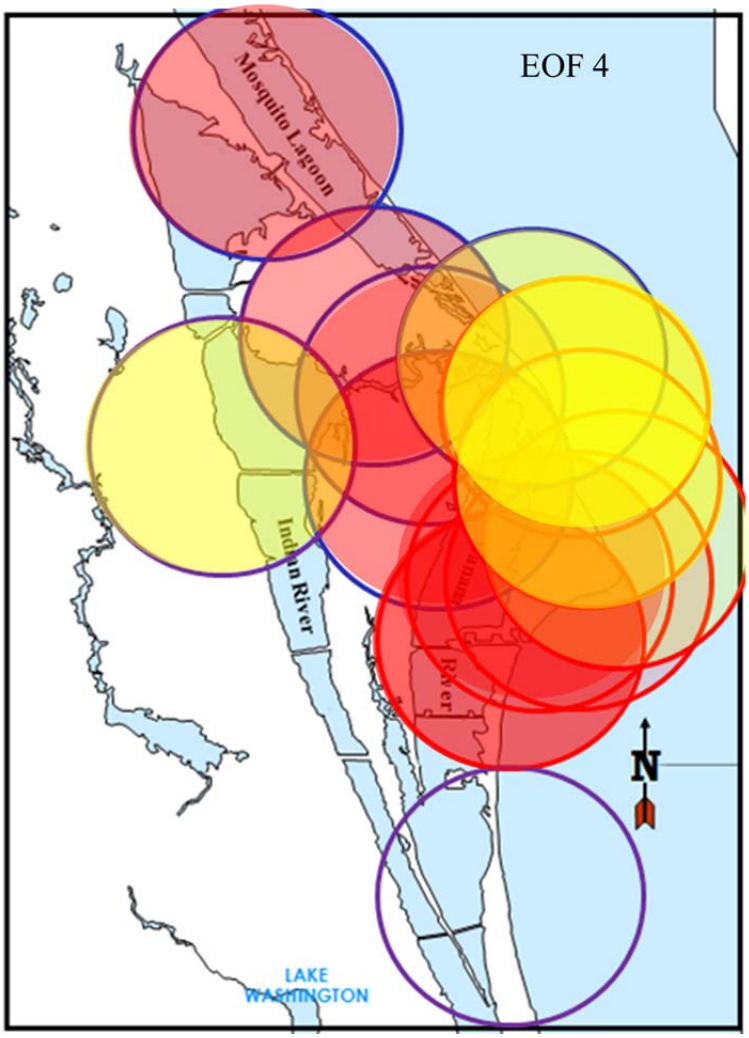

Figure 20. Values for EOF 4 of Phase II Lightning Warnings. Red shaded circles indicate negative values; yellow shaded circles indicate positive values. Level of shading indicates relative magnitude of the EOF value (more transparency indicates less magnitude).

Overall, EOFs 1 through 4 explain 84.5% of the total variability (Table 3). There is a distinct division between EOF 1 and EOFs 2, 3 and 4 and a lesser divide between EOF 4 and 5. By the methods of North et al. (1982), EOFs 5-12 are not physically meaningful as the standard deviation of EOFs 5-12 are comparable and overlap.

It is possible to associate specific weather regimes with these EOF patterns. The co-variability pattern in EOF1 could be associated with the east coast sea

breeze front and a local southeasterly flow (Reap (1994) Type A). Under this regime, the east coast sea breeze front develops along the southern portion of the Cape and pushes inland during the afternoon. The pattern defined in EOF2 can be associated with the locally coined "Merritt Island Thunderstorm Complex" which is associated with enhanced convergence of the sea breeze and river breeze, particularly at the northwest side of KSC (presumably due to the circular shape of the river bank there), leading to enhanced lightning in the northern circles with simultaneous suppressed lightning in the southeast circles. Haulover and Astrotech vary oppositely of the KSC circles, which may be a result of subsidence in that region generated by the Merritt Island Thunderstorm Complex. This pattern is consistent with a study by Laird et al. (1995) that indicates the creation and maintenance of a quasi-stationary convergence zone in this region. In EOF3, the circles with the most change in co-variability likely have the most complex warning variability due to their location relative to the Indian and Banana Rivers. The river breeze circulations associated with these bodies of water are complex and can interact to initiate and enhance thunderstorm formation at CCAFA/KSC as documented by Cetola (1997). The east-west pattern of co-variability in EOF4 may be related to southwesterly flow (Reap (1994) Type B) across the region which allows the west coast sea breeze front to propagate across the Florida peninsula with a north-south orientation.

While it is possible to associate weather regimes and patterns with these EOF patterns, caution should be used in linking the patterns strictly to meteorology because this data set has human bias when setting and canceling warnings. The pattern of co-variability in EOF1 is strongly facility based and indicates a possible human or administrative process that may be affecting the pattern. A sampling of pair and quadruple combinations shows that warnings are canceled at the same time more often than they are set at the same time (Table 5). This is indicative of a tendency of the forecasters to over-warn at the end of a warning. Reasons for this include a tendency of forecasters to err on the side of caution, errors in over-warning due to workload management during periods of increased lightning and the need for improved lightning cessation forecast techniques.

Table 5. Sampling of the percentage of identical start and stop times for pair and quadruple combinations with high temporal overlap.

Pair		% Temporal Overlap	% Start time same	% Stop Time Same
3	4	0.93	85.70	96.70
4	5	0.91	84.20	98.70
5	6	0.91	79.00	98.60
3	7	0.89	76.12	90.54
1	6	0.88	83.30	95.50
3	5	0.86	77.90	95.40
11	12	0.85	74.41	94.49
10	12	0.85	68.50	95.80
4	7	0.84	67.74	88.50
4	6	0.84	68.24	97.15
1	5	0.81	68.45	94.17
5	7	0.80	59.13	86.54
3	6	0.80	62.50	93.75
10	11	0.78	59.00	92.00
9	12	0.77	73.53	94.54
6	7	0.76	51.98	86.63
9	11	0.75	64.68	92.77
1	4	0.75	61.00	93.50
1	3	0.72	55.89	90.26

Facility	Quad				% Temporal Overlap	% Start time same	% Stop Time Same
CCAFS	3	4	5	6	0.78	45.42	70.33
KSC	9	10	11	12	0.63	34.42	61.69

b. 4DLSS Data

The 4DLSS data set (as detailed in section II.A.2) contains actual lightning strike data from May 2008 through September 2009. The amount of variance explained by the first six EOFs from the PCA of the 4DLSS Lightning Events are listed in Table 6 and displayed in Figure 21. The resulting first six EOFs from the PCA of 4DLSS Lightning Events are displayed in Table 7.

Table 6. Percent of variance explained by EOFs 1– 6 of 4DLSS Lightning Events for CCAFS/KSC warning circles.

EOF	Variance
1	54.8%
2	20.0%
3	15.1%
4	3.5%
5	2.6%
6	1.8%

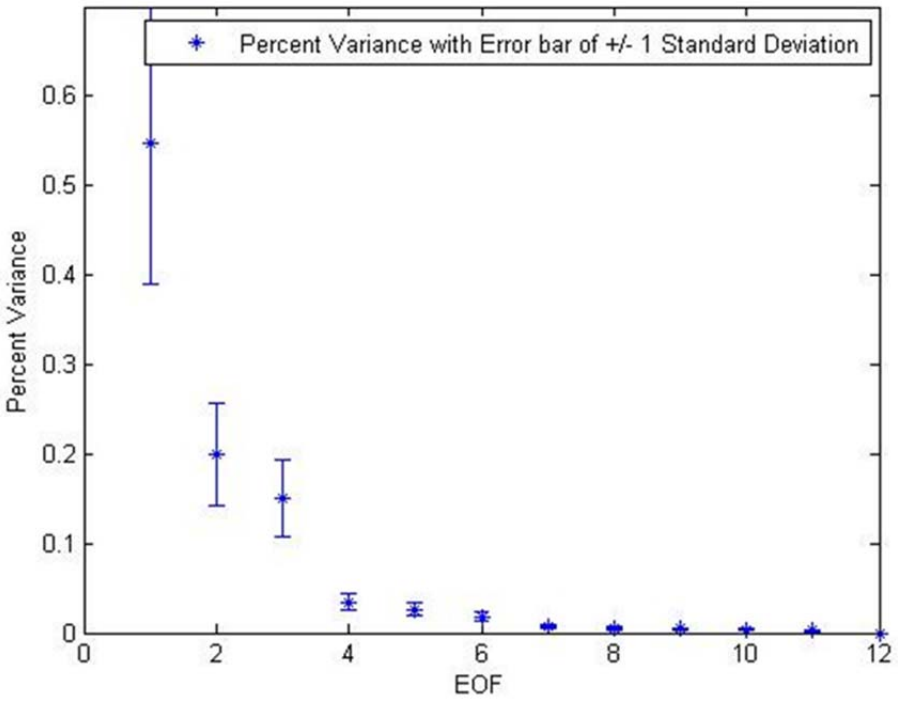

Figure 21. Percent variance explained by each EOF of the 4DLSS lightning events. Error bars are defined by +/- 1 standard deviation.

Table 7. Empirical Orthogonal Functions (EOFs) 1 – 6 of 4DLSS Lightning Events for CCAFS/KSC warning circles. Locations shaded in light blue are located on Kennedy Space Center. Locations shaded in light green are located on Cape Canaveral Air Force Station. Locations not shaded are not located on either CCAFS or KSC. EOF values with red fill and dark red text are positive values. EOF values with yellow fill and dark yellow text are negative values.

	EOF1	EOF2	EOF3	EOF4	EOF 5	EOF 6
Haulover	-0.30271	0.088569	0.098965	-0.32108	-0.18759	0.030298
39 A/B	-0.36028	-0.13567	0.047556	-0.31597	0.468516	0.06056
SLF	-0.47268	-0.13675	-0.42287	0.696756	-0.01886	0.031804
VAB	0.342045	0.550015	-0.62776	-0.15678	0.248444	0.103691
40/41	0.201822	-0.2074	0.090452	-0.01921	-0.09668	0.396642
Astrotech	-0.12	-0.06828	0.248031	-0.06846	0.454408	0.197611
KSC IA	0.07928	0.420607	0.325549	0.173678	-0.11298	-0.31651
ITL/20/37	0.244544	-0.32604	-0.01662	-0.05354	-0.02331	-0.05725
CCAFS IA	0.363894	-0.25377	-0.00533	0.076933	-0.32461	0.381743
CX36/46	0.117978	0.306556	0.466324	0.366937	0.081042	-0.00849
CX17	0.241306	-0.37871	-0.12118	-0.05463	0.089633	-0.72765
Port Area	-0.3352	0.140874	-0.08312	-0.32464	-0.57802	-0.09244

The first EOF accounts for 54.8% of the overall variability (Table 6) and indicates an almost north-south split (Figure 22) in lightning event co-variability. The three northernmost circles and the Astrotech circle vary together and inversely to the remaining circles to the south, with the exception of the CCAFS Port Area circle. The magnitude of the EOF values for the northernmost circles is similar to that of the CCAFS Port Area circle, while the Astrotech circle is less than half that of those with which it varies. The southern circles also have similar magnitude EOF values to each other and the northern circles.

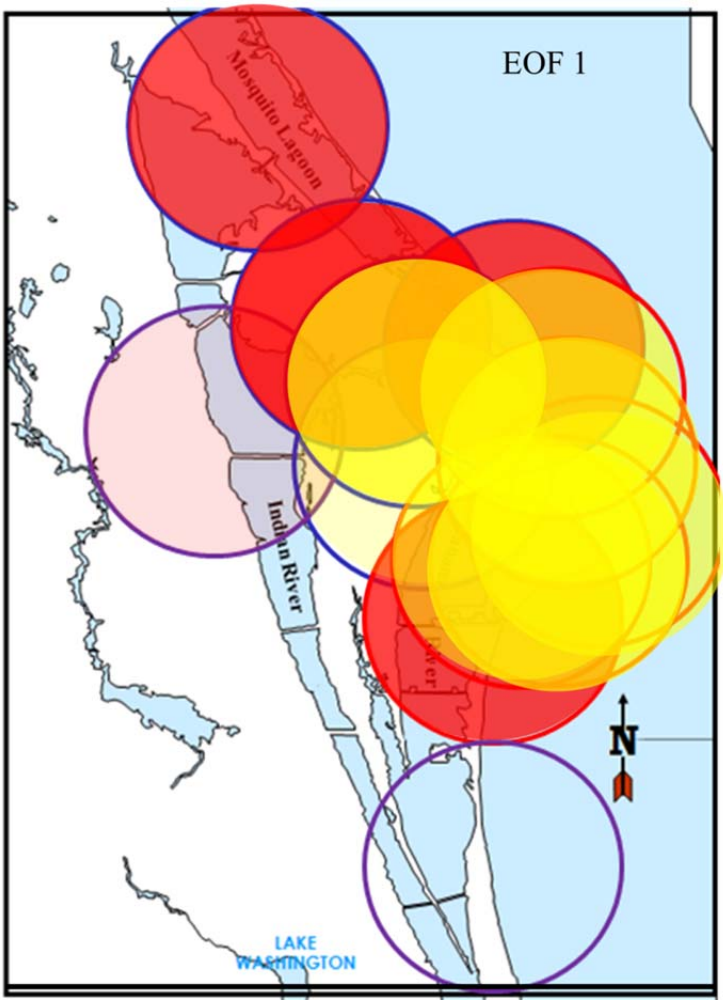

Figure 22. Values for EOF 1 for 4DLSS Lightning Events. Red shaded circles indicate negative values; yellow shaded circles indicate positive values. Level of shading indicates relative magnitude of the EOF value (more transparency indicates less magnitude).

The second EOF accounts for 20.0% of the overall variability (Table 6). As seen in Figure 23, there is a slight east-west pattern in lightning event co-variability. Given the orthogonal nature of the analysis, this is not unexpected, but it is also not as strong a signal as the north-south split in EOF, which is likely due to the lesser amount of overall variability explained by this EOF.

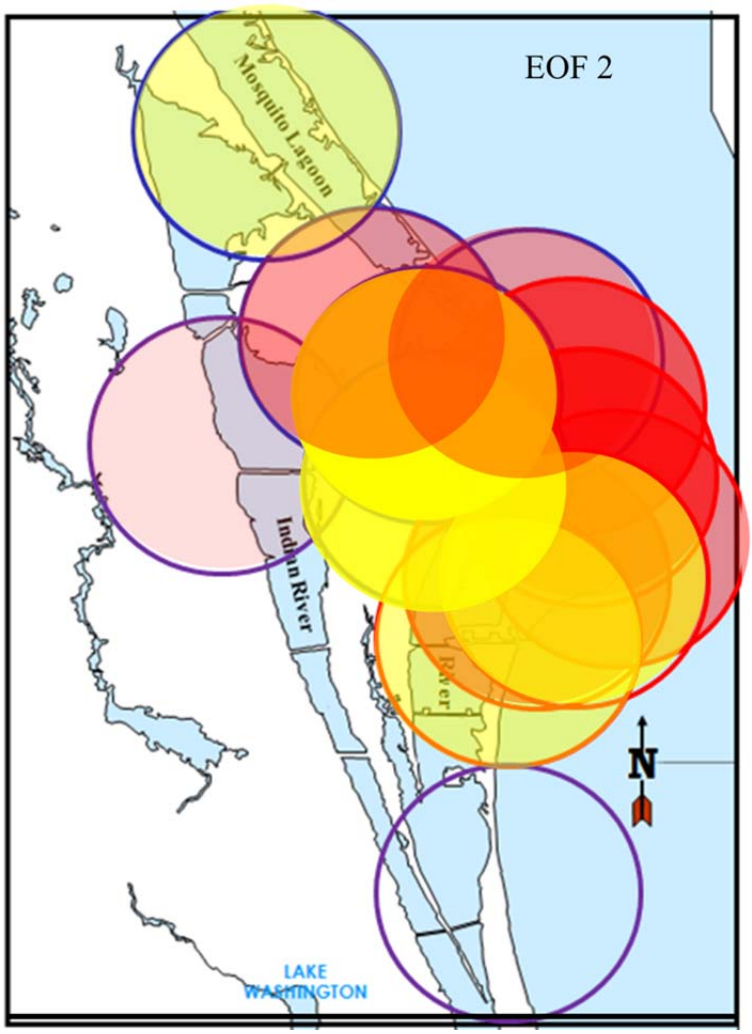

Figure 23. Values for EOF 2 for 4DLSS Lightning Events. Red shaded circles indicate negative values; yellow shaded circles indicate positive values. Level of shading indicates relative magnitude of the EOF value (more transparency indicates less magnitude).

The third EOF accounts for 15.1% of the overall variability (Table 6). There is no clear north-south split in this EOF, and the EOF has little pattern to the co-variability (Figure 24).

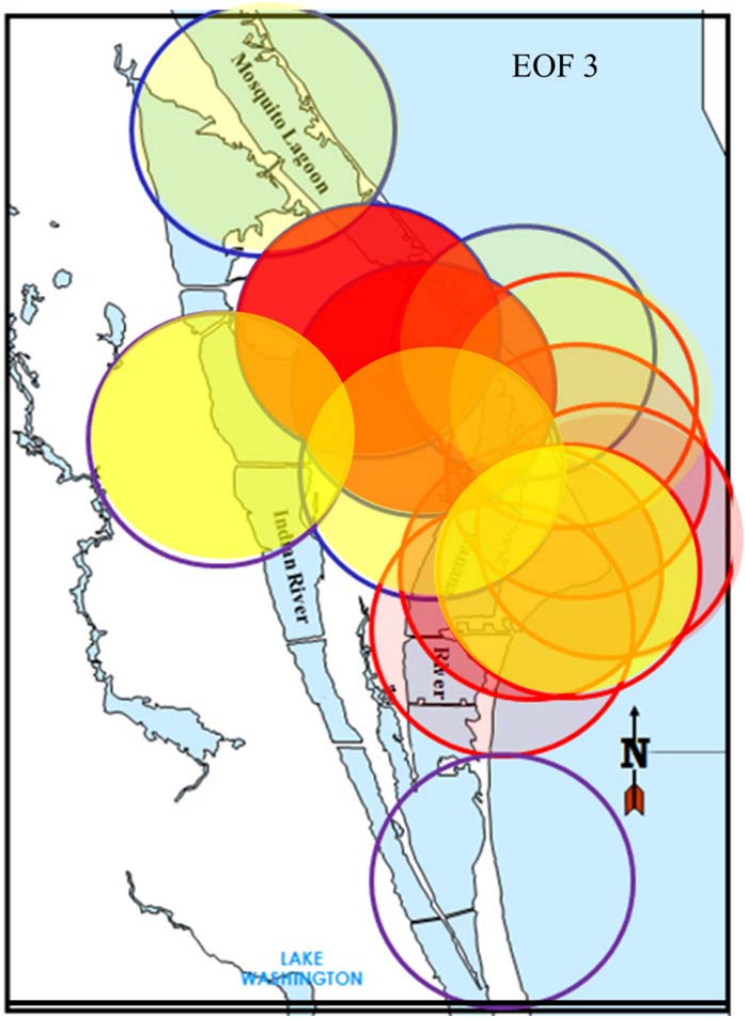

Figure 24. Values for EOF 3 for 4DLSS Lightning Events. Red shaded circles indicate negative values; yellow shaded circles indicate positive values. Level of shading indicates relative magnitude of the EOF value (more transparency indicates less magnitude).

Overall, EOFs 1 through 3 explain 89.9% of the total variability (Table 6). There is a distinct division between EOF1 and EOFs 2 and 3 followed by another distinct division between EOF 3 and 4. EOFs 4 through 12 account for a total of only 10.1% of the total variability and based on the methods of North et al. (1982), can be excluded from the analysis as not physically meaningful.

The EOFs for the 4DLSS data can be more objectively associated with flow regimes and other local weather effects than the Phase II warnings data as there is no human bias or error. In EOF1, when considering the bodies of water and their

interactions with the sea breeze fronts, this north-south split is not unexpected. The local sea breeze front often has the apparent motion of moving from southeast to northwest, which is likely due to the enhanced thunderstorm formation due to enhanced river breeze convergence at the northwest end of KSC. Over Cape Canaveral itself, the directions of the sea breeze vary considerably north or south of the point of the Cape. South of the point, the flow is often more out of the southeast. North of the point, the flow is often more out of the northeast. This is all superimposed on the general flow depending whether the subtropical ridge is north or south of the Cape. More often the ridge is to the south, which adds a southeast component to the overall sea breeze with local modifications as noted above. When the general flow is weak, the southeast and northeast sea breezes south and north of the point of the Cape lead to a convergent line bisecting the Cape from the Point inward, called the "Trailing Convergence Line." This leads to enhanced convection bisecting the Cape behind the sea breeze front itself and documented by Laird et al (1995). This can lead to a small line of Cumulus, to showers, to even thunderstorms in extreme events. In addition, while the thunderstorm enhancing vertical motion at the sea breeze front is important, the thunderstorm suppressing subsidence behind the sea breeze front is also important. When combined with the locally coined "Merritt Island Thunderstorm Complex" associated with enhanced convergence of the sea breeze and river breeze, particularly at the northwest side of KSC (presumably due to the circular shape of the river bank there), frequent enhanced lightning in the northern circles with simultaneous suppressed lightning in the southeast circles could be expected.

In EOF2, an east-west pattern in co-variability is possibly related to southwesterly flow (Reap (1994) Type B) that moves the west coast sea-breeze front across the peninsula where it merges with the east coast sea breeze front. Under this regime there is a maximum flash density just inland of Cape Canaveral.

In EOF3, the lack of obvious physical pattern that clearly explain the co-variability in this EOF may be explained by the meso- and micro-scale phenomena which can lead to thunderstorm development in this area. Small scale boundaries related to soil moisture and cloud shadows interacting with other low-level boundaries can lead to

convection and thunderstorms in patterns not clearly explained by the climatological and synoptic weather patterns.

2. Time Series Analysis of the Principal Components

a. Phase II Lightning Warnings

The resulting PC time series corresponding to EOFs 1 through 4 are plotted in Figures 25 through 28. The seasonal dependence of Phase II warnings is apparent in all four PC plots as the amplitudes (both positive and negative) increase during the summer months. The periodicity for each mode (1 through 4) is near daily, indicating that there is no strong synoptic scale forcing of the co-variability of the warnings. Table 8 lists the zero-crossings used to determine the average number of days spent in each mode. For the first four modes, the average number of days per mode is just over one day. Figure 29 depicts PC1 values for the summer months of 2008 and clearly displays the day to day oscillation in the PC values. There is no indication of long-term periodicity to the warning variability.

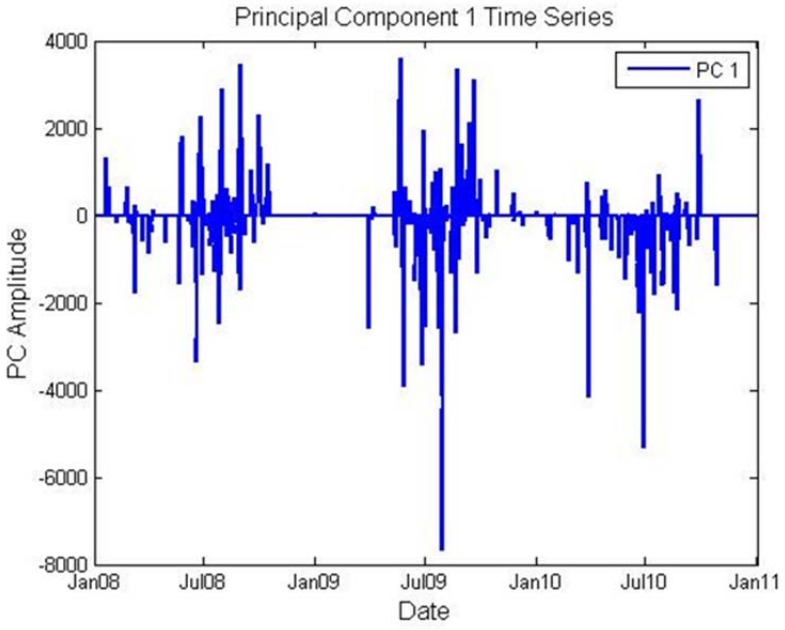

Figure 25. Phase II lightning warning principal component 1 time series.

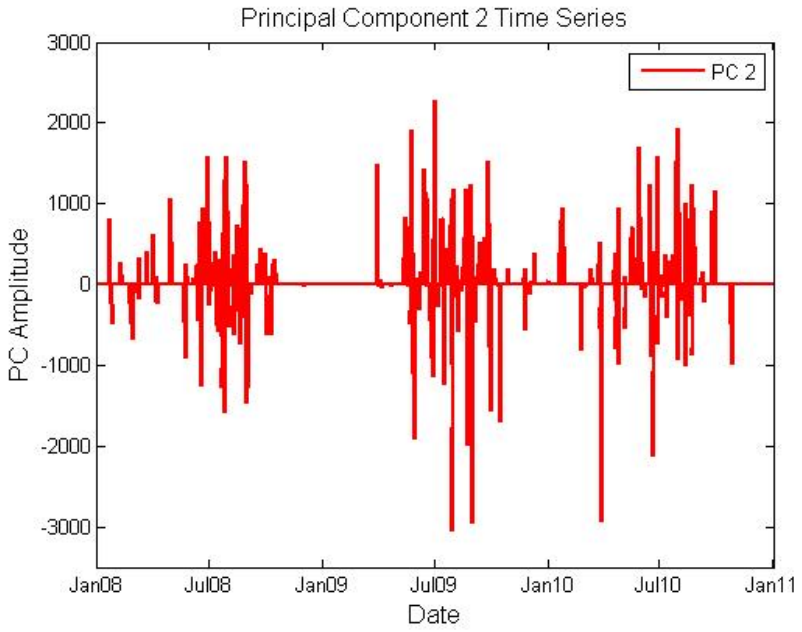

Figure 26. Phase II lightning warning principal component 2 time series.

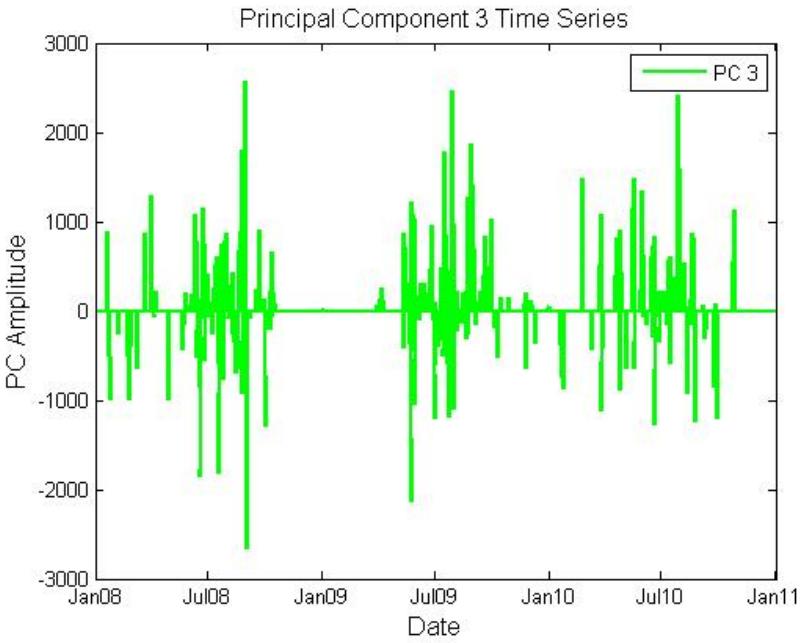

Figure 27. Phase II lightning warning principal component 3 time series.

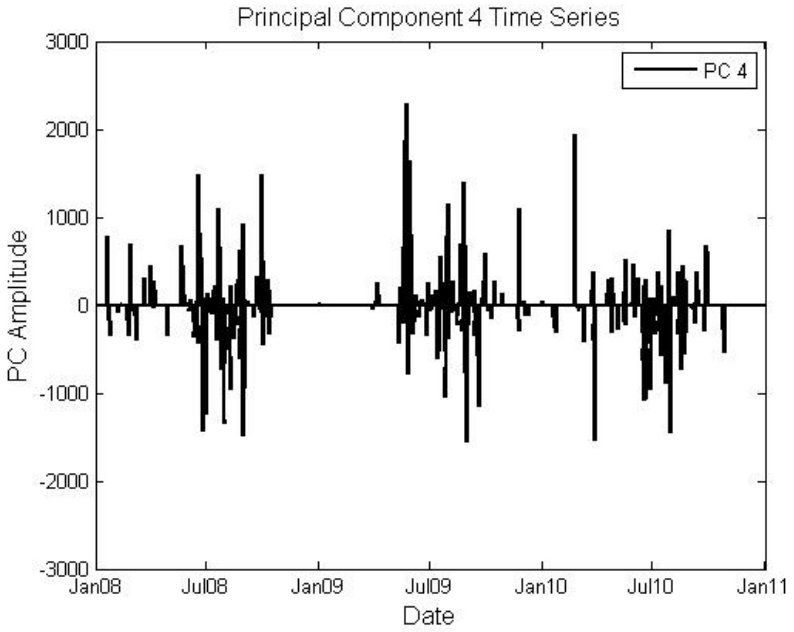

Figure 28. Phase II lightning warning principal component 4 time series.

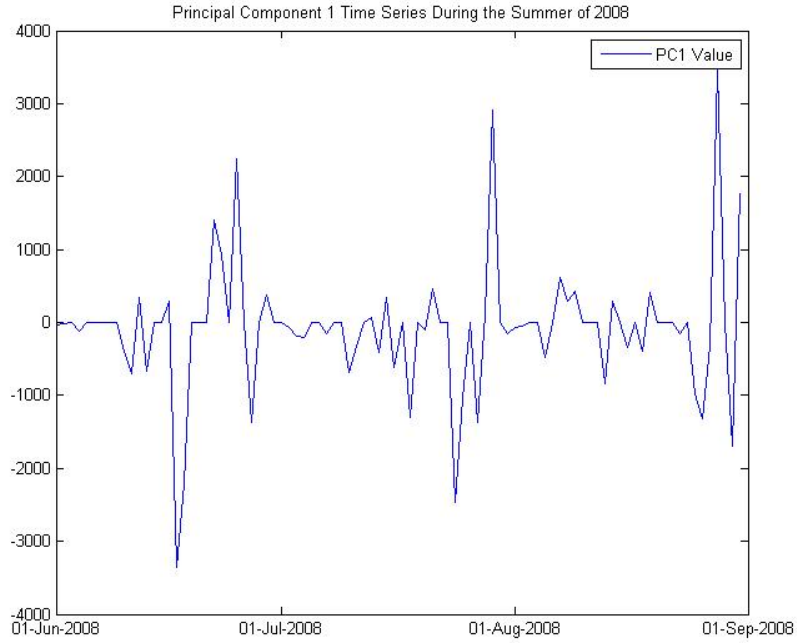

Figure 29. Phase II Lightning Warning principal component 1 time series during the summer of 2008.

Table 8. Average amount of time per mode for phase II lightning warning for PC 1 through 4.

	# Zero Crossing	# Days in Series	Avg. # Days Per Mode
PC1	1009	1098	1.09
PC2	1009	1098	1.09
PC3	1015	1098	1.08
PC4	1021	1098	1.08

b. 4DLSS Data

The resulting PC time series corresponding to EOFs 1 through 3 are plotted in Figures 30 through 32. The seasonal dependence of lightning events is apparent in all three PC plots as the amplitudes (both positive and negative) increase during the summer months. The periodicity based on zero-crossings of each mode (1 through 3) is slightly greater than daily indicating no strong synoptic scale forcing of the co-variability of the warnings. Table 9 lists the zero-crossings used to determine the average number of days spent in each mode. PC1 is highly negative with a mean value of -31.0523. PC2 is generally positive with a mean value of 3.9957. PC3 has the smallest magnitude mean value of 1.5848 and oscillates nearly equally between positive and negative amplitudes. During the summer of 2008, PCs 1 and 2 are nearly the inverse of each other; however, in November and December 2008, PCs1 and 2 are both negative (Figure 33). During the summer of 2009, PC 1 is less negative than it was during the summer of 2008 and PC 2 has similar values between the summer of 2008 and 2009 (Figure 33). Averaging the PC values during these time periods supports this observation (Table 10). Sea level pressure composite anomalies for the summer of 2008 and 2009 indicate that lower than normal pressure existed along the eastern seaboard of the United States (Figures 34 and 36). The summer of 2008 had greater pressure anomalies than the summer of 2009. The same sea level pressure composite anomalies for November to December 2008 define higher than normal pressures over the Florida peninsula (Figure 35). The synoptic difference between the summer and early winter of 2008 may account for the change in relationship between PCs 1 and 2.

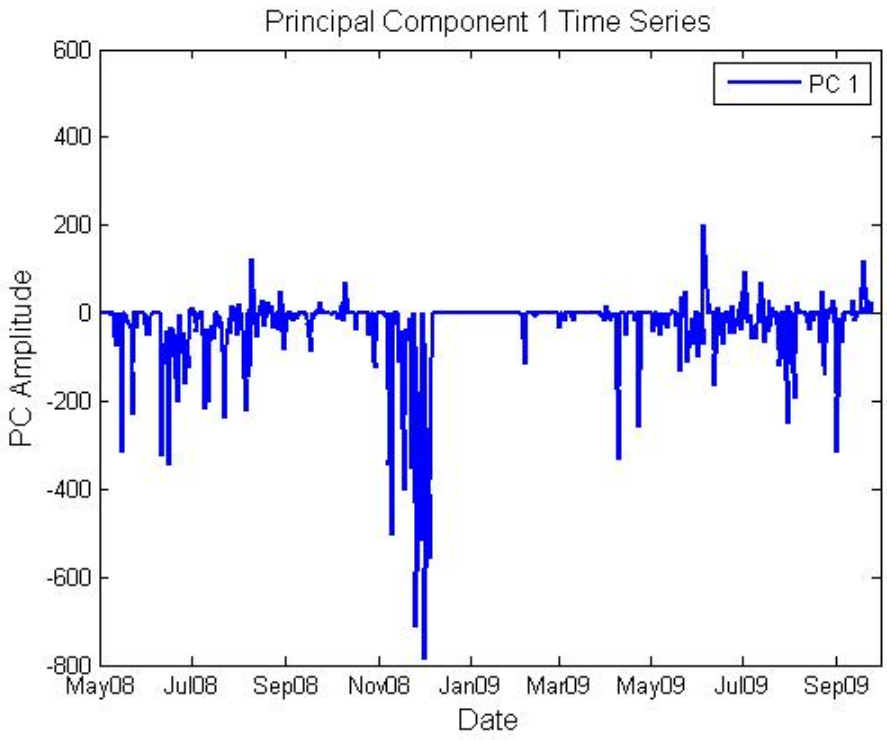

Figure 30. 4DLSS lightning event principal component 1 time series.

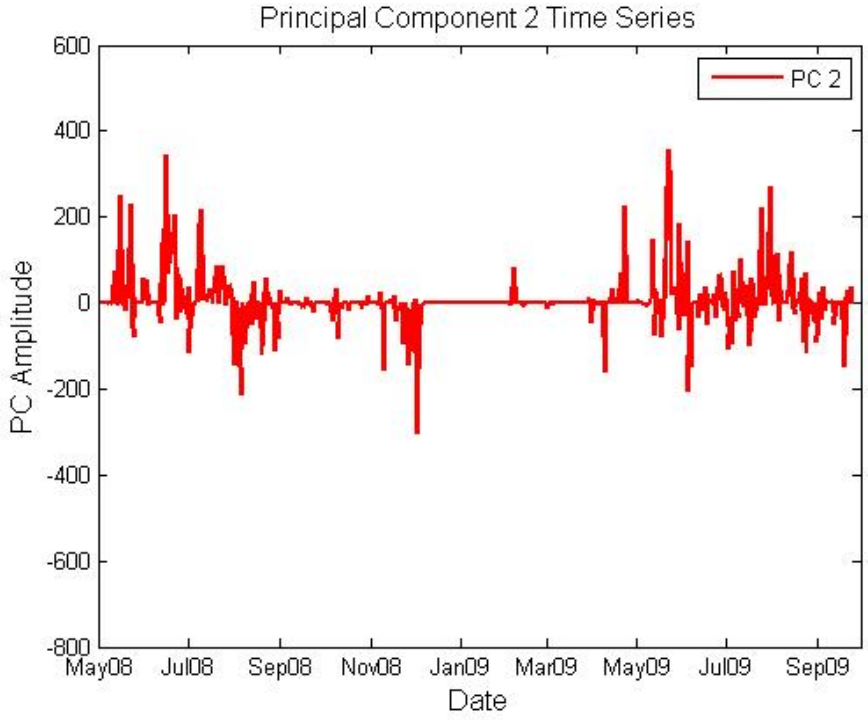

Figure 31. 4DLSS lightning event principal component 2 time series.

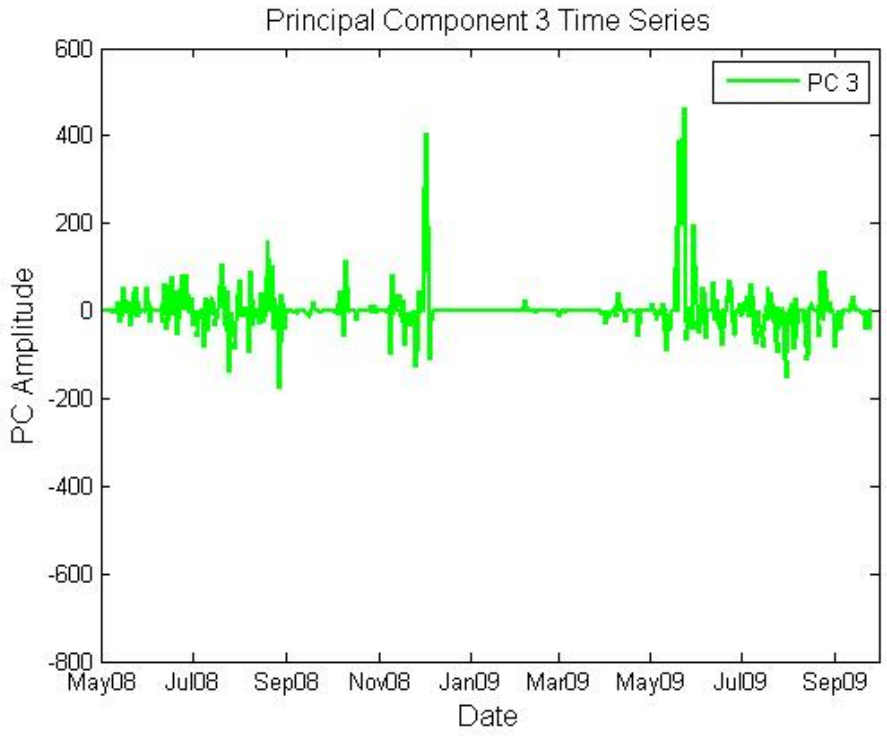

Figure 32. 4DLSS lightning event principal component 3 time series.

Table 9. Average amount of time per mode for 4DLSS lightning events for PC 1 through 3.

	# Zero Crossing	# Days in Series	Avg. # Days Per Mode
PC1	387	513	1.33
PC2	411	513	1.25
PC3	406	513	1.26

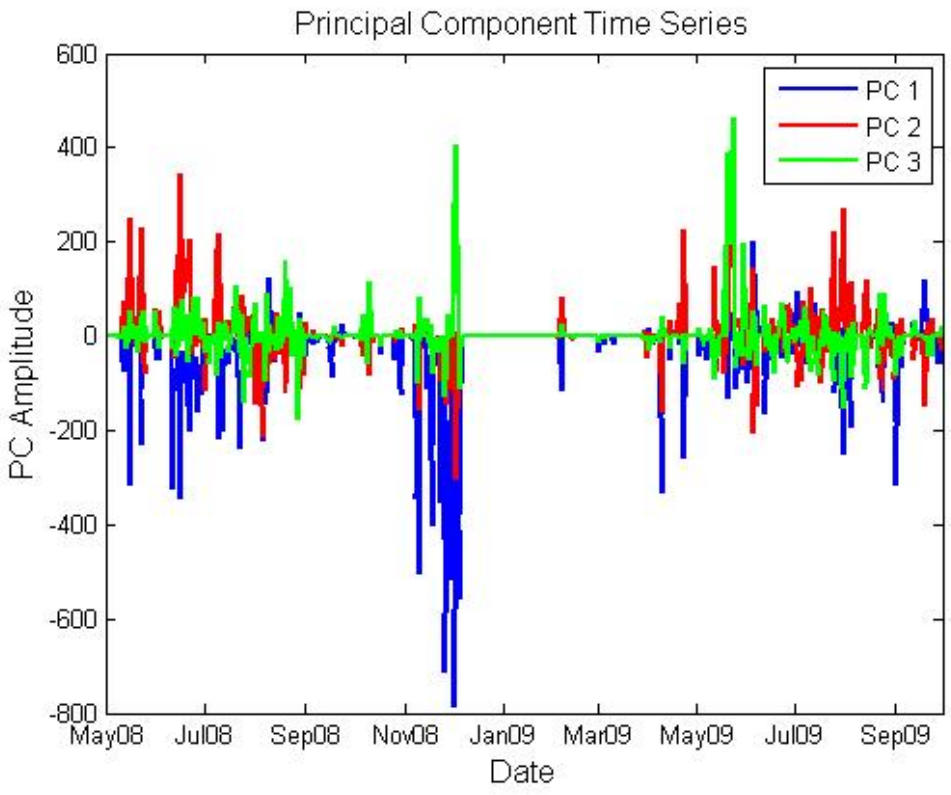

Figure 33. 4DLSS lightning event principal components1 through 3 time series.

Table 10. Mean and standard deviations of principal components 1 through 3 during summer and winter months.

	Overall			Nov08-Dec08	
	Mean	**St. Dev**		**Mean**	**St. Dev**
PC1	-31.0523	89.9955	**PC1**	-110.053	195.4863
PC2	3.9957	57.3355	**PC2**	-20.6668	57.2271
PC3	1.5848	49.9202	**PC3**	2.1312	65.7572
	May08-Sept08			**May08-Sept09**	
	Mean	**St. Dev**		**Mean**	**St. Dev**
PC1	-35.8422	69.0081	**PC1**	-17.5154	55.3298
PC2	11.6536	64.2313	**PC2**	10.1565	69.922
PC3	2.0145	40.0377	**PC3**	2.738	71.7488

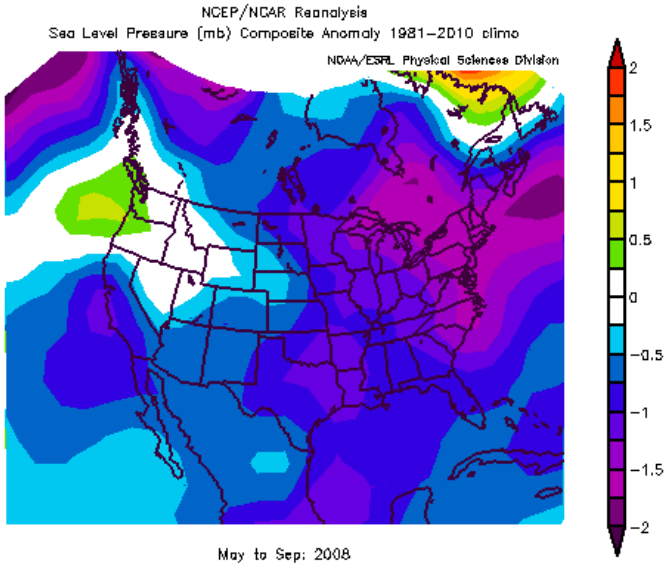

Figure 34. Sea level pressure (hPa) composite anomaly for May to September 2008. Image provided by the NOAA/ESRL Physical Sciences Division, Boulder Colorado from their Web site at http://www.esrl.noaa.gov/psd/.

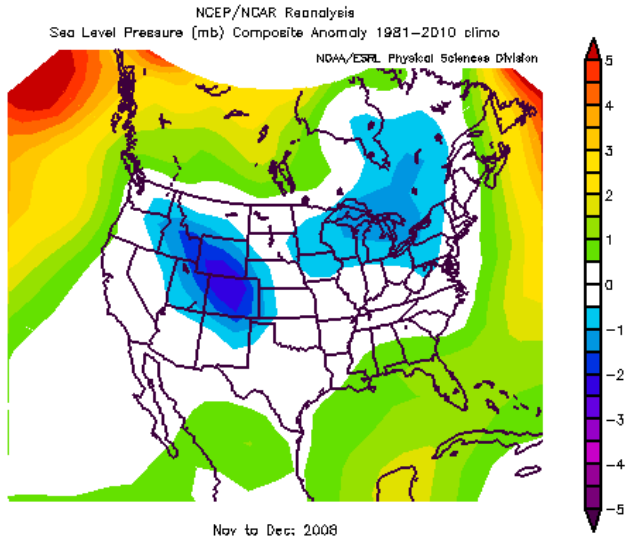

Figure 35. Sea level pressure (hPa) composite anomaly for November to December 2008. Image provided by the NOAA/ESRL Physical Sciences Division, Boulder Colorado from their Web site at http://www.esrl.noaa.gov/psd/.

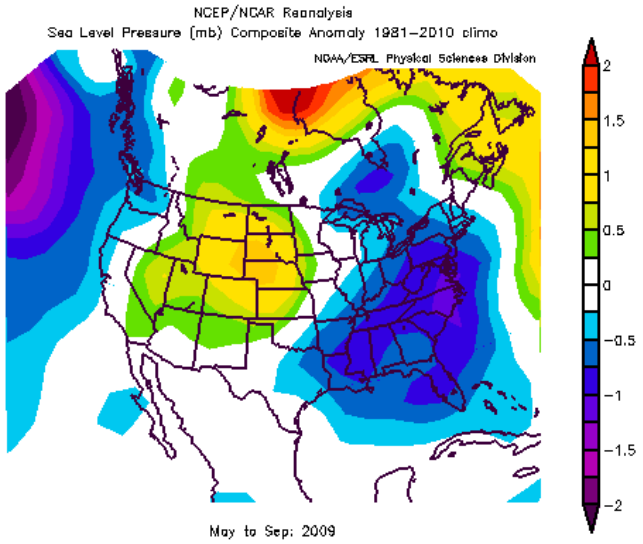

Figure 36. Sea level pressure (hPa) composite anomaly for May to September 2009. Image provided by the NOAA/ESRL Physical Sciences Division, Boulder Colorado from their Web site at http://www.esrl.noaa.gov/psd/.

3. Summary of PCA Results

Intuitively, it is easy to separate the circles based upon their location on either KSC or CCAFS. There are also meso-scale meteorological phenomena that would cause the circles to vary together with a north-south split, such as a northeast versus southeast sea-breeze front. Additionally, the 45 WS knew anecdotally that there was considerable overlap between some of the lightning warning circles, which was confirmed in the initial study conducted by Bowman (2009). However, to group these circles together based solely on these reasons would lack rigor and objectivity in analysis needed in this type of decision. By conducting a basic EOF/PC Analysis on the Phase II warning data and the 4DLSS data, it allows the data to indicate for which circles warnings are issued together as well as meteorologically which circles should have warnings issued together, providing an objective means of breaking the circles into subsets for evaluation.

a. Phase II Lightning Warnings

As expected, there is a clear grouping of the warning circles based on their location on either KSC or CCAFS. Across the first three EOFs, which collectively

account for 76.4% of the variability of the data set (Table 3), there is an overall north-south divide. The second EOF indicates east-west variability associated with the two most geographically distance circles, Haulover and Astrotech. The third EOF indicates variability among the circles located in the center, where KSC and CCAFS border each other. Additionally, the PC periodicity indicates that there is nearly daily variation in the modality of the EOF.

The north-south pattern is strongly tied to the facilities CCAFS and KSC, such that even where CCAFS and KSC circles have large spatial overlap, the co-variability in the warnings is still split by facility. Based on these results, there appears to be some bias by the forecasters to issue warnings based on the different administrative organization at each facility (Air Force for CCAFS and the National Aeronautics and Space Administration (NASA) for KSC) vice strictly meteorological events.

b. 4DLSS

The results the 4DLSS PCA show a much more complex picture of the lightning co-variability at CCAFS/KSC. The first EOF defines a similar north-south pattern in co-variability to that seen in the Phase II Lightning Warning PCA, but EOFs 2 and 3 illustrate the complexities of thunderstorm formation over CCAFS/KSC. The first EOF is clearly the dominant mode as defined by the high variance explained (54.8%). EOFs 2 and 3 each explain nearly the same amount of co-variability and are separated from EOF1 by more than 1 standard deviation. The differences in co-variability between EOFs 2 and 3, particularly in the region of overlap between the facilities illustrates that there are numerous meso- and micro-scale features which affect thunderstorm initiation and enhancement.

Identifying the differences between the results of the PCA conducted on the Phase II Warning Data and the 4DLSS data is important. The clear forecaster bias in the warnings issuance could cause an analysis of temporal overlap of only warning data to be skewed by organizational structure vice meteorological occurrence of lightning. Only using the 4DLSS data would likely lead to a more meteorologically sound analysis of temporal overlap, but forecaster and customer perceptions may lead them to distrust or

reject the 4DLSS results. Recognizing the differences in the perceived co-variability of warning circles with the actual warning circles is critical to the decision process.

B. TEMPORAL OVERLAP

1. Phase II Lightning Warnings

All pair, triple, quadruple, quintuple and sextuple combinations with a percentage of temporal overlap greater than 50% are listed in Appendix A. The combinations listed were limited to those with greater than 50% temporal overlap as these are the only combinations that overlap temporally more than not, which makes them candidates for consolidation. Various pair combinations of circles 3, 4, 5, 6, 7 and 1 had the greatest percent of temporal overlap. All of these circles are located on CCAFS. Various pair combinations of circles 11, 12 and 10 had the next highest percent of temporal overlap. These three circles are all located on KSC. There were no pair combinations that contained one circle from CCAFS and one circle from KSC with a percentage of temporal overlap greater than 70%. There were no pair combinations of circles that contained circles 2 and 8 with a percentage of temporal overlap greater than 70%.

As the number of circles in combination increases beyond pairs to triples through sextuples, the combinations with the greatest percentage of temporal overlap contain circles 3, 4, 5, 6, 7 and 1. The first triple combination containing only KSC circles is 10, 11 and 12 with a 75% temporal overlap. Other combinations of KSC circles are interspersed with triple combinations from CCAFS.

The only quadruple combination containing all KSC circles (9, 10, 11, and 12) had 63% temporal overlap. All quadruple combinations with percentage of temporal overlap between 50% and 63% contained at least one KSC circle. The first quadruple combination to contain circles located on both CCAFS and KSC contained circles 1, 6, 10, and 12 (60% temporal overlap).

Again, the quintuple combinations with the greatest percentage of temporal overlap all contain circles 3, 4, 5, 6, 7 and 1. The first two quintuple combinations to contain circles located on both CCAFS and KSC were separated by 0.1% at 56%. The first was the combination of 3, 4, 5, 6, and 10. The second was 1, 5, 6, 10 and 12. All

quintuple combinations with a percentage of temporal overlap between 50% and 56% contained at least 1 KSC circle.

The sextuple combination with the highest percentage of temporal overlap is 1, 3, 4, 5, 6 and 7 with an overlap of 64%. All other sextuple combinations between 50% and 64% contained at least one KSC circle.

2. Phase II Lightning Warnings Overlap Comparison to EOF Results

The first EOF indicated that the CCAFS and KSC circles varied together by facility, but inversely from each other. Additionally, the EOF values for the CCAFS circles were larger than those for KSC circles. The CCAFS circles, which had larger EOF1 values, had combinations (from pairs to sextuples) with higher percentages of temporal overlap than the KSC circles. As the number of circles in combination increases, the next circle added appears to be the circle with the most spatial overlap with the previous combination. Circle 1 with the least spatial overlap to the other circles at CCAFS is the last to be grouped with the CCAFS circles in combination. At KSC, circles 11 and 12 are the most spatially overlapped and have the largest magnitude EOF1 values at KSC (-0.27 and -0.21 respectively). As observed at CCAFS, as the number of circles in combination increases, the next circle added at KCS also appears to be the circle with the most spatial overlap with the previous combination. In this case, circle 10 is added in the triple combination and then circle 9 for the quadruple combination.

The second EOF indicated that circles 2 and 8 varied together as geographical outliers. Circles 2 and 8 were not among any of the highest percentages of temporal overlap. The maximum percentage of temporal overlap for either of these circles with any other circle was 56% for circles 2 and 11 and 55% for circles 8 and 11. Most likely circles 2 and 8 will remain separate and individual warning circles.

The third EOF indicated that there was increased co-variability among the circles along the borders of each of the facilities, likely associated with Indian and Banana River Breeze interaction. Circles 1 and 6 (located on CCAFS) clearly shift to vary with the KSC circles in EOF 3, however circle 10 (located on KSC) shifts to vary with the CCAFS circles. The first triple combination to include circles from both facilities is 1, 6

and 10 and the first quadruple combination to include circles from both facilities is 1, 6, 10 and 12. These circles have some shared latitudes but differ in their distance from the coast. Circles 1 and 12 share a latitude, as do 6 and 10. The shift in co-variability across facilities does not exactly match the combinations with highest percentage of temporal overlap, but it does identify the circles that will be the first to group together across facilities. Again, as the number of circles in combination increase, circles with the most spatial overlap with the previous combination are added next.

3. 4DLSS Lightning Events

All pair, triple and quadruple combinations with a percentage of temporal overlap greater than 50% are listed in Appendix B. There were no quintuple or higher order combinations with a temporal overlap greater than 50%. Various pair combinations of circles 1, 5, 3 and 6 have the greatest percent of temporal overlap. These four circles are located on CCAFS. The pair combinations of circles 7 and 8, 2 and 9, and 8 and 9, had the next highest percentages of temporal overlap, but raise questions as they are all geographically separated as pairs, with none overlapping spatially. This suggests that this level of overlap is not important and should not be considered for consolidation. In particular, is the combination of circles 7 and 8 which are the most geographically separated circles of the 12, with approximately 20 nm between the circle centers. The two circles that are geographically displaced from the rest, 2 and 8, appear in pair combinations with other circles with a percentage of temporal overlap greater than 50% eight and six times respectively.

As the number of circles in combination increases beyond pairs to triples and quadruples, the combinations with the greatest percentage of temporal overlap contain circles 1, 3, 5, and 6. The first triple combination containing KSC circles is 7, 8 and 9 with a 62.8% temporal overlap. Circle 7 is on CCAFS while circles 8 and 9 are on KSC. None of these circles overlap spatially with each other, suggesting that this level of consolidation may not be justified. Again the two circles which are geographically displaced from the rest, 2 and 8, appear in triple combinations with other circles with a percentage of temporal overlap greater than 50% twelve and eleven times respectively.

The quadruple combination with the greatest percent of temporal overlap is circles 1, 3, 5 and 6, followed closely by the combination containing circles 2, 7, 8 and 9. Only 1 additional quadruple combination had a percentage of temporal overlap greater than 50% and contained circles 1, 2, 5 and 6.

4. 4DLSS Lightning Events Overlap Comparison to EOF Results

The first EOF indicated a similar north-south split in co-variability as that seen in the Phase II Lightning Warning PCA, however it was less facility based. Circles 1, 3, 4, 5, 6, 10 and 12 vary together positively in EOF 1, and with the exception of circle 12, all appear in pair combinations with temporal overlap greater than 50%. Circles 2, 7, 8, 9 and 11 vary together negatively in EOF1 and all appear in pair combinations with temporal overlap greater than 50%. Pair combinations containing one circle from the positive and negative EOF1 groupings only occur with temporal overlap of less than 70%. As the number in combinations increase from pairs to triples and quadruples, circles with high spatial overlap have the higher percentages of temporal overlap. Specifically, circles 1, 3, 5 and 6 (southern circles) and 2, 7, 8 and 9 (northern circles, plus Port Area) group together in triple and quadruple combinations. EOF1, which explained 54.8% of the co-variability, dominates the temporal overlap groupings.

The second EOF indicated an east-west split in the co-variability while EOF3 lacked a clear pattern in the co-variability. A comparison of the circles that warn together across all three EOFs, inducates that circles 3, 5, and 6 consistently vary together as do circles 4 and 10. In EOF1, these five circles vary together, while in EOFs 2 and 3, circles 3, 5 and 6 vary together positively while circles 4 and 10 vary together negatively. Of the combinations with temporal overlap greater than 50%, combinations including these 5 circles have the greatest amount of spatial overlap. Other combinations with high temporal overlap that are grouped in at least 2 EOFs have little or no spatial overlap, making their operational consolidation unlikely. Combinations that fall into this category are any that include 2 or 8 and also where 7 is in combination with 9 and 10.

C. ALTERNATIVES

Based on the 4DLSS temporal overlap percentage results, five pairs and one triple combination met the alternative criteria of having temporal overlap greater than or equal to 66% and spatially overlap (see section II.B.4., criteria 1 and 3.) The circles that make up these combinations are also those that varied together in all three EOFs and are listed in Table 11. Using these combinations, and using the previously defined criteria for alternatives (section II.B.4.), 13 alternative warning area sets were identified, labeled A through M, and listed in Table 12. These 13 alternative warning area sets were created using the 4DLSS temporal overlap percentage results to eliminate the human bias exhibited in the Phase II warning data and link the warning areas strictly by meteorology. Three additional facility based alternatives, labeled N through P and a status quo alternative were also created to provide a more complete set of alternatives for consideration based on the temporal overlaps of warnings issued and the perceived co-variability of warning circles by the forecasters.

Table 13 contains the attributes for each of these alternatives. The values in the first two columns are summed over the entire data period of May 2008 through September 2009. The values in the second two columns are the average attribute values for days when warnings would be issued (i.e., days when lightning occurred in one or more warning circles). The attributes values summed over the entire 18 month period were difficult to interpret and understand. For example, how meaningful over 18 months is the difference between 5,841 warnings and 4,728 warnings? To make the attribute numbers more meaningful, they were averaged over the number of days when lightning occurred in one or more warning circles. This yielded a much more meaningful number to interpret, 22 vs. 18 warnings in a day. Figure 37 is a plot of the average number of minutes over-warned versus average number of warnings on days when warnings would be issued for all alternatives. A pattern in the grouping of alternatives exists. There are three clusters near the top left. The alternatives in cluster 1 all contain one pair of circles and 10 single circles. The alternatives in cluster 2 (with the exception of L) contain two pairs of circles and eight single circles. Alternative L contains one triple set of circles and nine singles. The alternatives in cluster 3 contain alternative M which consists of one

triple, one pair and seven single circles and alternative K which contains three pairs of circles and six single circles. The three facility-based alternatives are in the bottom half of the figure and are clearly separated from each other and the three clusters at the top.

Clusters 1 to 3 (Figure 38) spread out at a smaller scale than is seen in Figure 37. An Efficient Frontier, or subset of alternatives consisting of all alternatives not dominated by another alternative, appears along a line from alternative A to F to K with each of these 3 alternatives at least slightly dominating the other alternatives within their grouping (Kirkwood 1997). Figures 39-42 define how the warm season dominates this chart. Patterns from the warm seasons in 2008, 2009 and the composite warm season are the same as the overall pattern of alternatives. The spread of the number of warnings issued is greater in 2008 than 2009. Analysis of the 500 hPa geopotential height anomalies for the warm seasons of 2008 and 2009 and the PNA Index show a clear positive phase of the Pacific-North American teleconnection pattern (PNA) for the entirety of the 2009 warm season (Figures 43-45). The positive phase of the PNA pattern features above-average heights in the vicinity of Hawaii and over the intermountain region of North America, and below-average heights located south of the Aleutian Islands and over the southeastern United States. The positive phase of the PNA pattern is associated with below average temperatures across the south-central and southeastern United States. Summer (Climate Prediction Center 2013a). The cool season shows greater spread among the alternatives, but the total number of warnings for the cool season versus either warm season is significantly less (only 15-20% of total warnings in a year).

Table 11. 4DLSS Combinations having a percent of temporal overlap greater than or equal to 66% and overlap spatially.

Pairs		
Combination		% Overlap
1	5	82.07%
5	6	79.42%
3	6	76.84%
4	10	74.91%
1	6	74.69%

Triples			
Combination			% Overlap
1	5	6	69.68%

Table 12. Alterative Warning Areas. Orange boxes contain pairs of circles to be combined. Red boxes contain triples of circles to be combined. Yellow boxes contain circles which will not be combined.

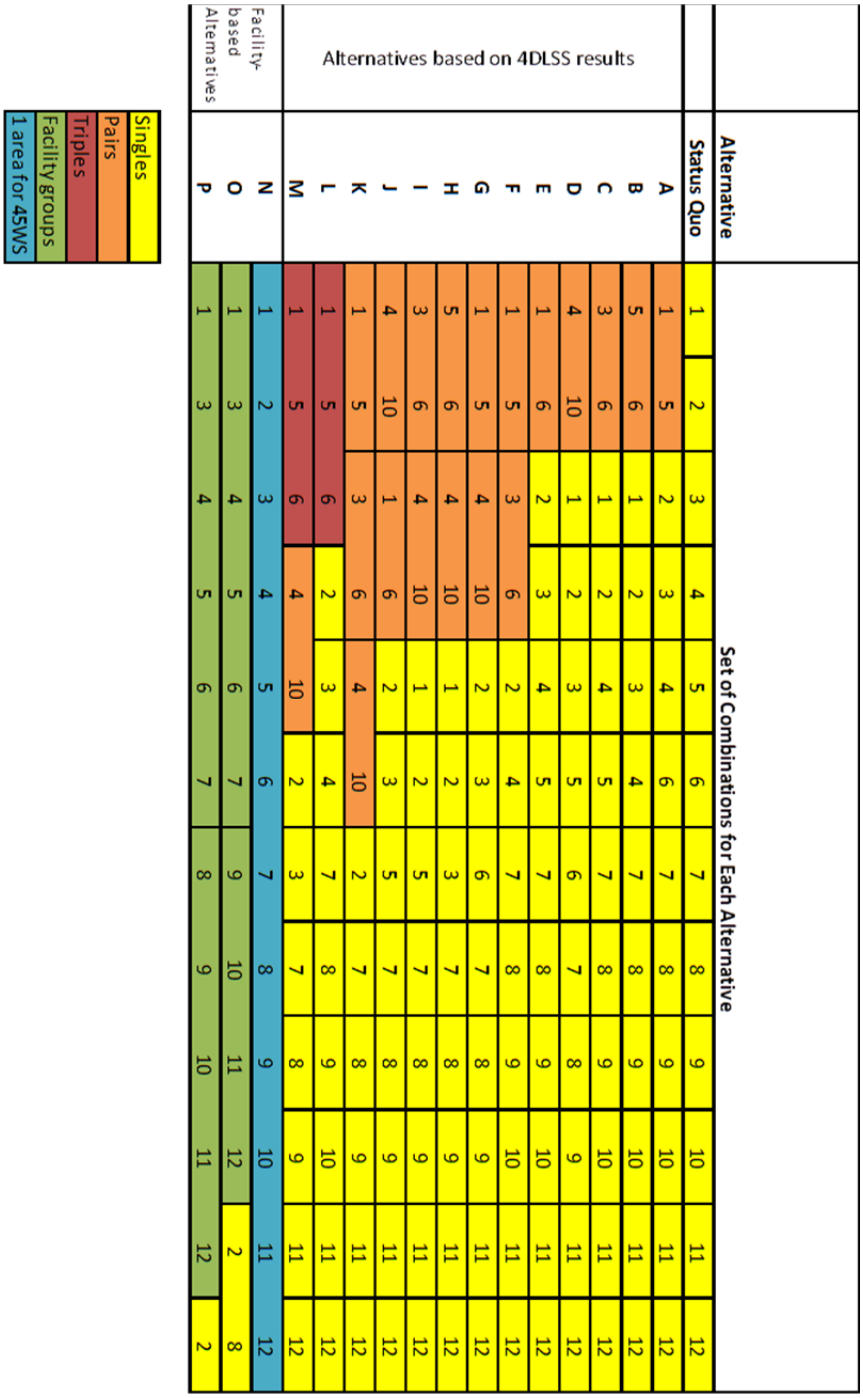

Table 13. Attribute measures of effectiveness for the alternative warning areas.

Alternative	Minutes Overwarned	Number of Warnings	Average Minutes Overwarned on Days Warnings Issued	Average Num of Warnings on Days Warnings Issued
StatusQuo	0	5841	0.00	22.29
A	4076	5512	15.55	21.89
B	4222	5511	16.11	21.89
C	4847	5482	18.5	21.79
D	6538	5432	24.95	21.58
E	5252	5473	20.05	21.75
F	8923	5153	34.06	20.47
G	10614	5103	40.51	20.27
H	10760	5102	41.07	20.26
I	11385	5073	43.45	20.16
J	11790	5064	45	20.12
K	15461	4744	59.01	18.85
L	9636	5137	36.78	20.41
M	16174	4728	61.73	18.78
N	211568	911	807.51	3.63
O	93899	2745	281.13	7.99
P	111025	2158	342.67	6.95

Figure 37. Average number of minutes over-warned versus average number of warnings on days when warnings were issued for the alternatives.

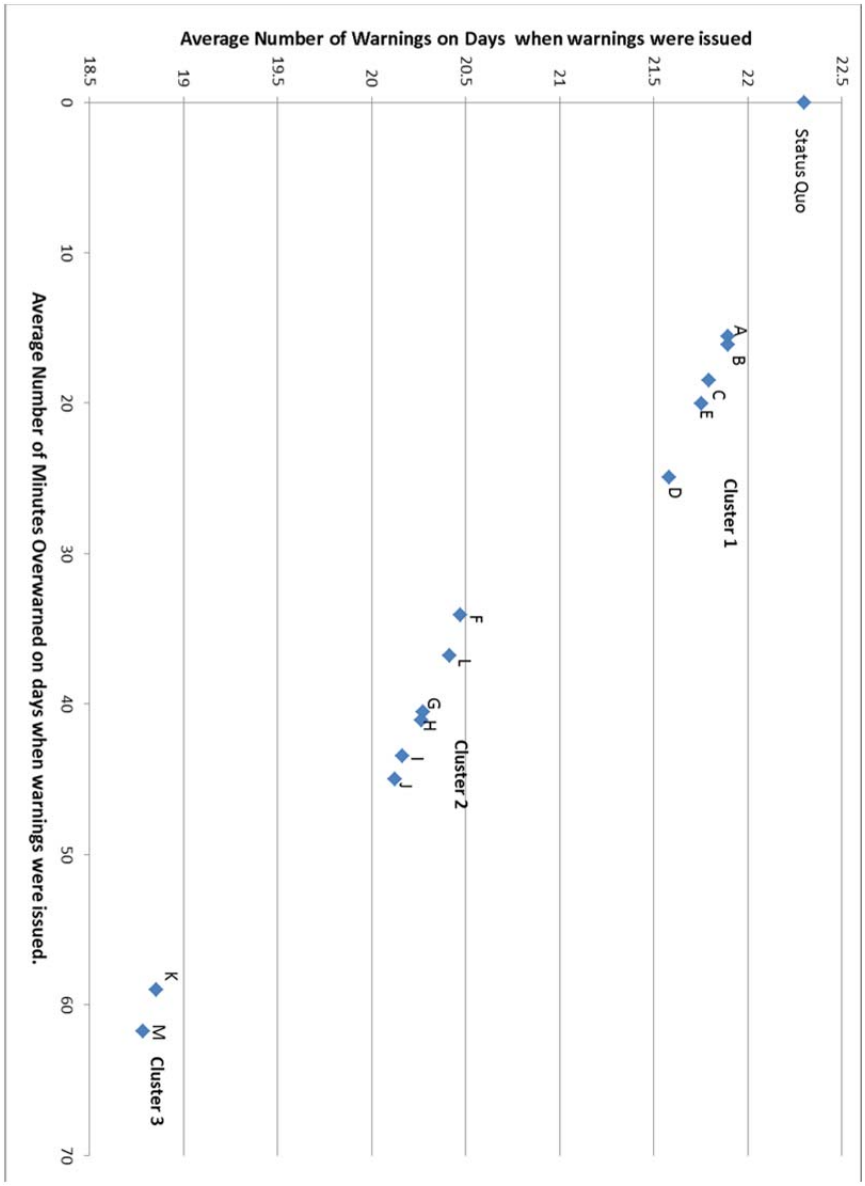

Figure 38. Average number of minutes over-warned versus average number of warnings on days when warnings were issued for the status quo and alternatives in clusters 1 to 3.

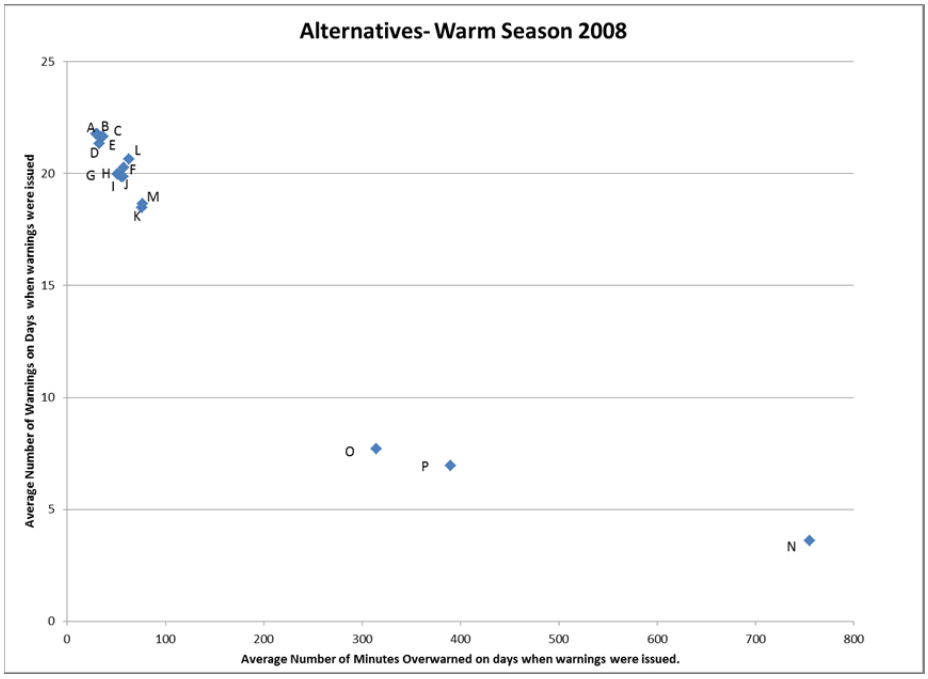

Figure 39. Number of minutes over-warned versus number of warnings during the warm season 2008. The warm season is defined as May through September.

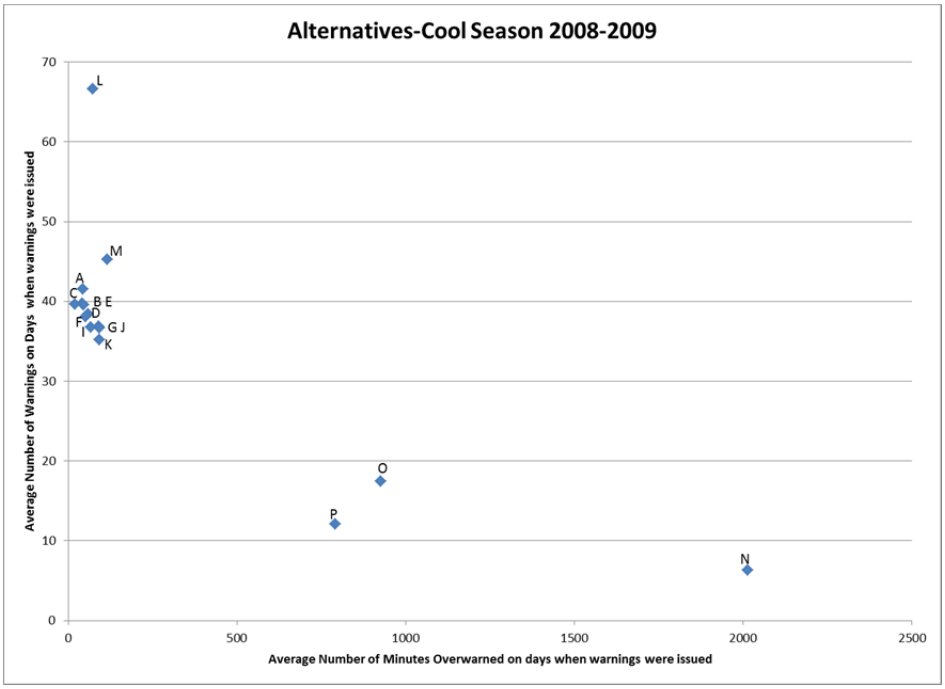

Figure 40. Number of minutes over-warned versus number of during the cool season 2008-2009. The cool season is defined as December through February.

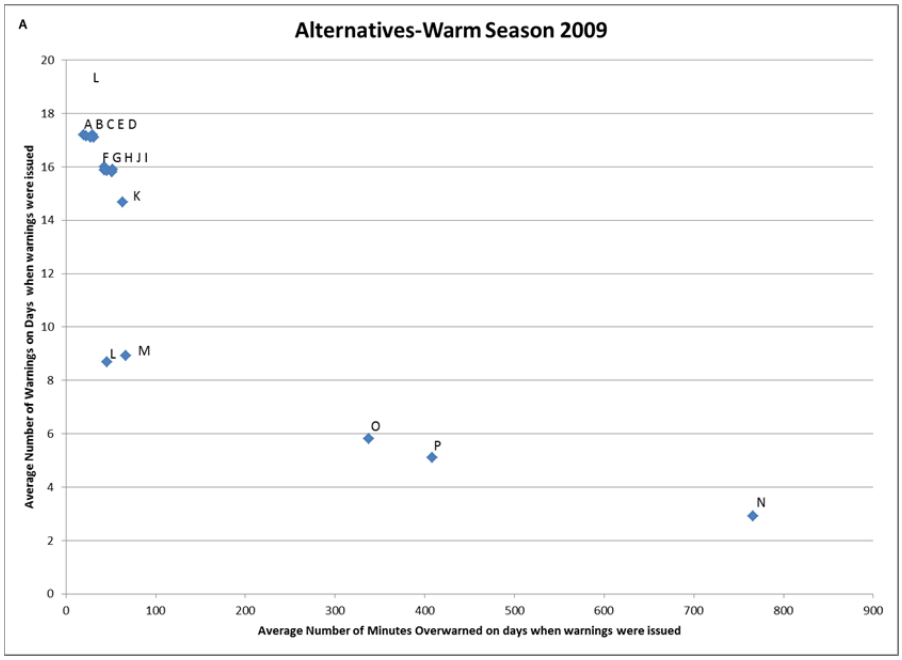

Figure 41. Number of minutes over-warned versus number of warnings during the warm season 2009. The warm season is defined as May through September.

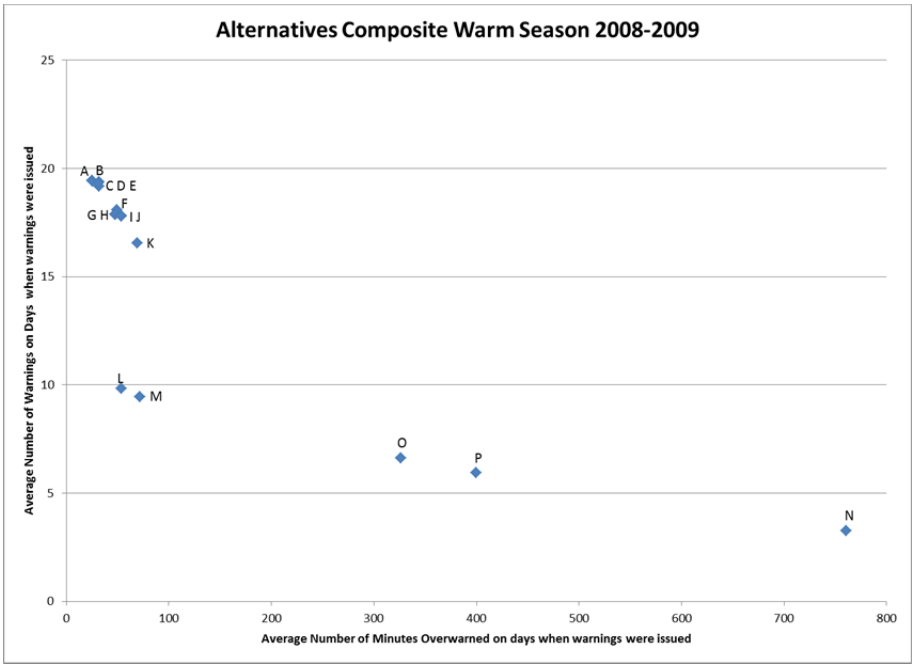

Figure 42. Number of minutes over-warned versus number of warnings during the warm seasons of 2008 and 2009. The warm season is defined as May through September.

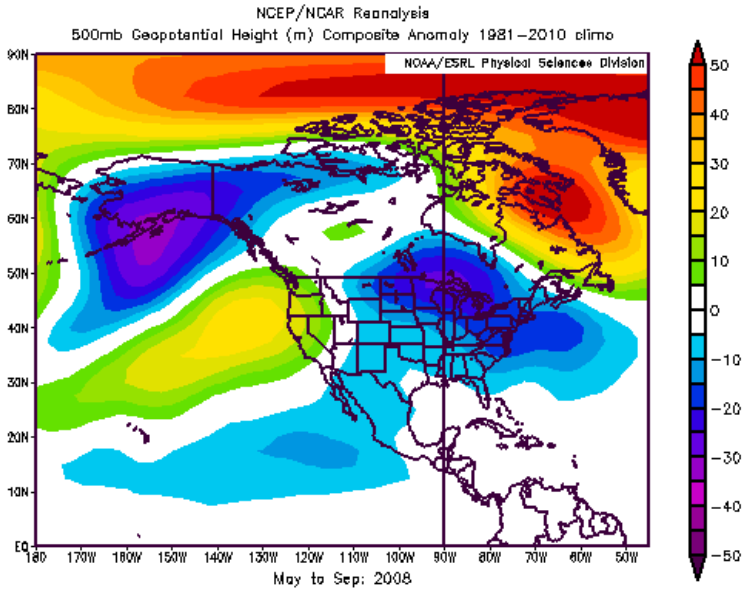

Figure 43. 500 hPa geopotential height anomalies May to September 2008. Image provided by the NOAA/ESRL Physical Sciences Division, Boulder Colorado from their Web site at http://www.esrl.noaa.gov/psd/.

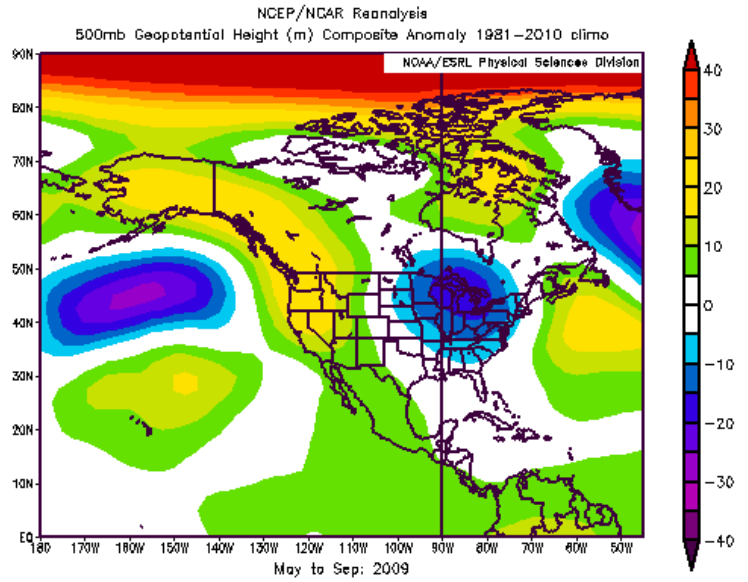

Figure 44. 500 hPa geopotential height anomalies May to September 2009. Image provided by the NOAA/ESRL Physical Sciences Division, Boulder Colorado from their Web site at http://www.esrl.noaa.gov/psd/.

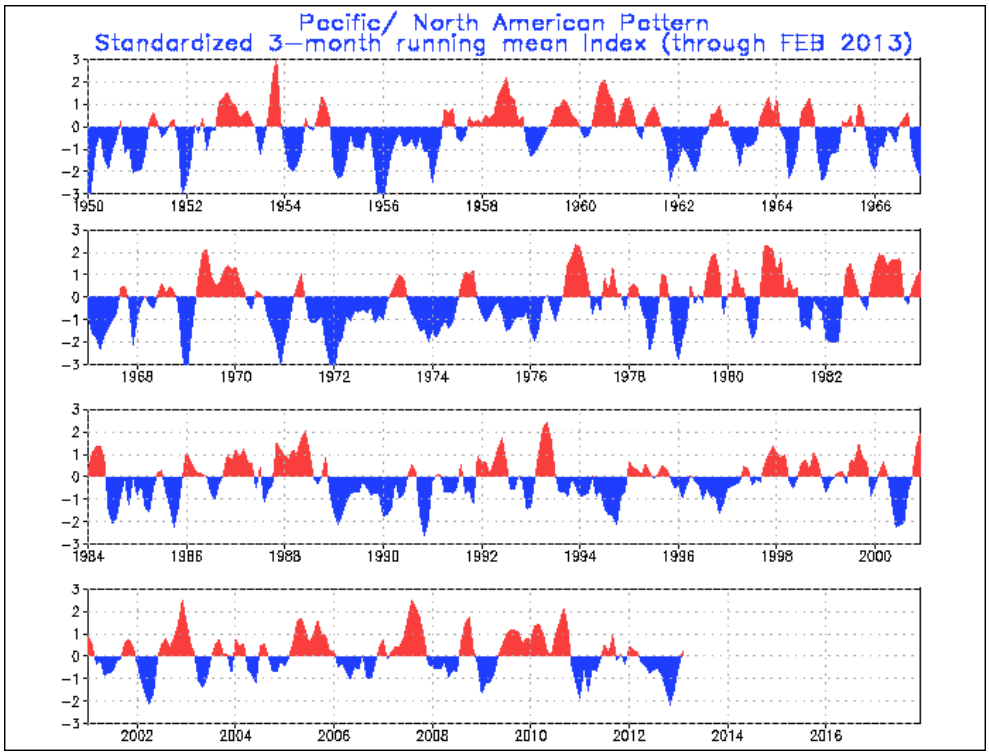

Figure 45. Pacific/North American Index values from 1950 through 2013. (From Climate Prediction Center 2013b)

D. MULTI-OBJECTIVE DECISION ANALYSIS

1. Single-Dimension Value Functions

The Direct Rating Method was used to develop the single-dimension value function for attribute 1 (number of warnings). The direct rating of the number of warnings issued was completed using the worksheet in Appendix C by the primary thunderstorm coordinator for the summer months as a subject matter expert. His ratings given to the number of warnings issued are shown in Table 14. The associated piece-wise linear single-dimension value function for attribute 1 is plotted in Figure 46.

Table 14. Direct rating results for the number of warnings issued.

Number of Warnings (X_w)	Value Function $v_w(X_w)$
22	0
20	10
19	20
15	50
8	80
7	90
4	100

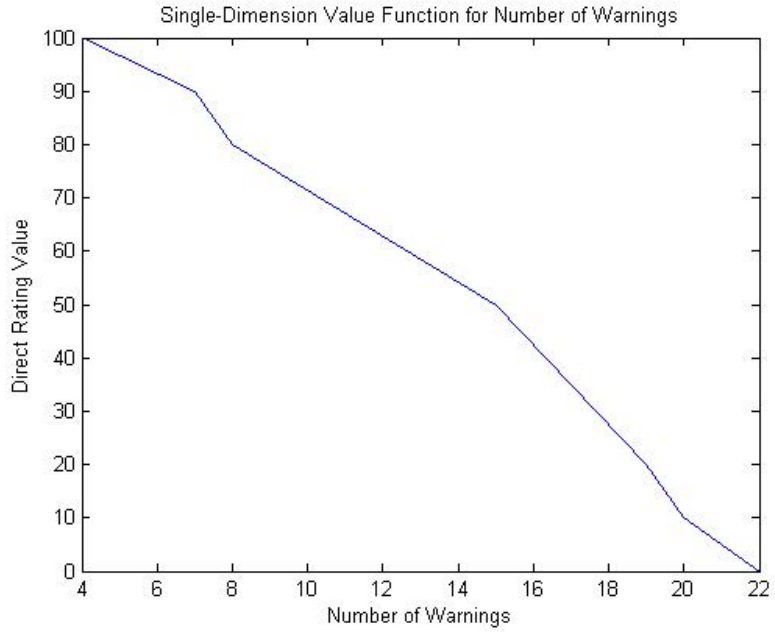

Figure 46. Piece-wise linear single-dimension value function for the number of warnings issued.

The Direct Rating Method was also applied to the number of minutes over-warned to create a single-dimension value function. The direct rating of the number of minutes over-warned was completed using the worksheet in Appendix C by four Launch Weather Officers at the 45 WS. Direct input from the customers at each facility was not available at the time of this thesis, so the median value of the Launch Weather Officer inputs was used for the single-dimension value function. The Launch Weather Officers interact directly with the customers on each of the facilities and are best suited at the 45

WS to provide this input. These values are listed in Table 15. The associated piece-wise linear single-dimension value function for attribute 4 is plotted in Figure 47.

Table 15. Direct rating results for the number of minutes over-warned.

Minutes Overwarned (X_{ow})	Value Function $v_{ow}(X_{ow})$
1	100
60	70
310	18
808	0

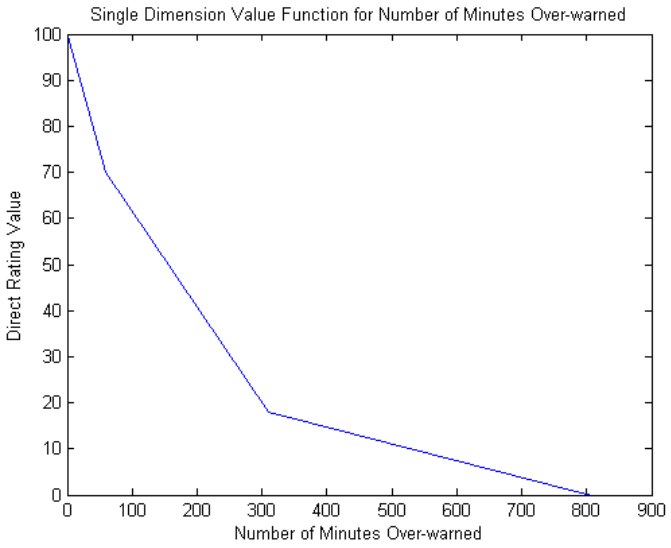

Figure 47. Piece-wise linear single-dimension value function for the number of minutes over-warned.

2. Weights for Single-Dimension Value Functions

Just as determining the single-dimension value functions required subject matter experts, so does determining weights for each of the single-dimension value functions. Given that there are only 2 attributes that require weights, a single-variable sensitivity analysis can provide insight into which alternatives would be preferred based on different weights of the attributes. This will be discussed in detail in a later section.

3. Final Multi-Objective Value Function

Using an additive model, the final multi-objective value function is:

$$v(X_W, X_{OW}) = w_w v_w(X_w) + w_{ow} v_{ow}(X_{ow})$$

where X_w is attribute 1 (number of warnings), X_{ow} is attribute 4 (number of minutes over-warned), w_w is the weight for attribute 1, w_{ow} is the weight for attribute 4, $v_w(X_w)$ is the single-dimension value function for attribute 1 and $v_{ow}(X_{ow})$ is the single-dimension value function for attribute 4 (minutes over-warned).

4. Sensitivity Analysis

a. Sensitivity of Weights

Table 16 contains the final multi-objective value function results using the values for number of warnings, $v_w(X_w)$, and the estimated values for number of minutes over-warned, $v_{ow}(X_{ow})$, and weights of w_w=0 to w_w=1. Figure 48 was created using the method outlined in section III.B.4. The lines for each alternative define the value each alternative would have for each value of w_{ow}. Based on the single-dimension value functions defined by the preferences provided, the Status Quo alternative is best for weights w_w=0 to 0.48, alternative P is best for weights w_w=0.48 to 0.63 and alternative N is best for weights w_w=0.63 to 1. Given that the single-dimension value function for the number of minutes over-warned was based on subject matter experts at the 45 WS and not direct customer input, additional sensitivity analysis on the single-dimension value function for the number of minutes over-warned is warranted to test the robustness of the results.

Table 16. Multi-objective value function values for number of warnings, $v_w(X_w)$, and the estimated values for number of minutes over-warned, $v_{ow}(X_{ow})$, and weights of $w_{ow} = 1$ and $w_{ow} = 0$.

Alternative	Final Value Function (W_w=0)	Final Value Function (W_w=1)
StatusQuo	100	0
A	92.225	0
B	91.945	0
C	90.75	0
D	87.525	0
E	89.975	0
F	82.97	10
G	79.745	10
H	79.465	10
I	78.275	10
J	77.5	10
K	70.495	20
L	81.61	10
M	69.64016	20
N	0	100
O	24.0039824	80
P	16.82062022	90

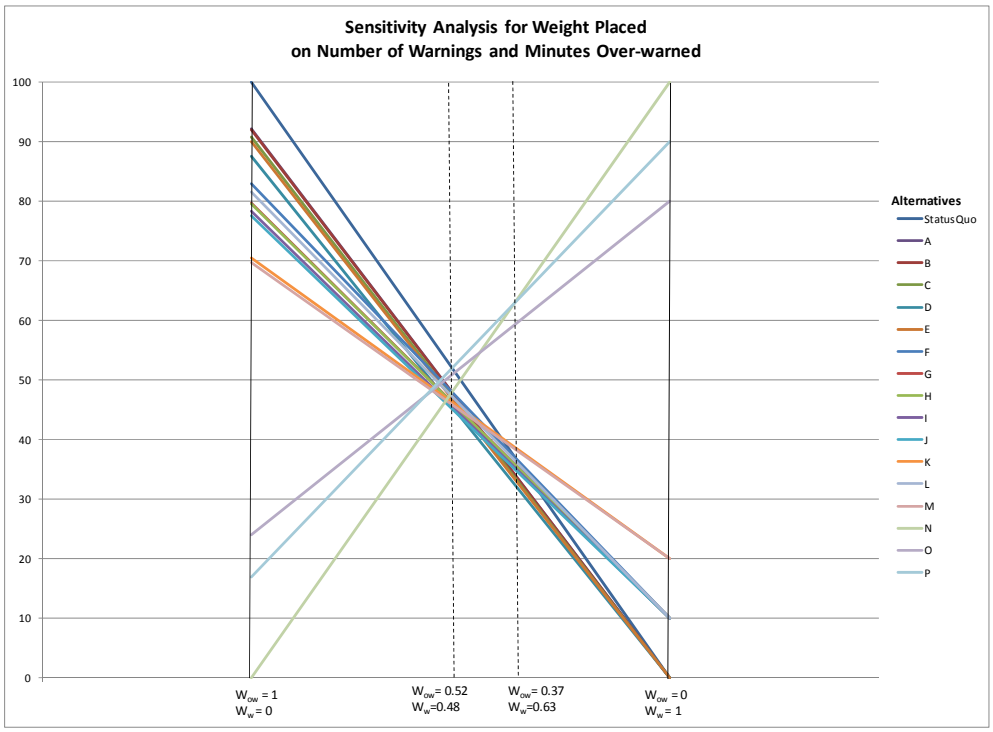

Figure 48. Sensitivity analysis of the weights for number of warnings issued and number of minutes over-warned.

b. Sensitivity with respect to the Single-Dimension Value Function for Number of Minutes Over-warned

There are three basic shapes that the single-dimension value function for number of minutes over-warned is likely to have. Figure 49 displays these shapes. The blue line is an exponential curve fit to the values provided by the 45 WS. In this case, as the number of minutes over-warned increases, the value decreases rapidly to approximately 310 minutes over-warned, and less rapidly from 310 to 808. The red line is a linear value function, where value decreases linearly with the number of minutes over-warned. The green line is a polynomial relationship, where, as the number of minutes of over-warning increases, the value slowly decreases to approximately 310 minutes and rapidly decreases from 310 to 808 minutes.

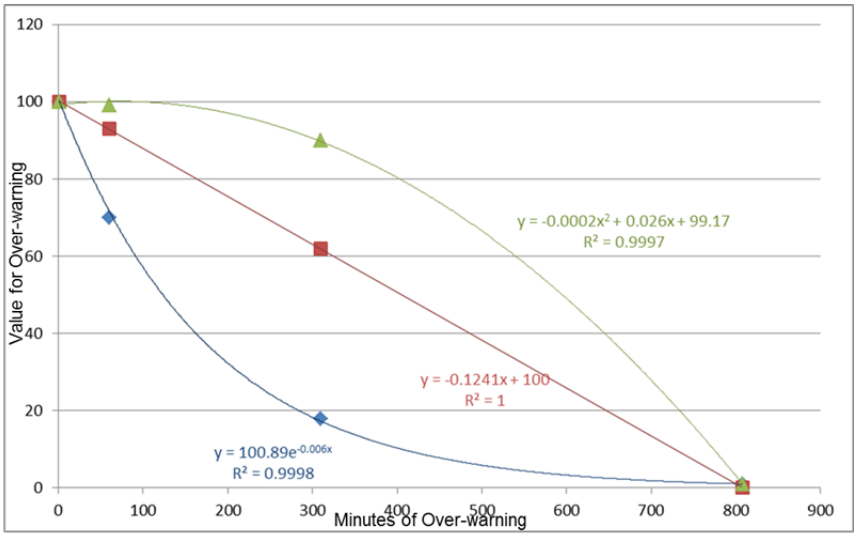

Figure 49. Three basic shapes for the single-dimension value functions for the number of minutes over-warned. The blue line is the current estimated single-dimension value function. The red line is a linear value function. The green line is a similar, but inverse shape, to the blue line.

By examining the shape of the estimated single-dimension value function there appears to be a point near 300 minutes over-warned for which the value would have to change (likely increase) to make alternatives O or P options to consider. To evaluate the sensitivity of the single-dimension value function for number of minutes over-warned, the parameter, γ_{ow}, was defined as the single-dimension value function value at 310 minutes over-warned. A two-part piece-wise linear function was calculated to describe the single-dimension value function for γ_{ow} for values of 10 to 90 in increments of 10 and 18 which is the γ_{ow} value from the single-dimension value function provided by the 45 WS. Using the method outlined in section III.B.4. sensitivity analysis plots for each γ_{ow} were created. Figures 50 to 53 contain the plots for γ_{ow} values 18, 30, 60 and 90. As γ_{ow} increases, additional alternatives enter into consideration and the range of weights over which alternatives P and O are preferred increases. The Status Quo alternative dominates at smaller values of w_{ow} while alternative N dominates at higher values of w_{ow}. Figure 54 displays the alternatives that dominate for each γ_{ow} and w_{ow} value.

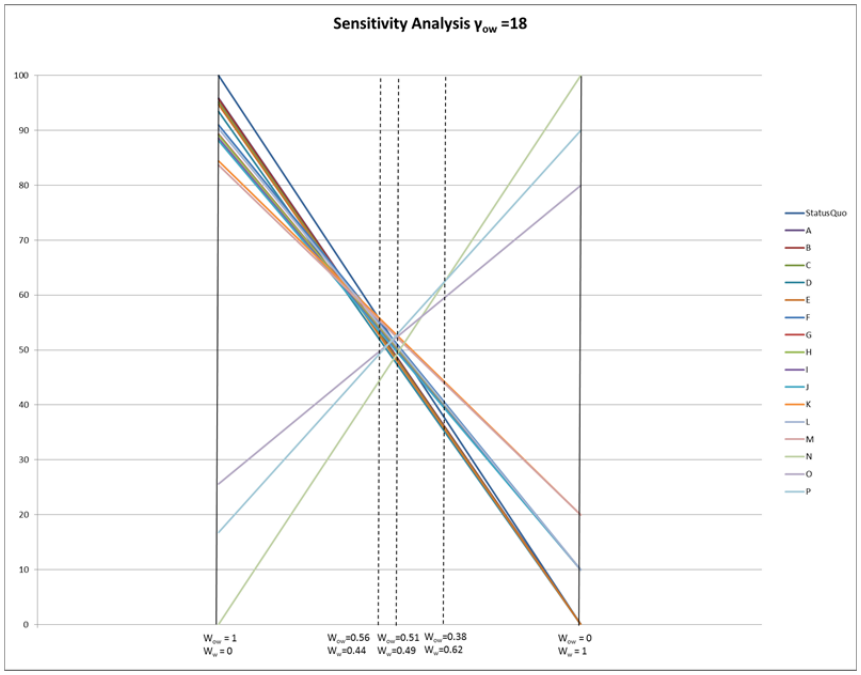

Figure 50. Sensitivity analysis with respect to weights for γ_{ow} = 18.

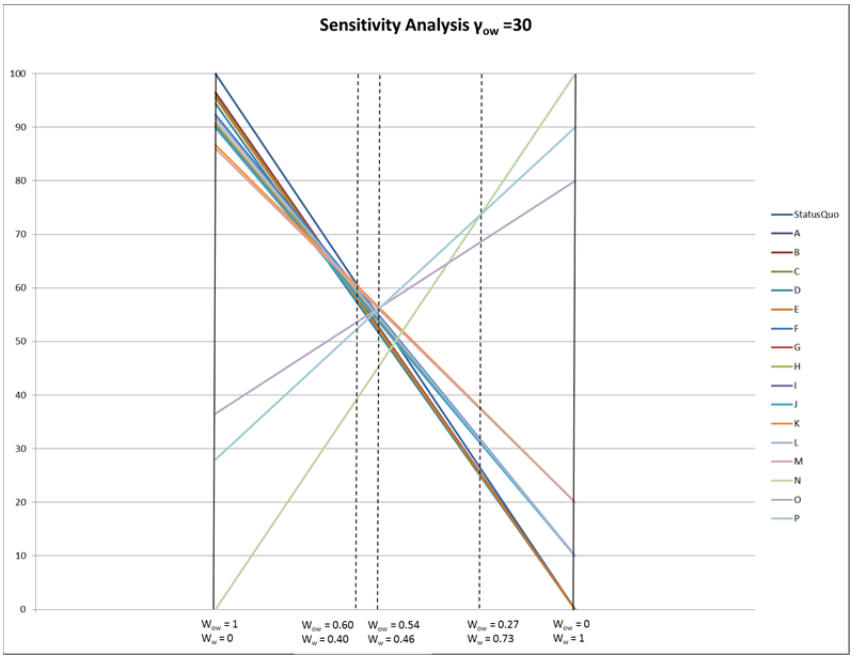

Figure 51. Sensitivity analysis with respect to weights for γ_{ow} = 30.

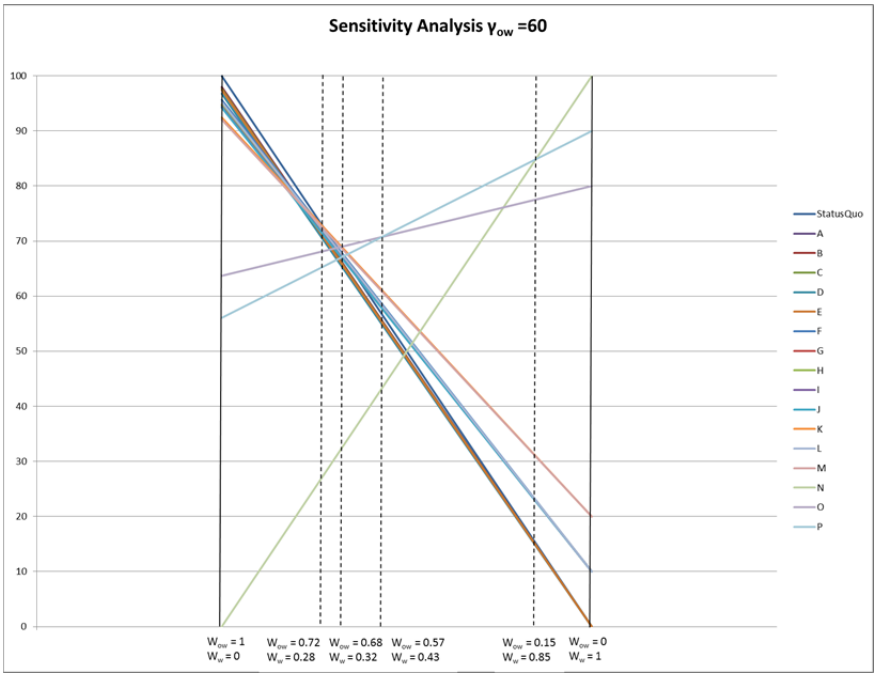

Figure 52. Sensitivity analysis with respect to weights for $\gamma_{ow} = 60$.

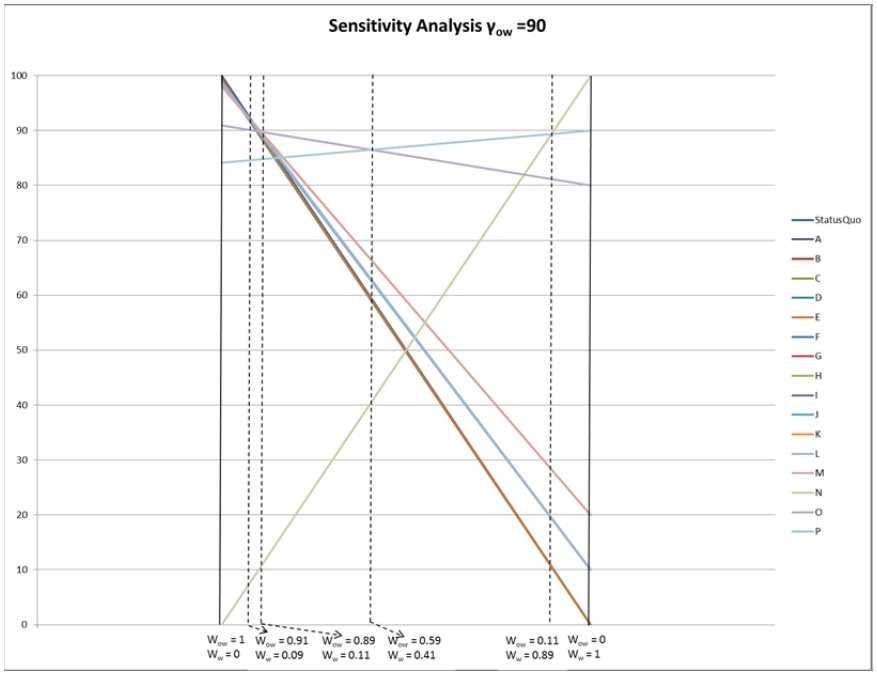

Figure 53. Sensitivity analysis with respect to weights for $\gamma_{ow} = 90$.

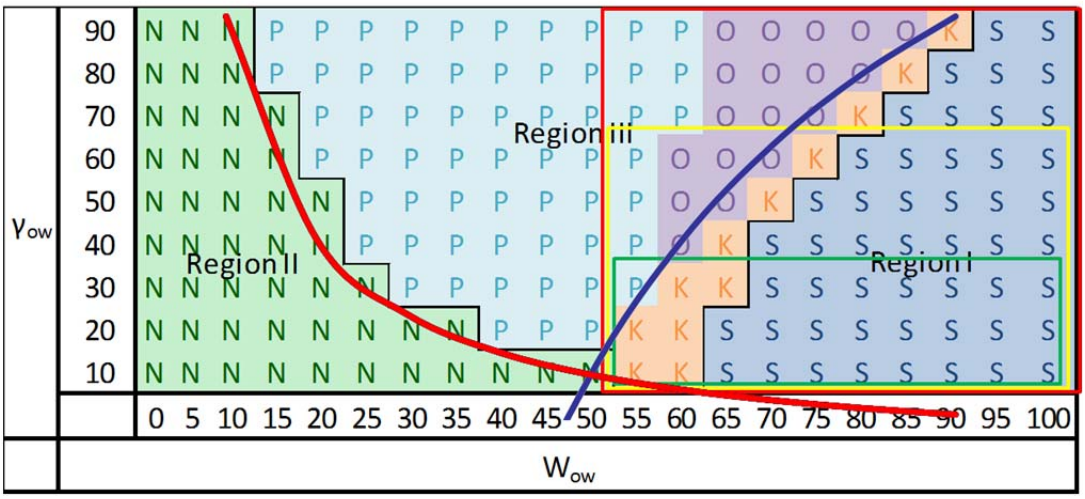

Figure 54. Dominant alternatives for γ_{ow} and w_{ow} values.

Figure 54 has 3 distinct regions. Region I is dominated by the Status Quo (S) alternative, Region II is dominated by alternative N (total consolidation) and Region III is dominated by 3 other alternatives (O, P and K), primarily P. The boundaries between these regions represent the boundaries between sets of preferences of the decision makers. To determine these boundaries, the final value functions for alternatives were compared. For simplicity, since alternative K dominates over a narrow band of w_{ow} (for most γ_{ow}, the range of w_{ow} is less than 0.05) and because alternatives O and P (with similar number of minutes over-warned) dominate Region III, alternative X is defined as the average of alternatives O and P at 310 minutes over-warned. Using the final multi-objective value functions for alternatives X and S to relate γ_{ow} and w_{ow}, the boundary between Region I and Region III is plotted as a blue line defined for γ_{ow} values for where

$$\gamma_{ow} = 190 - \frac{90}{w_{ow}}$$

Using the final multi-objective value functions for alternatives N and P to relate γ_{ow} and w_{ow}, the boundary between Region II and Region III is plotted as a red line defined for γ_{ow} values where

$$\gamma_{ow} = 10 \times \frac{1 - w_{ow}}{w_{ow}}$$

The blue and red lines can be interpreted with respect to the preferences of the decision maker. Following the either of the lines, as γ_{ow} increases, it means that it is not as bad to have 310 minutes over-warned, and as w_{ow} increases, it means over-warning is more important. Each value along the line represents a tradeoff associated with over-warning. For example, if γ_{ow} is 75, that means the difference between 310 and 808 minutes over-warned is 3 times as important as the difference 0 and 310 minutes over-warned.

To justify any consolidation of warning circles, the preferences must be such that the combination of γ_{ow} and w_{ow} values lie to the left of the blue line (Regions II and III). This occurs when

$$\gamma_{ow} > 190 - \frac{90}{w_{ow}}$$

Justification for total consolidation of warning areas requires the preferences to be such that the combination of γ_{ow} and w_{ow} values lie to the left of the red line (Region II). This occurs when

$$\gamma_{ow} < 10 \times \frac{1 - w_{ow}}{w_{ow}}$$

To justify consolidation of circles in some intermediate alternative such as O or P, the preferences must be such that the combination of γ_{ow} and w_{ow} values lie to the right of the red line and to the left of the blue line (Region III). This occurs when:

$$\gamma_{ow} > 190 - \frac{90}{w_{ow}} \text{ and } \gamma_{ow} < 10 \times \frac{1 - w_{ow}}{w_{ow}}$$

When looking at the table in Figure 54, there is a preference expressed by experts at the 45 WS to weight the number of minutes over-warned more heavily than the number of warnings issued. This is based on the need to minimize the impact to the operators while maintaining safe operations. Given this preference, the alternatives worth considering are then limited to those on the right-hand side of the table in Figure 54, contained in the red box. Additionally, the value of 310 minutes over-warned is also not likely to be greater than 60 (γ_{ow} = 60), which corresponds to the linear single-dimension value function. This limits the preferrable options to those within the yellow

box in Figure 54. Finally, none of the Launch Weather Officers rated 310 minutes over-warned greater than 30 (γ_{ow} = 30), limiting the options to those within the green box, giving strong evidence to maintain the current warning circles of the Status Quo alternative.

THIS PAGE INTENTIONALLY LEFT BLANK

V. CONCLUSIONS AND RECOMMENDATIONS

A. CONCLUSIONS

The co-variability of warning circles based on the Phase II lightning warnings issued by the 45 WS shows a strong facility-based bias. The first EOF defined strong co-variability among the circles located at KSC and at CCAFS and explains 45.2% of the overall variability, which is more than EOF2, EOF3and EOF4 combined. While the EOF patterns can be associated with specific weather regimes, there is a clear human bias in the data as indicated in the high percentages of identical stop times for a sample of pair and quadruple combinations. From the results of the PCA of the Phase II lightning warnings it can be concluded that forecasters are already consolidating warning areas and in doing so, there is greater over-warning with respect to stop times than start times.

The co-variability of warning circles based on the 4DLSS lightning data shows the complexity in lightning patterns over the CCAFS/KSC area. The first EOF defined a north-south split in co-variability among the circles accounting for 54.8% of the overall variability. The first three EOFs can be associated with flow patterns and local convergence patterns to explain the associated co-variability. The lack of human bias and error in this data set enables more objective matching of regimes to the EOF patterns. Ultimately, recognizing the differences in the perceived co-variability of warning circles with the actual warning circles is critical to the decision process and ensuring that forecaster perceptions of co-variability are weighed against the meteorological data.

Analysis of the temporal overlap of warning circles based on the Phase II lightning data found that facility-based (CCAFS and KSC) combinations had the greatest percentage of overlap. This was true for combinations ranging from pairs to sextuples. The temporal overlap of warning circles based on the 4DLSS data did not show as strong a tendency for facility-based combinations to dominate the temporal overlap percentages. While some combinations of circles located at CCAFS and KSC did group together with high percentages, there were additional non-facility based combinations with similar percentages.

Based on sensitivity analysis of the weights w_w and w_{ow} and the single-dimension value function v_{ow}, there are five alternatives (Status Quo, K, N, O and P) out of a set of 17 evaluated, which should be considered for selection based on the preferences reflected in the γ_{ow} parameter and weights.

In order to justify consolidation of warning circles, the preferences must be such that the combination of γ_{ow} and w_{ow} values lie within Regions II and III in Figure 54, which occurs when

$$\gamma_{ow} > 190 - \frac{90}{w_{ow}}$$

Finally, based on the expressed preferences of the 45 WS that w_{ow} is greater than 0.5 and the maximum value for γ_{ow} provided by the Launch Weather Officers of 30, the most likely options are those contained within the green box of Figure 54, giving strong evidence to maintain the current warning circles of the Status Quo alternative

B. RECOMMENDATIONS

Given the relatively small size of the 4DLSS observed lightning data set (18 months), conducting the same or a similar analysis on a larger data set would provide increased robustness and statistical significance to the results. Additionally, a resampling approach to PCA could be conducted on an independent data set to determine if the EOF patterns observed in this thesis can be repeated and are thus more likely to be physically real. Spectral analysis of the data would also provide additional insight to the timing of variability.

Stratification of the temporal overlap of the 4DLSS data by flow regime and identifying any significant changes between flow regimes would improve forecaster knowledge and potentially increase warning accuracy.

A subject matter expert was not available to provide ratings for the values with respect to minutes over-warned. The multi-objective decision analysis could be repeated once a subject matter expert is made available. This would result in value functions and weights that more accurately reflect the preferences of the stakeholders.

While processing the data, there were differences discovered between the observed lightning (4DLSS) and warned lightning data sets. Verification of the warnings issued again the actual lightning strikes could identify errors in the warning process. Given the time sensitive nature of lightning warnings, an evaluation of the process associated with warning issuance may yield increased forecaster efficiency.

THIS PAGE INTENTIONALLY LEFT BLANK

APPENDIX A. TEMPORAL OVERLAP FOR PHASE II LIGHTNING WARNINGS

Combinations with a temporal overlap of at least 50% are included in the tables below. The combinations are listed in order of decreasing temporal overlap.

Pair Combinations					
Combination		% Temporal Overlap	Combination		% Temporal Overlap
3	4	0.93	5	10	0.65
4	5	0.91	1	11	0.62
5	6	0.91	4	10	0.61
3	7	0.89	6	9	0.61
1	6	0.88	5	12	0.61
3	5	0.86	7	10	0.61
11	12	0.85	6	11	0.60
10	12	0.85	3	10	0.60
4	7	0.84	4	12	0.57
4	6	0.84	7	12	0.57
1	5	0.81	5	9	0.56
5	7	0.80	2	11	0.56
3	6	0.80	2	10	0.56
10	11	0.78	3	12	0.56
9	12	0.77	5	11	0.56
6	7	0.76	2	12	0.55
9	11	0.75	8	11	0.55
1	4	0.75	4	9	0.53
1	3	0.72	7	11	0.52
9	10	0.69	4	11	0.52
1	12	0.69	8	12	0.52
6	10	0.68	3	9	0.51
1	7	0.68	3	11	0.51
1	9	0.67	7	9	0.51
1	10	0.67	8	10	0.50
6	12	0.66			

Triple Combinations							
Combination			% Temporal Overlap	Combination			% Temporal Overlap
3	4	5	0.85	6	9	12	0.56
4	5	6	0.83	5	7	10	0.56
3	4	7	0.83	6	7	10	0.56
1	5	6	0.81	4	5	12	0.56
3	5	6	0.79	4	6	12	0.56
3	4	6	0.79	1	5	9	0.56
3	5	7	0.79	5	6	11	0.55
4	5	7	0.78	1	4	10	0.55
10	11	12	0.75	4	10	12	0.55
1	4	6	0.74	3	4	12	0.54
5	6	7	0.74	1	4	12	0.54
1	4	5	0.74	5	11	12	0.54
3	6	7	0.73	7	10	12	0.54
4	6	7	0.73	6	9	10	0.54
1	3	6	0.71	3	6	12	0.54
9	11	12	0.71	3	5	12	0.54
1	3	5	0.71	3	10	12	0.53
1	3	4	0.70	3	7	12	0.53
9	10	12	0.68	1	5	11	0.53
1	6	7	0.67	1	3	10	0.53
1	5	7	0.66	5	10	11	0.53
1	3	7	0.66	6	7	12	0.53
1	4	7	0.65	6	9	11	0.53
9	10	11	0.64	5	7	12	0.52
1	6	10	0.63	1	3	12	0.52
1	6	12	0.63	4	7	12	0.52
5	6	10	0.63	1	7	10	0.52
1	10	12	0.63	4	6	9	0.52
6	10	12	0.62	4	5	9	0.52
1	11	12	0.61	1	4	9	0.52
1	6	9	0.60	2	11	12	0.52
1	9	12	0.60	5	9	12	0.52
5	6	12	0.60	2	10	12	0.51
4	5	10	0.60	1	7	12	0.51
4	6	10	0.59	4	5	11	0.51
1	5	10	0.59	4	6	11	0.51
1	5	12	0.58	4	11	12	0.51
6	11	12	0.58	7	11	12	0.50
3	4	10	0.58	5	9	10	0.50
5	10	12	0.58	3	4	9	0.50
1	6	11	0.58	4	10	11	0.50
3	5	10	0.57	3	6	9	0.50
1	10	11	0.57	1	3	9	0.50
3	7	10	0.57	3	4	11	0.50
3	6	10	0.57	3	5	9	0.50
6	10	11	0.57	3	11	12	0.50
1	9	11	0.56	7	10	11	0.50
5	6	9	0.56	2	10	11	0.50
4	7	10	0.56	8	11	12	0.50
1	9	10	0.56				

Quadruple Combinations									
Combination				% Temporal Overlap	Combination				% Temporal Overlap
3	4	5	6	0.78	3	4	6	12	0.53
3	4	5	7	0.78	1	3	6	10	0.53
1	4	5	6	0.74	1	3	5	10	0.53
3	5	6	7	0.73	5	6	10	11	0.53
4	5	6	7	0.73	6	9	11	12	0.52
3	4	6	7	0.72	1	3	4	10	0.52
1	3	5	6	0.70	1	9	10	11	0.52
1	3	4	6	0.70	3	4	10	12	0.52
1	3	4	5	0.70	1	6	7	10	0.52
1	5	6	7	0.66	1	4	10	12	0.52
1	3	6	7	0.65	1	6	9	11	0.52
1	4	6	7	0.65	5	10	11	12	0.52
1	4	5	7	0.65	3	6	10	12	0.52
1	3	5	7	0.65	5	6	7	12	0.52
1	3	4	7	0.65	1	5	11	12	0.52
9	10	11	12	0.63	3	5	10	12	0.52
1	6	10	12	0.60	1	3	6	12	0.52
1	5	6	10	0.59	4	5	6	9	0.52
4	5	6	10	0.59	3	4	7	12	0.52
1	5	6	12	0.58	1	4	6	9	0.52
5	6	10	12	0.57	1	3	5	12	0.52
1	10	11	12	0.57	1	4	5	9	0.52
3	4	5	10	0.57	5	6	9	12	0.52
1	6	11	12	0.56	1	5	7	10	0.51
3	5	6	10	0.56	1	3	4	12	0.51
3	4	6	10	0.56	6	7	10	12	0.51
1	9	11	12	0.56	3	6	7	12	0.51
6	10	11	12	0.56	3	5	7	12	0.51
1	5	10	12	0.56	4	5	7	12	0.51
1	5	6	9	0.55	3	7	10	12	0.51
4	5	6	12	0.55	4	6	7	12	0.51
3	4	7	10	0.55	1	6	7	12	0.51
1	6	9	12	0.55	1	5	9	12	0.51
1	4	6	10	0.55	5	7	10	12	0.51
1	9	10	12	0.55	4	5	6	11	0.51
5	6	7	10	0.55	1	3	7	10	0.51
1	4	5	10	0.55	1	4	7	10	0.51
3	5	7	10	0.55	4	7	10	12	0.51
4	5	7	10	0.54	1	5	10	11	0.51
1	6	10	11	0.54	6	9	10	11	0.50
3	6	7	10	0.54	1	5	7	12	0.50
1	4	6	12	0.54	1	3	10	12	0.50
4	6	7	10	0.54	5	6	9	10	0.50
4	5	10	12	0.54	1	3	7	12	0.50
4	6	10	12	0.54	1	5	9	10	0.50
1	4	5	12	0.54	1	7	10	12	0.50
5	6	11	12	0.54	4	5	11	12	0.50
1	6	9	10	0.53	1	4	7	12	0.50
3	5	6	12	0.53	3	5	6	9	0.50
3	4	5	12	0.53	1	3	6	9	0.50
1	5	6	11	0.53	5	9	10	12	0.50
6	9	10	12	0.53	4	6	11	12	0.50

Quintuple Combinations

Combination					% Temporal Overlap
3	4	5	6	7	0.72
1	3	4	5	6	0.70
1	4	5	6	7	0.65
1	3	5	6	7	0.65
1	3	4	6	7	0.65
1	3	4	5	7	0.64
3	4	5	6	10	0.56
1	5	6	10	12	0.56
1	4	5	6	10	0.55
1	6	10	11	12	0.54
3	4	5	7	10	0.54
1	4	5	6	12	0.54
3	5	6	7	10	0.54
4	5	6	7	10	0.54
4	5	6	10	12	0.54
3	4	6	7	10	0.53
3	4	5	6	12	0.53
1	3	5	6	10	0.53
1	6	9	10	12	0.53
1	3	4	6	10	0.52
1	9	10	11	12	0.52
1	3	4	5	10	0.52
1	4	6	10	12	0.52
1	4	5	10	12	0.52
1	6	9	11	12	0.52
1	5	6	11	12	0.52
5	6	10	11	12	0.52
3	5	6	10	12	0.52
1	3	5	6	12	0.52
1	4	5	6	9	0.51
3	4	5	10	12	0.51
1	5	6	7	10	0.51

Combination					% Temporal Overlap
1	3	4	6	12	0.51
3	4	6	10	12	0.51
1	3	4	5	12	0.51
1	5	6	9	12	0.51
4	5	6	7	12	0.51
3	5	6	7	12	0.51
3	4	5	7	12	0.51
1	3	6	7	10	0.51
1	4	6	7	10	0.51
5	6	7	10	12	0.51
3	4	6	7	12	0.51
1	5	6	10	11	0.50
1	4	5	7	10	0.50
6	9	10	11	12	0.50
1	5	10	11	12	0.50
1	5	6	7	12	0.50
1	3	5	7	10	0.50
1	3	6	10	12	0.50
1	3	4	7	10	0.50
3	4	7	10	12	0.50
1	6	9	10	11	0.50
3	6	7	10	12	0.50
1	3	5	10	12	0.50
3	5	7	10	12	0.50
4	5	7	10	12	0.50
1	3	4	10	12	0.50
4	6	7	10	12	0.50
1	5	6	9	10	0.50
1	3	6	7	12	0.50
1	6	7	10	12	0.50
1	4	6	7	12	0.50

Sextuple Combinations						
Combination						% Temporal Overlap
1	3	4	5	6	7	0.64
3	4	5	6	7	10	0.53
1	3	4	5	6	10	0.52
1	4	5	6	10	12	0.52
1	3	4	5	6	12	0.51
3	4	5	6	10	12	0.51
1	4	5	6	7	10	0.50
3	4	5	6	7	12	0.50
1	3	5	6	7	10	0.50
1	5	6	10	11	12	0.50
1	3	4	6	7	10	0.50
1	3	4	5	7	10	0.50
1	6	9	10	11	12	0.50
1	3	5	6	10	12	0.50
1	3	4	6	10	12	0.50
1	3	4	5	10	12	0.50
4	5	6	7	10	12	0.50
3	5	6	7	10	12	0.50

THIS PAGE INTENTIONALLY LEFT BLANK

APPENDIX B. TEMPORAL OVERLAP FOR 4DLSS LIGHTNING EVENTS

Combinations with a temporal overlap of at least 50% are included in the tables below. The combinations are listed in order of decreasing temporal overlap.

Pair Combinations		
Combination		% Temporal Overlap
1	5	0.82
5	6	0.79
7	8	0.79
3	6	0.77
2	9	0.76
8	9	0.75
4	10	0.75
1	6	0.75
1	2	0.69
8	10	0.68
2	4	0.67
2	8	0.67
7	9	0.66
3	5	0.63
4	8	0.62
7	10	0.62
7	11	0.61
1	3	0.60
2	10	0.60
2	6	0.59
1	9	0.58
2	5	0.58
2	7	0.57
1	4	0.57
4	9	0.57
9	10	0.56
8	11	0.55
9	11	0.54
6	9	0.54
4	7	0.52
2	3	0.52
3	9	0.51
1	8	0.50

Triple Combinations			
Combination			% Temporal Overlap
1	5	6	0.70
7	8	9	0.63
2	8	9	0.62
3	5	6	0.62
1	3	6	0.58
7	8	10	0.58
1	2	5	0.57
4	8	10	0.55
1	2	9	0.55
1	3	5	0.55
1	2	6	0.55
2	7	8	0.55
2	4	10	0.54
2	4	9	0.53
8	9	10	0.53
2	7	9	0.53
2	4	8	0.52
2	5	6	0.52
2	8	10	0.51
1	2	4	0.51
4	8	9	0.51
7	8	11	0.51
4	7	8	0.50

Quadruple Combinations				
Combination				% Temporal Overlap
1	3	5	6	0.55
2	7	8	9	0.52
1	2	5	6	0.51

There were no quintuple or sextuple combinations of 4DLSS Lightning Events with a percentage of temporal overlap greater than 50%.

APPENDIX C. DIRECT RATING METHOD WORKSHEETS

Direct Rating Method-Number of Minutes Over-Warned

As part of a study of lightning warning areas at CCAFS/KSC, potential alternative warning areas have been derived from the LDAR-II lightning data at CCAFS/KSC. To help measure how well each alternative performs relative to the attributes that are of concern to the decision makers, some additional information is required.

Attributes are measures of performance in relation to an objective. One objective of this study is to reduce forecaster workload. An attribute that measures this is the number of warnings issued. A second objective is to conduct safe operations. An attribute that measures this is the number of minutes over-warned (provides a measure of man-hours lost due to over-warning). These objectives alone do not indicate a clear best alternative, because as the number of warnings decreases, the number of minutes over-warned will increase, requiring a tradeoff. To ensure that the alternatives are properly ranked, these attributes must be combined into a single index of overall.

I will be using a direct rating method to determine the value function for each attribute. This is a simple method that requires subject matter expertise to rank values associated with alternatives on an interval scale so that a piece-wise linear function can be determined and used to specify the value function.

Below is a list of alternatives and the average number of minutes over-warned that each alternative would have on a day when warnings were issued.

A 0

B 60

C 310

D 808

Alternative A has the lowest number of minutes over-warned (0) and is assigned a value of 100. Alternative D with the highest number of minutes over-warned (810) will be assigned a value of 0.

0-----10-----20-----30-----40-----50-----60-----70-----80-----90-----100

D A

Please rate the alternatives B and C so that the space between the values for each alternative represents the strength of preference for one alternative over another in terms of the number of warnings issued per day when there are warnings issued. Note: it is the interval between points on the scale that should be compared. For example, if you give alternative B a rating of 10, you are indicating that change in the number of warnings issued for alternative A is 10 times more preferable than the improvement between D and B.

Direct Rating Method- Number of Warnings

As part of a study of lightning warning areas at CCAFS/KSC, potential alternative warning areas have been derived from the LDAR-II lightning data at CCAFS/KSC. To help measure how well each alternative performs relative to the attributes that are of concern to the decision makers, some additional information is required.

Attributes are measures of performance in relation to an objective. One objective of this study is to reduce forecaster workload. An attribute that measures this is the number of warnings issued. A second objective is to conduct safe operations. An attribute that measures this is the number of minutes over-warned (provides a measure of man-hours lost due to over-warning). These objectives alone do not indicate a clear best alternative, because as the number of warnings decreases, the number of minutes over-warned will increase, requiring a tradeoff. To ensure that the alternatives are properly ranked, these attributes must be combined into a single index of overall desirability.

I will be using a direct rating method to determine the value function for each attribute. This is a simple method that requires subject matter expertise to rank values associated with alternatives on an interval scale so that a piece-wise linear function can be determined and used to specify the value function.

Below is a list of alternatives and the average number of warnings that each alternative would have on a day when warnings were issued.

A	22	E	8
B	20	F	7
C	19	G	4
D	15		

Alternative G has the lowest number of warnings (4) and is assigned a value of 100. Alternative A has the highest number of warnings (22) has been assigned a value of 0.

0-----10-----20-----30-----40-----50-----60-----70-----80-----90-----100

A G

Please rate the other alternatives (B, C, D, E and F) so that the space between the values for each alternative represents the strength of preference for one alternative over another in terms of the number of warnings issued per day when there are warnings issued. Note: it is the interval between points on the scale that should be compared. For example, if you give alternative B a rating of 10, you are indicating that a change in the number of warnings issued for alternative G is 10 times more preferable than the improvement between A and B.

LIST OF REFERENCES

14th Weather Squadron, 2009: Operational Climatic Data Summary for NASA Shuttle Landing Facility, 14th Weather Squadron (https://notus2.afccc.af.mil/SCIS/), 5 pp.

45th Space Wing, 2007: 45th Space Wing Instruction 15-101 Weather Support. [Available from William P. Roeder, 45 WS/SYS, 1202 Edward H. White St., MS 7302, Patrick AFB, FL, 32925-3238]

45th Weather Squadron, 2011: Eastern Range Instrument Handbook, 4DLSS. [Available from William P. Roeder, 45 WS/SYS, 1202 Edward H. White St., MS 7302, Patrick AFB, FL, 32925-3238]

Bazelyan, E. M. and Y. P. Raizer, 2000: *Lightning physics and lightning protection.* Institute of Physics Pub, 325 pp.

Bjornsson, H., and S.A. Venegas, 1997, 1997. *A Manual for EOF and SVD Analyses of Climate Data*. McGill University, CCGCR Report No. 97-1, Montréal, Québec, 52 pp.

Bowman, J, 2009: Combining Lightning Warning Circles Outbrief to the 45th OWS. [Available from William P. Roeder, 45 WS/SYS, 1202 Edward H. White St., MS 7302, Patrick AFB, FL, 32925-3238]

Cetola, J.D., 1997: A climatology of the sea breeze at Cape Canaveral, Florida. M.S. thesis, Dept. of Meteorology, Florida State University, 56 pp.

Climate Prediction Center, cited 2013: Pacific/North American (PNA). [Available online at http://www.cpc.ncep.noaa.gov/data/teledoc/pna.shtml.]

Climate Prediction Center, cited 2013: Pacific North American Pattern Plotted Historical Time Series. [Available online at http://www.cpc.ncep.noaa.gov/data/teledoc/pna.timeseries.gif]

Cummins K. L., and M. J. Murphy, 2009: An overview of lightning locating systems: history, techniques and data uses, with an in-depth look at the U.S. NLDN. *IEEE Transactions on Electromagnetic Compatibility*, **51,** 499–518.

——, J. A. Cramer, C. J. Biagi, E. P. Krider, J. Jerauld, M. A. Uman, and V. A. Rakov, 2006: The U.S. National Lightning Detection Network: post-upgrade status. *Extended Abstracts, Second Conf. on the Meteorological Applications of Lightning Data,* Atlanta, GA, Amer. Meteor. Soc., P6.1.

——, E. P. Krider, and M. D. Malone, 1998: The U.S. National Lightning Detection Network and applications of cloud-to-ground lightning data by electric power utilities. *IEEE Transactions on Electromagnetic Compatibility*, **40,** 465–480.

Department of the Air Force, 1997: Air Force occupational safety and health standard 91-66, general industrial operations. [Available online at http://afpubs.hq.af.mil.]

Flinn, F. C., W. P. Roeder, M. D. Buchanan, T. M. McNamara, M. McAleenan, K. A. Winters, M. E. Fitzpatrick, and L. L. Huddleston, 2010a: Lightning reporting at 45th Weather Squadron: Recent improvements, *21st International Lightning Detection Conference*, Orlando, FL, 18 pp.

——, W. P. Roeder, D. E. Pinter, S. M. Holmquist, M. D. Buchanan, T. M. McNamara, M. McAleenan, K. A. Winters, P. S. Gemmer, M. E. Fitzpatrick, and R. D. Gonzalez, 2010b: Recent Improvements In Lightning Reporting At 45th Weather Squadron, *14th Conference on Aviation, Range, and Aerospace Meteorology*, 17-21 Jan 10, Paper 7.3, 14 pp.

Golde, R.H., 1977: *Lightning*. Vol 2. Academic Press, 849 pp .

Goodwin, P. and G. Wright, 2009: Decision Analysis for Management Judgment. 4th ed. John Wiley and Sons, 449 pp.

Grogan, M. J., 2004: Report on the 2002-2003 U.S. NLDN system-wide upgrade. [Available online at http://www.kelag.ch/meteosysteme/Blitz/NLDN_article_BR_E.pdf.]

Hodanish, S., D. Sharp, W. Collins, C. Paxton and R. E. Orville, 1997: A 10-yr monthly lightning climatology of Florida: 1986-95. *Wea. Forecasting*, **12,** 439–448.

Huffines, G. R., and R. E. Orville, 1999: Lightning ground flash density and thunderstorm duration in the continental United States: 1989-96. *J. Appl. Meteor.* **38,** 1013–1019.

Kirkwood, C. W., 1997: *Strategic Decision Making.* Wadsworth Publishing Company, 345 pp.

Laird, N. F., D. A. R. Kristovich, R. M. Rauber, H. T. Ochs and L. J. Miller, 1995: The Cape Canaveral sea and river breezes: kinematic structure and convective initiation. *Monthly Weather Review*, **123,** 2942–2956.

Lambert, W., and W. P. Roeder, 2008: Update to the Lightning Probability Forecast Equations at Kennedy Space Center/Cape Canaveral Air Force Station, Florida, *2nd International Lightning Meteorology Conference*, 24-25 April 2008, 16 pp.

Lambert, W., M. Wheeler, and W. P. Roeder, 2005: Objective Lightning Forecasting At Kennedy Space Center And Cape Canaveral Air Force Station Using Cloud-To-Ground Lightning Surveillance System Data, *(1st) Conference on Meteorological Applications of Lightning Data*, 9-13 Jan 05

Lambert W., M. Wheeler, and W. P. Roeder, 2006: Lightning Probability Forecasts at Kennedy Space Center/Cape Canaveral Air Force Station, Florida, *1st International Lightning Meteorology Conference*, 26-27 April 2006

Lericos, T. P., H. E. Fuelberg, A. I. Watson and R. L. Holle, 2001: Warm season lightning distributions of the Florida peninsula as related to synoptic patterns. *Wea. Forecasting,* **17,** 83-87.

Malan, D. J., 1963: *Physics of lightning.* English Universities Press LTD, 176 pp.

MacGorman, D. R. and W. D. Rust, 1998: *The Electrical Nature of Storms*. Oxford Univeristy Press, 422 pp.

McNamara, T. M., W. P. Roeder, and F. J. Merceret, 2010: The 2009 Update To The Lightning Launch Commit Criteria, Todd M. McNamara, *14th Conference on Aviation, Range, and Aerospace Meteorology*, Paper 469.

——, 2002: The horizontal extent of cloud-to-ground lightning over the Kennedy Space Center, Dept. of Engineering Physics, Air Force Institute of Technology, 101 pp.

Merceret, F. J., J. C. Willett, H. J. Christian, J. E. Dye, E. P. Krider, J. T. Madura, T. P. O'Brien, W. D. Rust and R. L. Walterscheid, 2010: A history of the lightning launch commit criteria and the lightning advisory panel for America's space program. NASA Tech. Rep. NASA/SP—2010–216283, 234 pp.

National Climatic Data Center, cited 2012: 2009 Annual Summaries. [Available online at http://www.ncdc.noaa.gov/oa/climate/sd/annsum2009.pdf]

North, G.R., T.L. Bell and R. F. Cahalan, 1982: Sampling errors in the estimation of empirical orthogonal functions. *Monthly Weather Review*, **110,** 699-706.

Rakov, V. A. and M. A. Uman, 2003: *Lightning: Physics and Effects.* Cambridge University Press, 687 pp.

Reap, R. M, 1994: Analysis and prediction of lightning strike distributions associated with synoptic map types over Florida. *Monthly Weather Review*, **122,** 1698-1715.

Roeder, W. P, 2010: The Four Dimension Lightning Surveillance System, *21st International Lightning Detection Conference*, 19-20 Apr 10, 15 pp.

Roeder, W. P. and T. M. McNamara, 2006: A Survey of the Lightning Launch Commit Criteria. American Meteorological Society, 45 Beacon St. Boston MA 02108-3693 USA, [URL:http://ams.confex.com/ams/htsearch.cgi.]

Roeder, W. P. and T. M. McNamara, 2011: Using Temperature Layered VIL As Automated Lightning Warning Guidance. *5th Conference on Meteorological Applications of Lightning Data, Seattle,* WA, American Meteorological Society, Paper 688. [Available online at http://ams.confex.com/ams/91Annual/webprogram/Paper185424.html]

Stano, G. T., 2007: Developing empirical lightning cessation forecast guidance for the Kennedy Space Center. Ph.D. dissertation, The Florida State Univeristy, 95 pp.

Sun, A. G., 2012: CGLSS strong local stroke misdetection rate analysis. AEROSPACE REPORT NO. TOR-2013(2221)-1, prepared by Aerospace Corporation for Space and Missile Systems Center Air Force Space Command 483 N. Aviation Blvd. El Segundo, CA 90245-2808, Contract No. FA8802-09-C-0001, 12 Oct 2012, 20 pp.

Uman, M. A., 2001: *The Lightning Discharge*. Dover Publications, 377 pp.

Uman, M. A. and E. P. Krider, 1989: Natural and artificially initiated lightning. *Science,* **246**, 457-464.

Valine, W. C. and E. P. Krider, 2002: Statistics and characteristics of cloud-to-ground lightning with multiple ground contacts. *Journal of Geophysical Research*. **107,** AAC 8-1 to AAC 8-11.

Vaisala, cited 2011: Vaisala's NLDN U.S. National Lightning Detection Network. [Available online at http://www.vaisala.com/Vaisala%20Documents/Brochures%20and%20Datasheets/NLDN-brochure-B210412EN-F-low.pdf.]

Vaisala, cited 2012a: Viasala's National Lightning Detection Network (NLDN) Cluot-to-Ground Lightning Incident in the Continental U.S. (1997 – 2011). [Available online at http://www.lightningsafety.noaa.gov/stats/97-11Flash_Density_miles.png.]

Vaisala, cited 2012b: Thunderstorm Total Lightning Sensor (TLS-200)-Identifies in-cloud and cloud-to-ground lightning. [Available online at http://www.vaisala.com/en/products/thunderstormandlightningdetectionsystems/Pages/TLS200.aspx.]

Ward, J. G., K. L. Cummins and E. P. Krider, 2008: Comparison of the KSC-ER Cloud-to-Ground Lightning Surveillance System (CGLSS) and the U.S. National Lightning Detection Network (NLDN), *20th International Lightning Detection Conference*, 22-23 April 2008, 7 pp.

Wahlin, L., 1986: *Atmospheric Electrostatics*. Research Studies Press, 120 pp.

Wilks, D. S., 2006: *Statistical Methods in the Atmospheric Sciences.* 2nd ed. Academic Press, 627 pp.

THIS PAGE INTENTIONALLY LEFT BLANK

INITIAL DISTRIBUTION LIST

1. Defense Technical Information Center
   Ft. Belvoir, Virginia

2. Dudley Knox Library
   Naval Postgraduate School
   Monterey, California